AFOSR-TR-78-0064

(2)

eirs
ENGINEERING & INDUSTRIAL RESEARCH STATION
ELECTRICAL ENGINEERING · MISSISSIPPI STATE UNIVERSITY

SOLID-STATE IMAGING DEVICE PARAMETER STUDY FOR USE IN ELECTRO-OPTIC TRACKING SYSTEMS

by

Jerry Rogers
Wilson E. Taylor

MSSU · EIRS · 78 · 2

COLLEGE OF ENGINEERING ADMINISTRATION

HARRY C. SIMRALL, M.S.
DEAN, COLLEGE OF ENGINEERING

WILLIE L. MCDANIEL, JR., PH.D.
ASSOCIATE DEAN

WALTER R. CARNES, PH.D.
ASSOCIATE DEAN

LAWRENCE J. HILL, M.S.
DIRECTOR, ENGINEERING EXTENSION

CHARLES B. CLIETT, M.S.
AEROPHYSICS & AEROSPACE ENGINEERING

WILLIAM R. FOX, PH.D.
AGRICULTURAL & BIOLOGICAL ENGINEERING

JOHN L. WEEKS, JR., PH.D.
CHEMICAL ENGINEERING

ROBERT M. SCHOLTES, PH.D.
CIVIL ENGINEERING

B. J. BALL, PH.D.
ELECTRICAL ENGINEERING

W. H. EUBANKS, M.ED.
ENGINEERING GRAPHICS

FRANK E. COTTON, JR., PH.D.
INDUSTRIAL ENGINEERING

C. T. CARLEY, PH.D.
MECHANICAL ENGINEERING

JOHN I. PAULK, PH.D.
NUCLEAR ENGINEERING

ELDRED W. HOUGH, PH.D.
PETROLEUM ENGINEERING

For additional copies or information
address correspondence to:

ENGINEERING AND INDUSTRIAL RESEARCH STATION
DRAWER DE
MISSISSIPPI STATE UNIVERSITY
MISSISSIPPI STATE, MISSISSIPPI 39762

TELEPHONE (601) 325-2266

SOLID-STATE IMAGING DEVICE PARAMETER STUDY FOR USE IN ELECTRO-OPTIC TRACKING SYSTEMS

By

Jerry Rogers

Wilson E. Taylor

Prepared for
Air Force Office of Scientific Research
Bolling Air Force Base
Washington, D. C. 20332

October 1977

The research reported in this document was sponsored under Grant number AFOSR-76-3022

TABLE OF CONTENTS

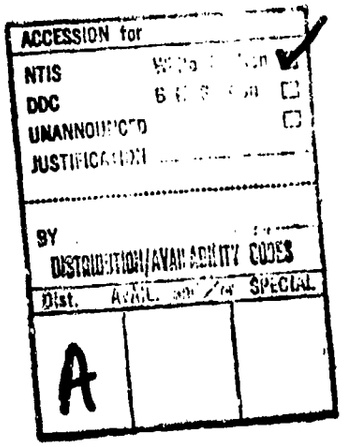

LIST OF FIGURES

LIST OF FIGURES (Continued)

LIST OF TABLES

LIST OF TABLES (Continued)

CHAPTER I

INTRODUCTION

The introduction of solid state arrays will have a major impact on at least three areas of semiconductor electronics:

1. As an analogue shift register or delay line
2. As a serial memory for binary data storage
3. As a solid state imaging device.

Imaging arrays have attractive military applications to terminal missile guidance, fire control, image reproduction, target or pattern recognition and similar areas.

Solid state devices (SSIDs) are attractive in many areas because arrays of charge coupled elements can be operated without the electron beam scanning mechanism and high-voltage vacuum technology of conventional vidicons. Most devices are compatible with other MOS devices or bipolar technology which might be used as peripheral circuitry, whether it be signal processing, clocking waveshapes, external amplifiers, or encoders.

One popular imaging device which shows much promise in state-of-the-art imaging is the charge coupled device (CCD). The CCD operates by a mechanism of charge storage and transfer of these packets of minority charge, which represent analogue or semi-analogue signals from under an array of MOS control gates. Information in this form is then transferred along the silicon surface in clocked shift register fashion by sequential manipulation of the voltages on the control gates. This transfer takes place in the bulk silicon

just beneath the silicon surface. There are basically two types of CCD, surface channel (SCCD) and buried channel (BCCD). In either case, the minimum potential energy of the depleted wells is determined by the voltage applied to the gate electrode, so that the appropriate manipulation of the phase voltages causes the charge packet transfer along the line, since the charge always moves to the local potential minimum. One section of a three-phase CCD is shown in Figure 1 to illustrate the potential well and development of the charge packet under the control electrode.

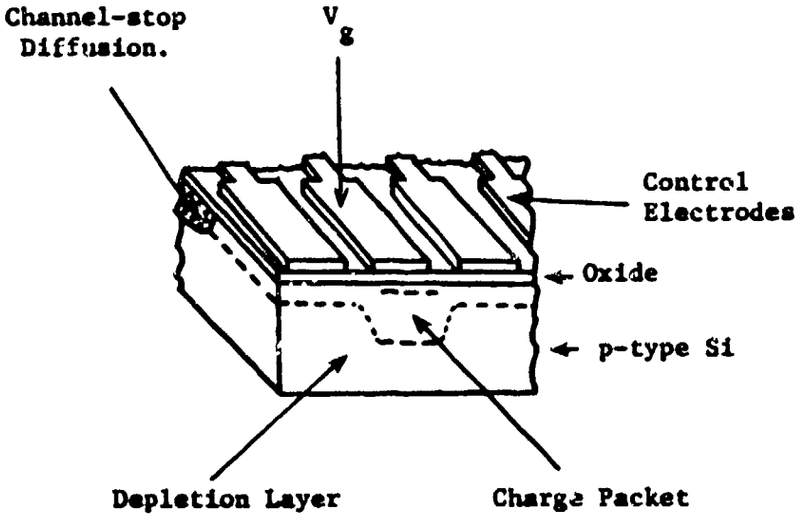

Figure 1. Section of a Three-phase CCD.

In the figure, V_g represents the electrode gate voltage. Once a charge packet has been produced on the surface of the device, it may be transferred along the structure as illustrated in Figure 2. At time t_o, a charge packet is developed under the electrode controlled by ϕ_2, which has an applied voltage of $+V_{cc}$. At this same time, electrodes ϕ_1 and ϕ_3 are maintained at the resting potential, $+V_{ss}$.

At time t_1, the electrode controlled by ϕ_3 is pulsed to $+V_{cc}$, producing a potential well under the control electrode. Since the electrodes are closely spaced, the charge begins to move slowly from the ϕ_2 electrode to the ϕ_3 controlled electrode. The voltage on the ϕ_2 electrode is then reduced to $+V_{ss}$ with a slowly falling edge. This slowly falling edge provides the finite amount of time necessary for the charge carriers to diffuse across the width of the electrode. Figure 2(c) shows the charge transfer complete at time t_2, with the charge stored in the well, or depletion region, under the electrode controlled by ϕ_3. ϕ_1 must be kept at a relatively low potential for this entire time to prevent the backflow of charge. Thus, in a three-phase device, three array elements, or electrodes, are necessary to store and transfer one charge packet. For this reason, these three control electrodes are usually referred to as "one element" of the CCD. This will be the notation used throughout the body of this work.

Thus, the electrodes of the three-phase CCD array are arranged in triplets and are connected sequentially to the drive lines carrying the three-phase clocking waveforms, or driving pulses. These

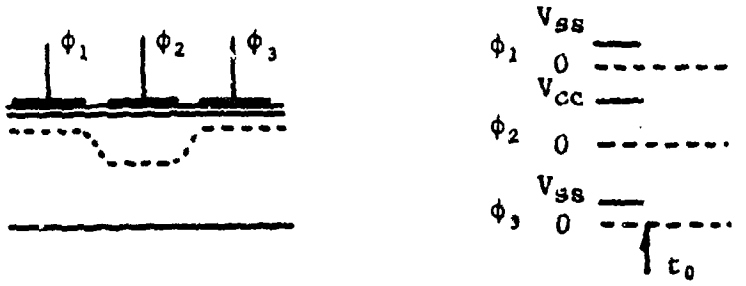

(a) Charge stored under ϕ_2

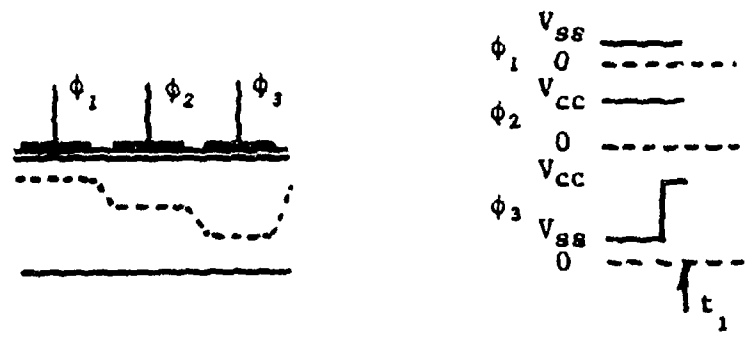

(b) ϕ_3 comes on

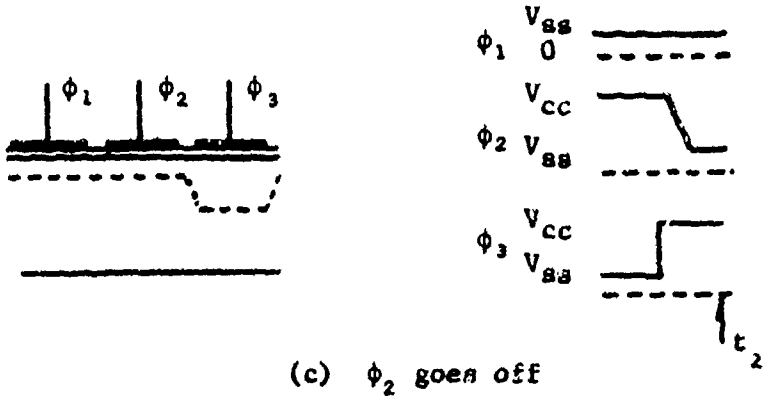

(c) ϕ_2 goes off

Figure 2. Charge Packet Transfer.

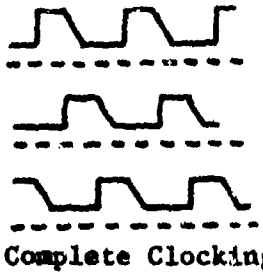

Figure 3. Complete Clocking Waveforms.

complete clocking pulses are illustrated in Figure 3. It should be noted that there can be charge under every third electrode in an array and that application of the clocking waveforms causes these charges to move simultaneously.[1]

The theoretical aspects of charge coupled device operation will not be dealt with explicitly, as they provide little insight into the operation parameters of the device in the manner of which they were examined. However, it is helpful to observe how the potential well depth is related to the applied gate voltage, and how the charge transfer time is related to element dimensions. The potential well depth may be expressed as

$$V_s = V_G' - B\left[\left(1 + \frac{2V_G'}{B}\right)^{\frac{1}{2}} - 1\right] \quad , \tag{1}$$

where

$$V_G' = V_G + \frac{Q_{ss}}{C_{ox}} \tag{2}$$

$$B = \frac{qN_d \varepsilon_s x_{ox}^2}{\varepsilon_{ox}^2} \tag{3}$$

V_G = gate voltage

Q_{ss} = oxide charge per unit area

C_{ox} = oxide capacitance per unit area

q = electronic charge in coulombs

N_d = substrate doping level in cm^{-3}

ε_s = silicon dielectric constant in F/cm

V_s = potential well depth

ε_{ox} = oxide dielectric constant in F/cm

x_{ox} = oxide thickness in cm.

The well depth is then determined by

$$\Delta V_s = \frac{Q_{sig}}{C_{ox} + C_d} \tag{4}$$

where C_d if the depletion-layer capacitance, and Q_{sig} is the signal charge.

The most important figure of merit for a charge transfer device is the transfer efficiency, η, the fractional part of charge that is transferred from one electrode to the next. Likewise, the portion which is not transferred, the transfer inefficiency, or transfer loss, is denoted by ε. Thus,

$$\eta + \varepsilon = 1 \quad . \tag{5}$$

Since CCD imaging devices require large numbers of transfers, ε must be very small to prevent excessive signal degradation.

The transfer efficiency is dependent on two aspects of the device--the transfer time and trapping effects. The trapping effects can be minimized by the continuous circulation of a small amount of charge (~10% of full signal level). This background charge is generally called "fat zero", and helps to keep the fast states continuously filled so that no states are empty to trap charge when a full well signal arrives.

The transfer time is essentially determined by either thermal diffusion or fringing field drift. Both of these mechanisms cause

an exponential decay of charge. The time constants for this decay determine the efficiency that can be achieved at any particular clock frequency, since this clock frequency determines the time available for charge transit.

The time constant for thermal diffusion can be determined by physical properties of the gate. The motivation is provided by the thermal voltage kt/q applied across the gate length. The transit time is therefore

$$\tau_{th} = \frac{L}{\mu E} = \frac{L}{\mu kt/qL} + \frac{L^2}{D} \quad . \tag{6}$$

To achieve efficiencies of 99.99% ($\varepsilon = 10^{-4}$) requires about ten time constants ($10^{-4} \cong e^{-10}$). Thus for typical values (L = 10um and $D = 10cm^2/sec$), efficiencies of 99.99% can be achieved at approximately 1 MHz. clock rates, assuming thermal diffusion is the only mechanism responsible for charge transfer. This speed is insufficient for many applications.

The transfer of charge is also aided by the externally applied voltages in the form of induced fields. The transit time constant for fringing-field drift is then given by

$$\tau_f = \frac{L}{\mu E_n} = \frac{L^3}{3.2 \mu V x_{ox}} \quad , \tag{7}$$

where E_m is the minimum fringing-field possible, given by

$$E_m = 3.2 \frac{V}{L} \frac{x_{ox}}{L} \quad . \tag{8}$$

V is the applied voltage, x_{ox} is the oxide thickness, and L is the gate length. Again, for 10 μm gates, the thermal time constant is 10^{-7} seconds. Assuming $\mu = 400$, $x_{ox} = 1000$ Å, and V = 10 volts, the fringing field time constant in 7.8×10^{-9} seconds, or a factor of 13 lower. Thus, for 10 μm gate lengths and low substrate doping, fringing field drift results in about 10–15 MHz. operation. Since τ_f is dependent on L^3, the increase in speed over that possible with thermal diffusion increases as gate length is decreased.[2]

The maximum amount of signal charge, Q, which can be stored under any one control electrode and transferred within the CCD is given by:

$$Q = kCV$$

where C is the total oxide capacitance of the storage electrode and V is the voltage swing on the control electrode. At full well, a constant fraction, k, of this is minority charge, where $k \tilde{=} 0.5$ for typical surface channel structures.[1]

The transfer efficiency can be calculated from the relative magnitude of the residual "trailing" charge ΔQ to the full charge packet Q:

$$\frac{\Delta Q}{Q} \tilde{=} \eta\varepsilon \qquad (9)$$

where η is the number of transfers. For example, for surface channel devices ε is typically in the range 5×10^{-3} to 10^{-4} (for medium frequency operation). The values for the ηε product can be

shown to be necessarily less than 0.1 for maximum bandwidth capabilities of the device to be realized.[3]

For imaging, an optical system focuses the light onto the CCD. The incident light quanta enter the substrate and impart their energy to the silicon causing the generation of free charge carriers. Depending on device structure, the quanta may enter between the control electrodes, through transparent electrodes or, in specially thinned devices, through the back face of the substrate. The generated carriers collect as a charge pattern under the array of electrodes. This pattern is a semi-analogue replica of the radiation of light intensity across the original image. Semi-analogue is a term that will be used to describe the sampled analogue image stored in the device. The charge pattern can be extracted from the CCD using the previously described sequential clocking technique by one of three different types of transfer. It appears as a train of pulses whose amplitudes vary with the grey scale of the image. The array is thus self-scanning.[1]

Three options of device organization are possible. These are frame transfer (FT), interline transfer (ILT), and line transfer (LT). These three options are illustrated in Figure 4. A listing of these options and design issues are also given in Table 1.

Frame transfer, which is a low frequency continuous transfer, and line step, which is also low frequency but discontinuous, make up the vertical transfer processes.

The frame transfer organization requires substantially more total device area to accommodate a buffer store, which is a major

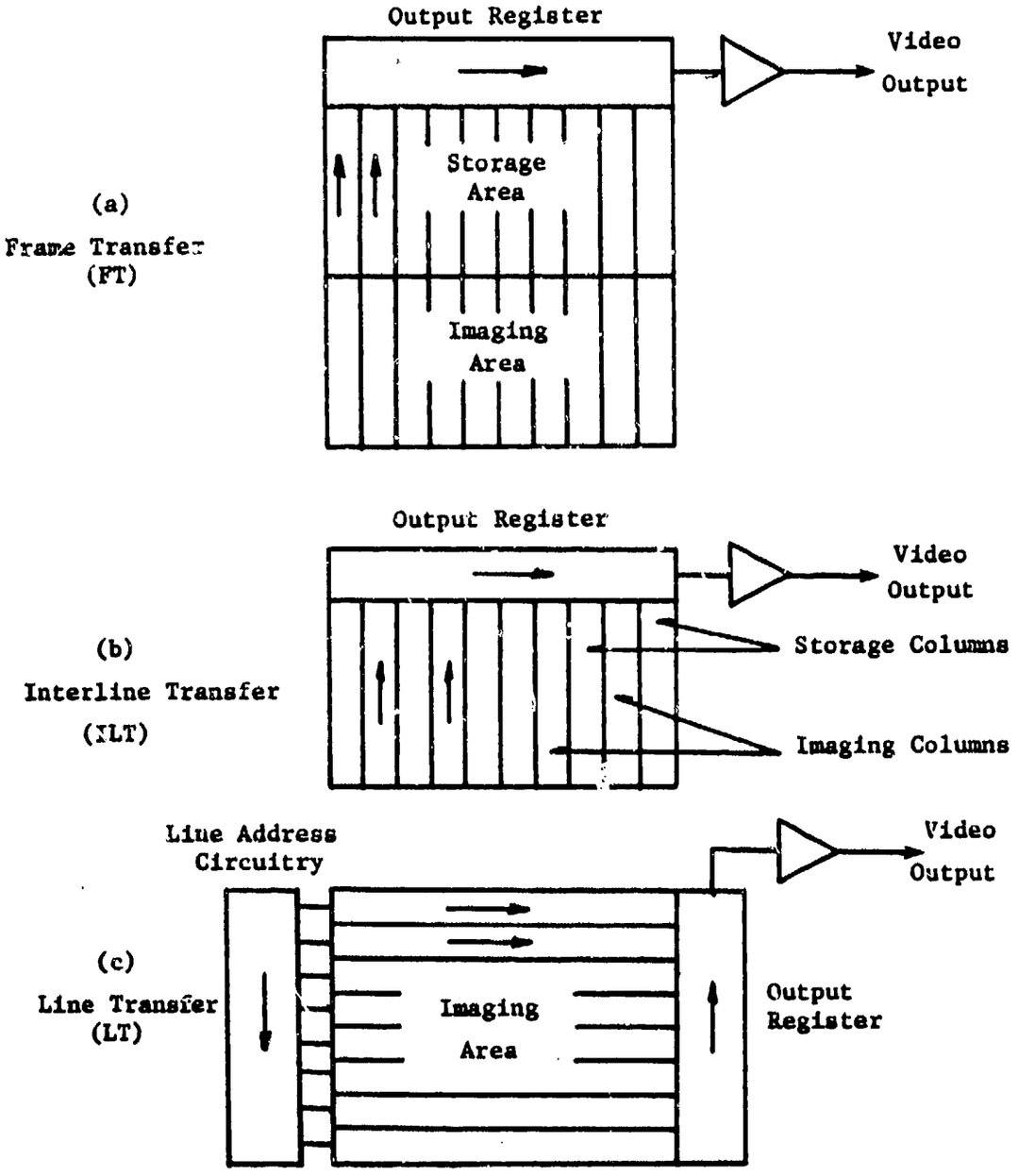

Figure 4. Three Basic Types of Organization for a Charge-Coupled Area Image Sensor.

Table 1. Design Issues and Options for Charge-Coupled Area Imagers

Issue	Options
1. Organization	Frame transfer, interline transfer, line transfer
2. Illumination side	Front, back
3. Channel mode	Surface, buried
4. Gate technology	Silicon, aluminum, refractory metal
5. Polarity	N-channel, P-channel
6. Clocking	2-Phase implanted barrier, 2-phase stepped oxide, 3-phase, 4-phase
7. Low light level mode	Electron imaging (with photocathode), direct optical imaging (with cooling)
8. Interlace mode	True, pseudo, sequential
9. On-chip preamplifier	None, GCI, FGA, DFGA
10. Anti-blooming control	None, element-type, column-type

disadvantage compared to the other two devices. However, it is functionally the simplest. The line transfer organization employs a scan generator. The interline transfer structure requires separate photosensitive elements and shift registers. The ILT simplicity is a definite advantage with regard to interlace and vertical resolution.[4]

In the frame-transfer structure, the top half of the chip is photosensitive. Field A is formed by collecting photoelectrons under the ϕ_1 electrodes for approximately 1/60 second. This charge configuration is shifted into the shielded storage register in typically 1/600 second. Field A is then read out a line at a time while Field B is being formed by collecting photoelectrons under the ϕ_2 electrodes.

In the interline transfer structure, the shielded vertical readout registers are interlaced with the photosensitive lines. Because the integrating cells and shift-out cells are separate, the effective integration time for both Field A and Field B is 1/30 second. After collecting photoelectrons in Field A for 1/30 second, the charge configuration is shifted into the shielded registers and down, a line at a time, into the horizontal output register. When Field A is completely read out (1/60 second), Field B is shifted into the shielded registers and out. It is important to note that the effective integration time for interline transfer structure is twice that of the frame-transfer structure or line transfer structure.[5]

Research has been performed by several aerospace companies to develop trackers which utilize imaging arrays such as the CCD as sensors. The Avionics Laboratory, Wright-Patterson Air Force Base,

Ohio initiated a program with the purpose of determining the performance characteristics of array trackers, providing useful test data to designers and exploring the potential of this new technology.

Tests are performed on array trackers from three companies: Honeywell Incorporated, McDonnell Douglas Astronautics, and Martin Marietta Aerospace.

The tests are performed using a Zoom Optical Target Simulator (ZOTS), an instrument designed specifically for testing electro-optical tracking systems. The ZOTS provides simulated parameters, such as brightness, contrast, motion, and range closures. Motion of the target carriage provided in x, y, and diagonal direction by a servo control system.

Both the ZOTS and the tracker under test are interfaced into a Data Aquisition System, and recorded in digital form on magnetic tape. The tape format is 9-track, 800 bpi, and IBM compatible. The run number, run time, x and y tracker outputs, ZOTS analogue voltages, and other information are recorded for each tracker frame.

These data are used in portions of the parameter investigation for CCD, charge injection device (CID), and photodiode arrays utilized in target and pattern tracking.

CHAPTER II

PROBLEM DESCRIPTION

The problem is three-fold. There is an analysis of data obtained from the available trackers, a parameter investigation utilizing these data as well as an extensive literature search, and a simulation of the CCD utilizing parameter variations. As an extension of this work the video data are encoded in order to reduce redundancy incurred. The Huffman coding of run-length sequences accomplishes this task easily.

The analysis task consists of identifying the sources of tracker error and where possible eliminating the systematic errors. A thorough investigation of the tracker responses to variations in the parameters in question is accomplished as well as the removal of system errors, revealing the actual tracker error.

Since the data are stored on 9-track magnetic tape, a program written to retrieve the data and transform the information into a usable form is utilized. The words are converted to a usable length and manipulated on the available Univac 1106 Multiprocessor Facility. A major portion of this work is, however, dedicated to the identification of these error sources and systematic error removal.

The results are used as a partial source of parameter study for the second portion of the study.

A synopsis of the computer software used in the error analysis is available in Appendix B of this text.

Several parameters are considered and trade-offs examined to evaluate the performance and establish the practicality of the SSID as a tracking sensor. There are several optical characteristics of the device itself that are significant. For example, polysilicon, which is used extensively to form the optically transparent electrodes, does provide some optical attenuation. Also, when multilayers of polysilicon electrodes are employed, as is the case in the manufacture of some devices, it is possible that the layers may act as an undesirable filter.

From a systems standpoint, there are a number of considerations that affect the eventual design decision. The close coupling of the photo elements, which is vital for the required charge transfer, to an output detector creates the atmosphere for a blooming problem. A heavy optical overload results in blooming; in fact, a small intense spot can create a disturbance as extensive as to cover the entire sensor. Partial cures for this blooming are proposed and evaluated for the tracking or imaging application.

A consideration along this same line is that of the intensity of the target and the background field of view. Besides the danger of high intensities causing blooming, there is the lower limit on target intensity which permits detection by the sensor or tracking algorithm. This means that there must be a significant difference between the intensity of the target and the intensity of both the background and the noise inherent in the device itself.

Inherent noise can degrade system performance while tracking. It develops in the following manner. If the object moves from one

active element or group of active elements to another, and if the amount of charge generated and stored in the second element or group is not comparable to that of the preceding element or group, the sensor might misjudge the direction of travel of the target, or lose the target altogether. Nonuniformities of this type are usually caused by limitations in the manufacturing process for the device.

The largest single cause of nonuniformity in sensor output is due to material properties. The generation of photo electrons varies according to the homogeneity of the bulk material in which the photons are absorbed. As devices get smaller and more dense the photolithographic process used in fabrication becomes a limiting factor. Irregularities become dependent on the irregularity in the geometry of the sensing cells. Many companies have thus gone to electronbeam lithography to provide smaller dimensions in cell size and intercell spacing.

The amount of nonuniformity which can be tolerated is, of course, dependent on device utilization. In tracking, as will be shown later, the nonuniformities only become a valid concern when contrasts and irradiances approach extremes. If inherent noise is present, schemes must be employed to reduce its effect on the video output of the device. For instance, corrections can be incorporated in the tracking algorithm or in the external circuitry.

This inherent noise is compounded by the introduction of a fixed-pattern "noise" on the signal. This fixed-pattern noise is imposed by an effect known as dark current nonuniformity.

This dark current is thermally generated in the silicon and also limits the storage time of the CCD. The limitation on storage time determines the lower limit on scan rate of the sensor. This storage time is very short at room temperature, but cooled devices are capable of storage times of up to an hour or two.

The scan rate of the sensor determines the maximum image velocity of a trackable target. The scan rate (data update) must be somewhat faster than the estimated velocity of the target image across the face of the device. If not, the target will be lost between frames. On the upper end of the scan rate, limitations are imposed by the integration time of the SSID. Integration time is a fundamental property of the device. If the device is scanned faster than the integration time necessary to adequately describe the scene in quantities of charge, blurring will result, and target definition suffers.

As scan rates and frame rates are increased, two interrelated quantities become crucial to system performance. These are transfer time and transfer efficiency. The loss of the small portions of information and the subsequent addition of these residual charges to trailing elements tend to degrade video output. Therefore, scan rates must allow for adequate charge transfer. System-wise, higher scan rates need wider bandwidth and wide band noise may prove undesirable.

Another area of concern is target acquisition. This aspect is a characteristic of both the tracking algorithm and the device parameters. Thus, various aspects are interdependent. The sensitivity

of the SSID to changes in the background, or the amount of grey level separation which is attainable, determine how well the target can be defined and tracked.

Several of the above listed problems are interrelated, and thus trade-offs are considered. For instance, integration time, scan rate, target velocity, transfer time, and transfer efficiency are all interdependent. Likewise, so are intensity, blur, sensitivity, inherent noise, and blooming effects.

It is necessary to study the extent of each problem as it is introduced by the device parameters and as it affects system performance. These results can be used to determine corrective measures. The data described previously are used as an experimental basis or applied starting point for the system effects of device parameters. They are used for analysis and investigation of projected system performance.

Portions of the projected performance are attained from a computer simulation of the CCD tracker array. The fortran program utilizes transfer efficiencies, target contrasts, background elimination, target pattern acquisition and grey level adjustment in each array element. The simulation provides information as to the degradation of the picture image as the analogue replica of each scene is clocked from the array, as well as the feasibility of target acquisition on large arrays. The target acquisitions can be utilized as a contrast tracker or a pattern recognition scheme.

The program is so written that the information clocked from the array can be encoded directly using Huffman encoding to reduce

scene redundancy as well as the space necessary for information storage. This portion of the work is backed by previous work done in the area of redundancy reduction by the coding of run-length sequences. Any code can be used since the scheme uses the table look-up procedure for coding.

CHAPTER III

DATA ANALYSIS

Each tracker tested in this study is listed in the order in which the original tests are made. The tracking algorithms are proprietary to the individual companies, and hence, are only discussed in a limited fashion. The programs used for extraction and reduction of the data for this study are located in Appendix B. A synopsis of each of these programs is also given.

TRACKER NUMBER 1, Honeywell Solid State Imaging Seeker (Photodiode)

The data from two Honeywell array trackers are available for investigation. Both utilize the same tracking algorithm, but have different detector arrays. Tracker Number 1 uses a Reticon 50 x 50 array of photodiodes in matrix form. Each cell stores charge in the p-n junction and is read serially once during each frame.

This device is designed as a terminal guidance seeker for a shoulder-launched anti-tank weapon. Its tracking algorithm is a correlation technique utilizing information from a specific number of array cells in the form of several levels of "grey" or internal target contrast.

TRACKER NUMBER 2, McDonnell Douglas Mosaic Tracker

Tracker Number 2 utilizes a General Electric 100 x 100 charge injected device (CID) array. This sensor consists of a matrix of

coupled MOS capacitors as does the CCD. Each cell is read once per frame by injecting the charge into the silicon substrate.

The tracking algorithm of this tracker consists of calculating the mathematical centroid of the target from the classical definition of the center of mass of a uniformly dense target. This target tracker uses two-level logic. A present threshold determines the presence of the target over a particular array element. Thus, any cell outputting a 1 (as determined by the threshold) is included in the tactical centroid calculation.

TRACKER NUMBER 3, Martin Marietta Area Correlation Tracker

This Martin Marietta tracker uses a Fairchild 201 CCD as a sensor. It is a 100 x 100 matrix of cells as is used in the simulation later on in the text of this study.

The tracking algorithm of this tracker utilizes target signature: characteristic of the target and background features within a fixed segment of the sensor field of view. The tracker stores a reference target area signature in memory and derives tracking information from the comparison of subsequent target signature with this reference. The target reference can be updated to enable tracking of relatively fixed targets during range closure. It is this idea that is utilized in the simulation.

TRACKER NUMBER 4, Martin Marietta Point Tracker

The point tracker once again uses the CCD array as does tracker number 3, the difference in the two being in the tracker electronics.

The point tracker algorithm processes sensor information to distinguish a target from its background and then calculates the relative location of the centroid. This tracker determines the contrast edges of the target and adjusts tracking to match the target window with the size of the target.

TRACKER NUMBER 5, Honeywell Solid State Imaging Seeker (CID)

This Honeywell device also uses the General Electric CID sensor. However, the sensor utilizes a 144 x 288 cell array. This tracker uses the same tracking algorithm as Tracker Number 1, the only modifications being to accommodate the array's larger size.

The dimensions of the target image on the sensor, the angular size and the approximate number of sensor cells subtended by the target are presented in Table 2.

Table 2

Geometric Target Sizes

Tracker Number	Target Size		Cells Subtended
	Mils	Milliradians	
1	12 x 12	2 x 2	3 x 3
2	16.4 x 16.4	2.7 x 2.7	5 x 6.5
3	24.1 x 24.1	4 x 4	15 x 20
4	13.3 x 13.3	2.2 x 2.2	8 x 11
5	7.2 x 4.2	1.7 x 1	3 x 3

In order to present the parameter study performed on the three companies' trackers, an identification and analysis of tracker error is necessary.

The error analysis is begun by reviewing sample runs and obtaining plots of the ZOTS position versus time for Tracker Number 1. The ZOTS position is the true position of the target and is measured in mils. The time is given in seconds. The x and y position on the array sensor are recorded as the x and y analogue outputs. The computer program TAPEREAD.DRIVE1 calculates the sensor error difference E_s as

$$E_s = Z - T \text{ (inches)} \quad , \tag{11}$$

where Z is the ZOTS indication of "true" target position and T is the tracker realization of target position.

The calculated error for the Honeywell tracker is plotted for investigation in Figure 5. Several types of error are evident from the plot. The error function has an average value which takes on a positive value during the first pass of the target on the image surface. When the target changes directions and begins its reverse pass, the value drops to a slightly negative quantity. This error, it seems, is due to tracker lag. This tracker lag might not be a characteristic of the imaging device itself, but an inconvenience encountered in the use of certain tracking algorithms. The lag error is evident in all of the trackers, but varies in its extent.

The higher frequency oscillations represent "electronic noise".

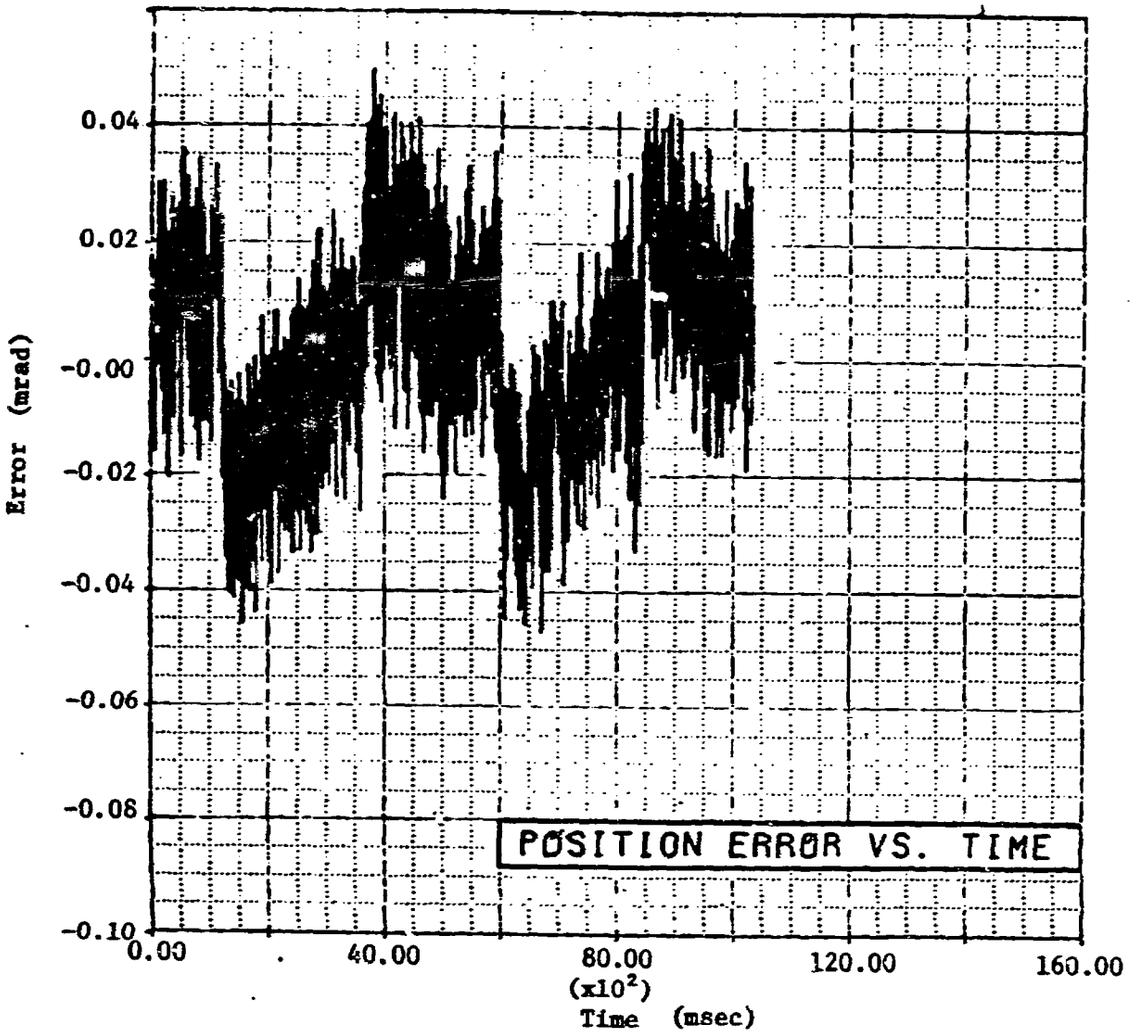

Figure 5. Error for Honeywell Tracker; Irr. = 12.1, Contr. = -58.0%, Vel. = 13.22, F.R. = 92.6; Run #37.

proportional to the location of the target. Superimposed on these d. c. voltages is a random "electronic noise", which is interpreted as "true" target motion by the tracker. This noise is easily removed in the computer analysis by simply obtaining a linear least-squares fit to the ZOTS output voltage. The removal of this noise reveals the actual tracker error as pictured in Figure 6. These results correspond much more closely to the reaction of an "ideal" tracker. An "ideal" tracker error occurs only between target position decisions. The difference error increases from zero until the tracking algorithm makes the decision that the target has indeed moved to another cell space or active element. At the predetermined time, the tracker output indicates a move and the error drops to near zero, where the procedure is itterated; resulting in a sawtooth waveform whose frequency is given by

$$f_{er} = v_t/d \quad , \tag{12}$$

similar to that of Figure 7. v_t is the target velocity and d is the width of an active element of the sensor. There is strong indication that this is indeed the case, in part, showing most of the error to be algorithm oriented rather than sensor oriented.

The other error element encountered in the analysis is that of calibration factor selection. The calibration factors for scaling outputs from the ZOTS and tracker determines the amplitude of the sweep for each. Lack of precision produces a large triangular component in the error difference as shown in Figure 8. This same

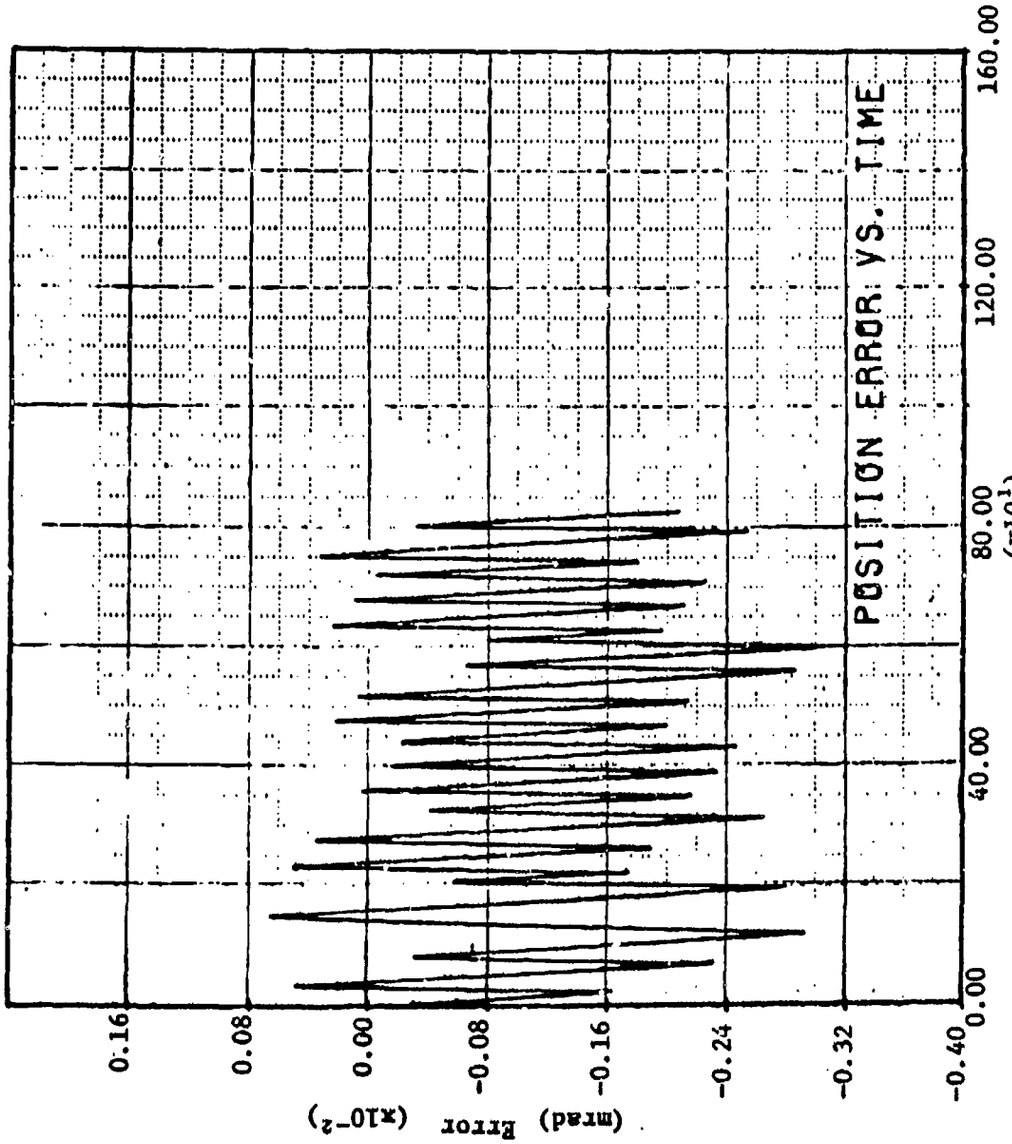

Figure 6. Error Without "Electronic" Noise, Run #1.

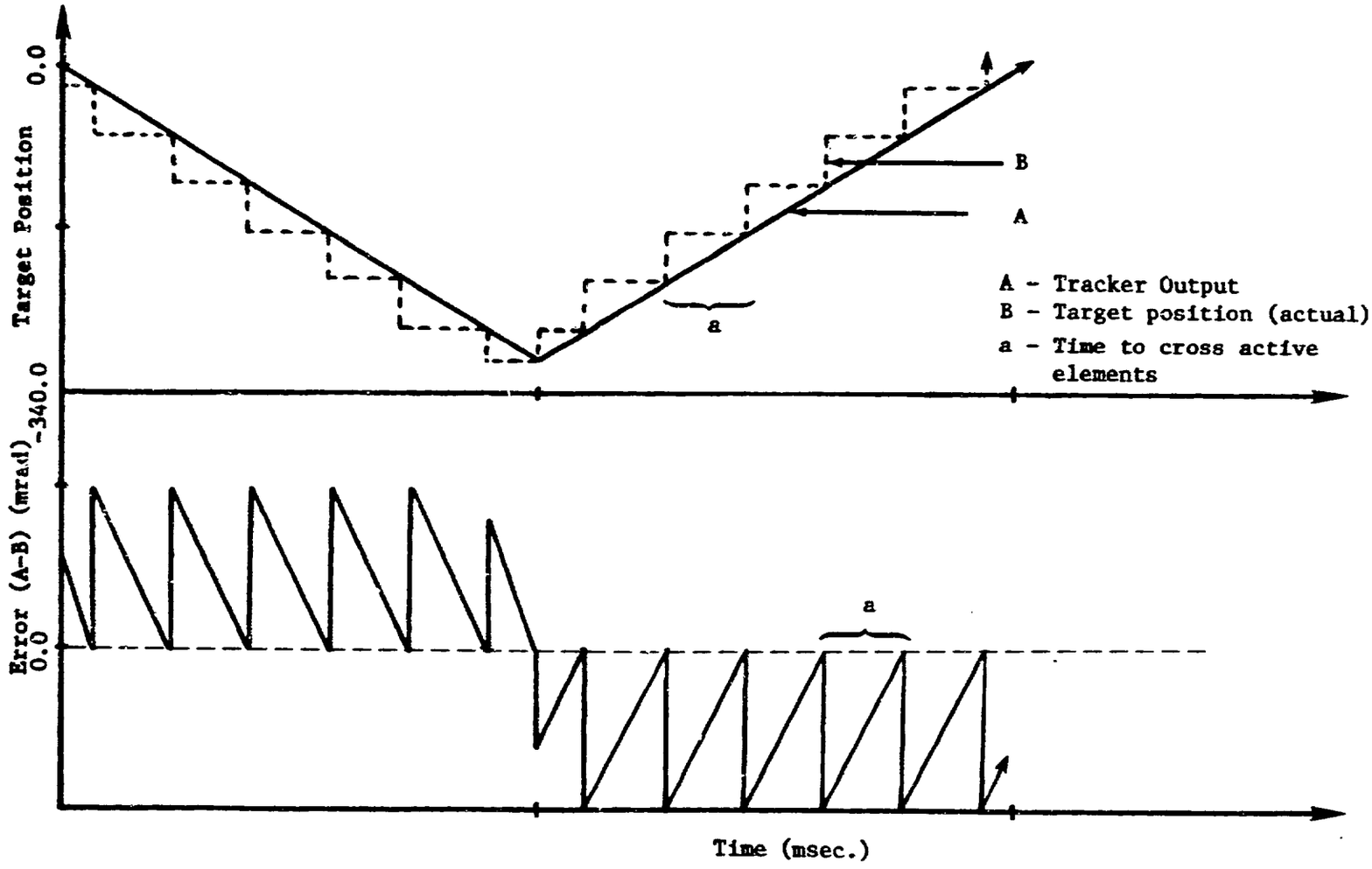

Figure 7. Explanation of Actual Error (Sawtooth).

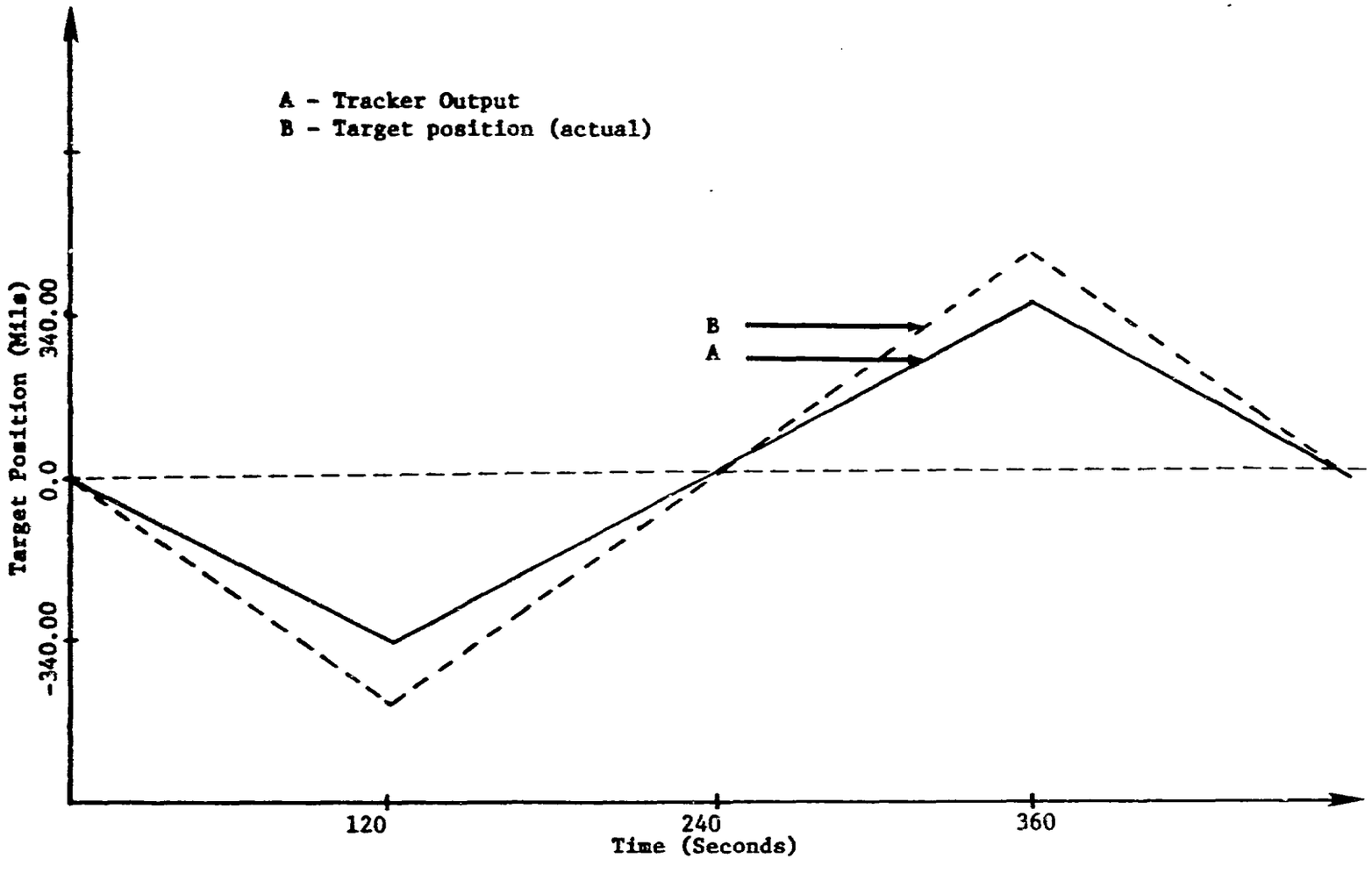

Figure 8. Explanation of Calibration Error Versus Time.

type of error would be evident if a lag in response of the target to ZOTS positioner, since the target would never cross the full expanse of the face of the imager. Each case is, however, a limitation of the test equipment and not of the tracker itself. It is not considered a restriction on the tracker.

Sample runs for obtaining the tracker error are shown in Figures 9 through 14. These runs provide illustrations of each type of error encountered in the tracker parameter analysis. The Fortran program also provides numerical values for the error differences, but an extensive listing would be cumbersome and provide little extra insight into the abilities of the tracker.

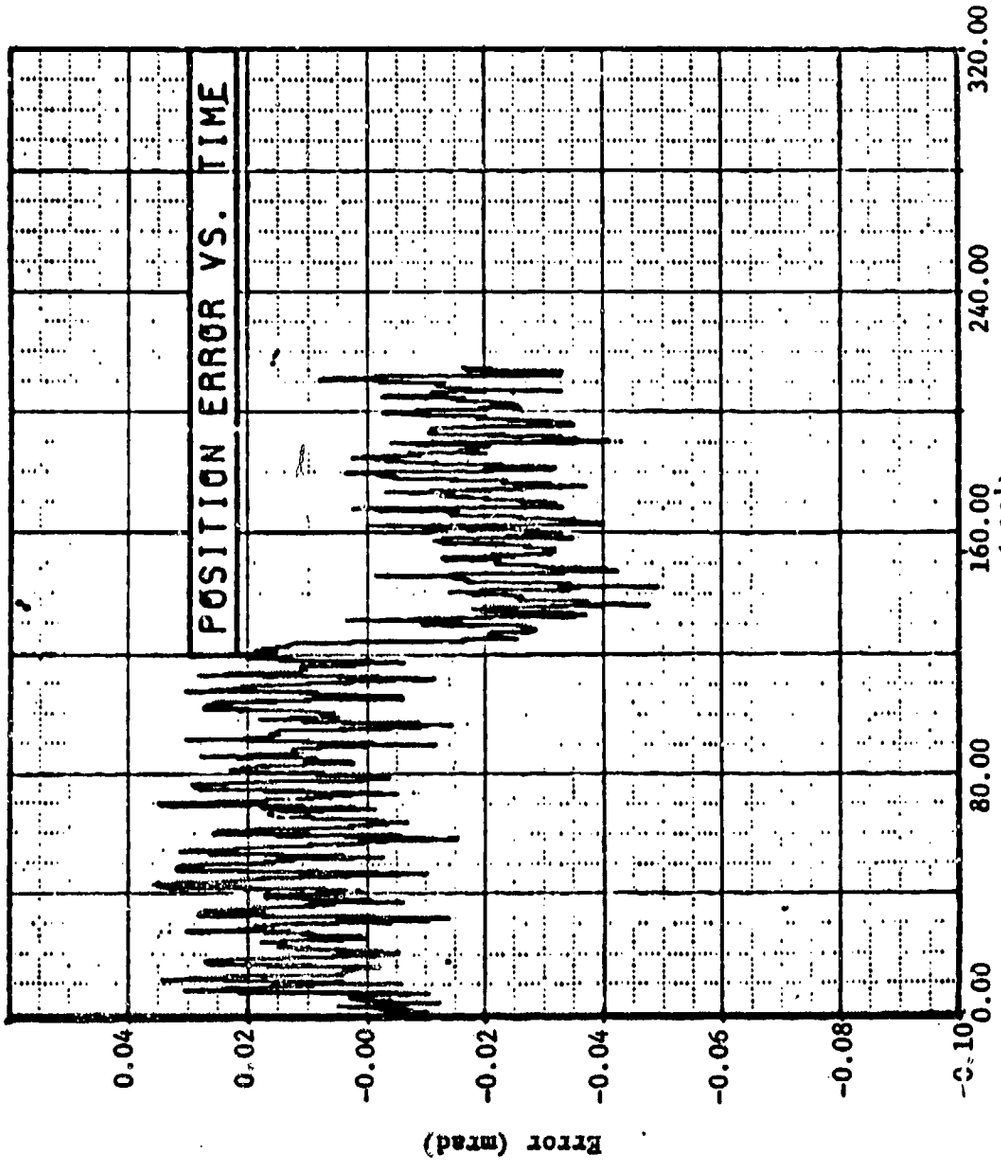

Figure 9. Error for Honeywell Tracker; Irradiance = 21.0, Contrast = -56.1%, Velocity = 13.22, F. R. = 92.6; Run #1.

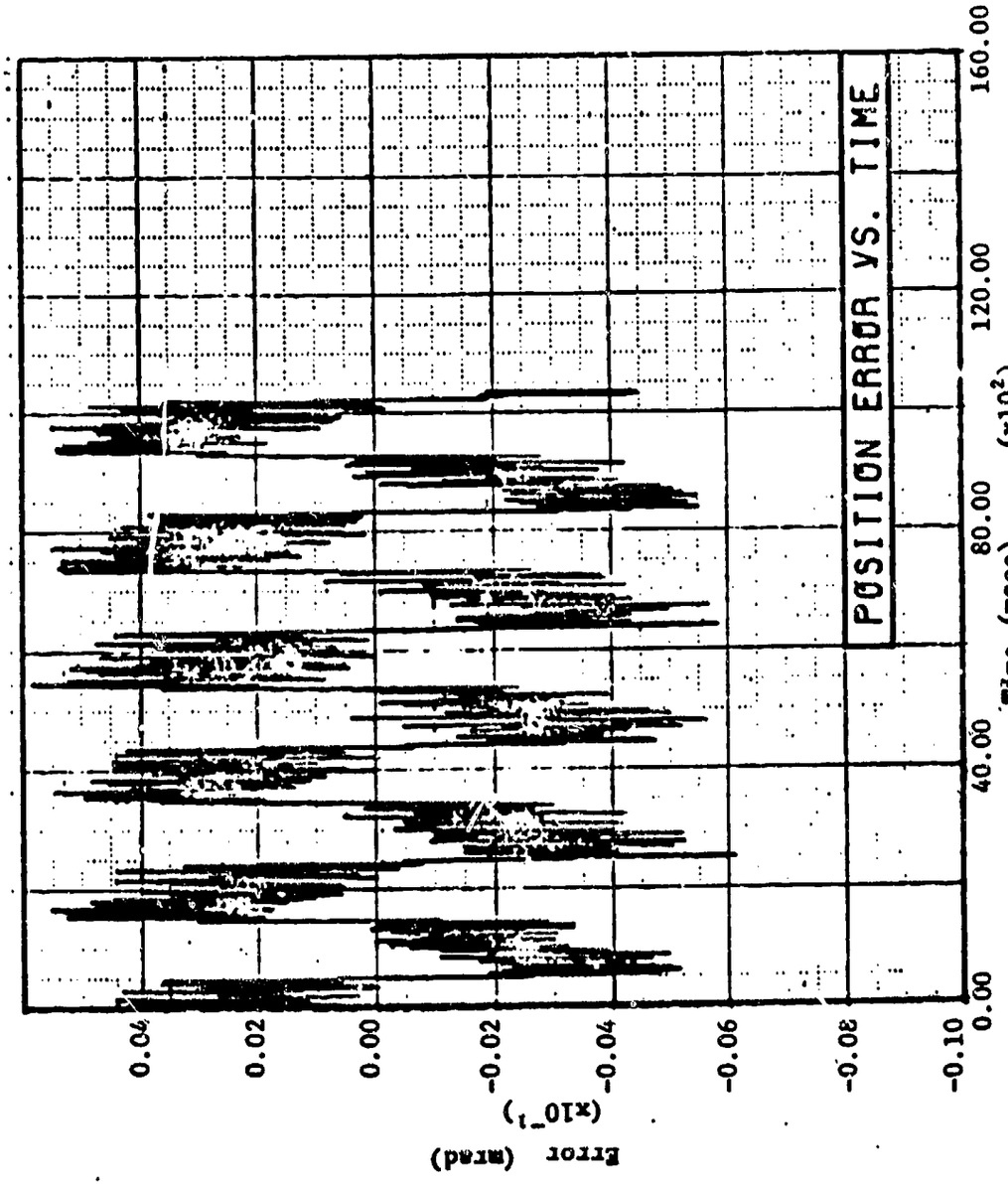

Figure 10. Error for Honeywell Tracker; Irr. = 21.0, Contr. = -56.1%, Vel. = 31.47, F.R. = 92.6; Run #31.

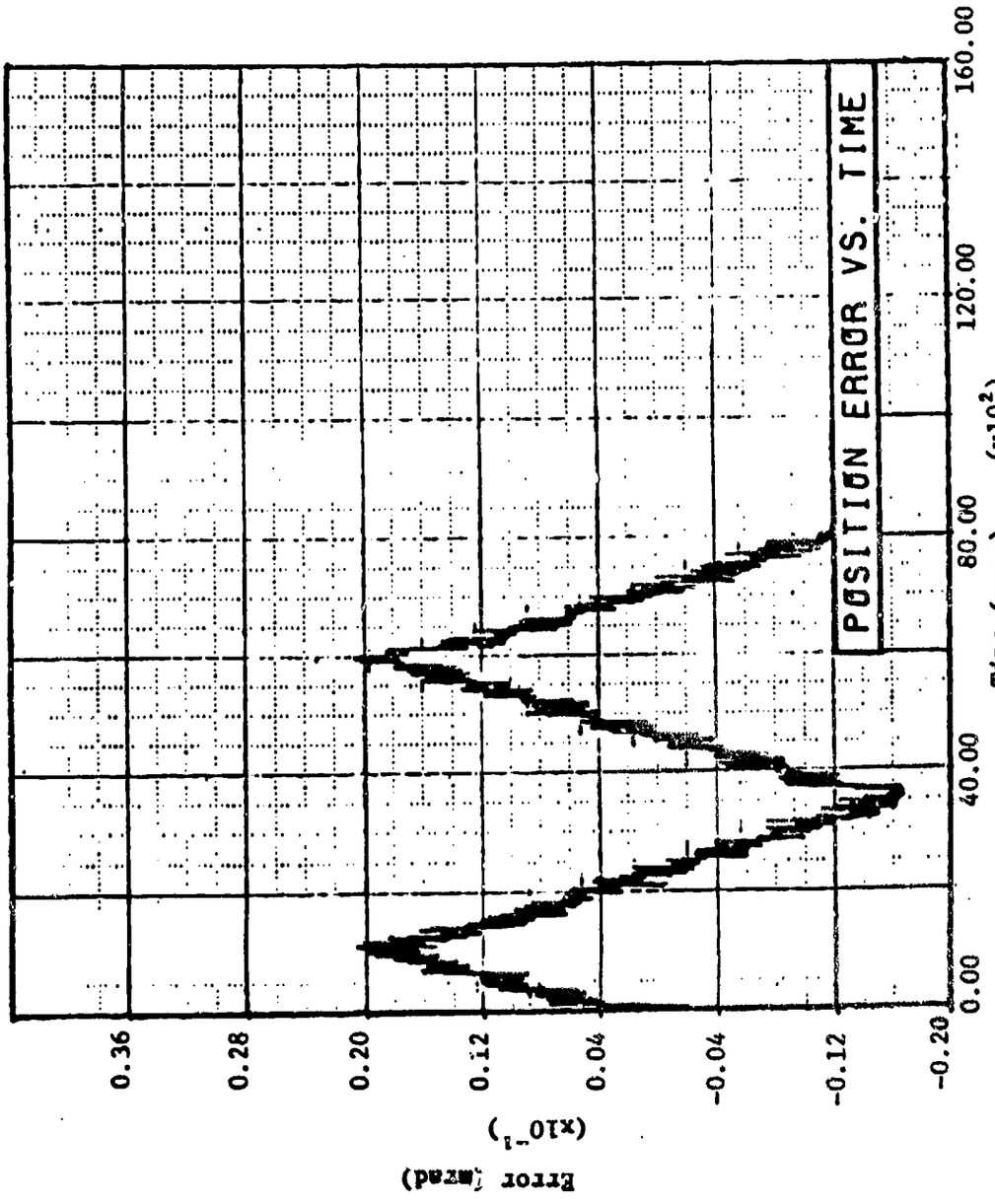

Figure 11. Tracker Error for Martin Marietta Correlation Tracker.

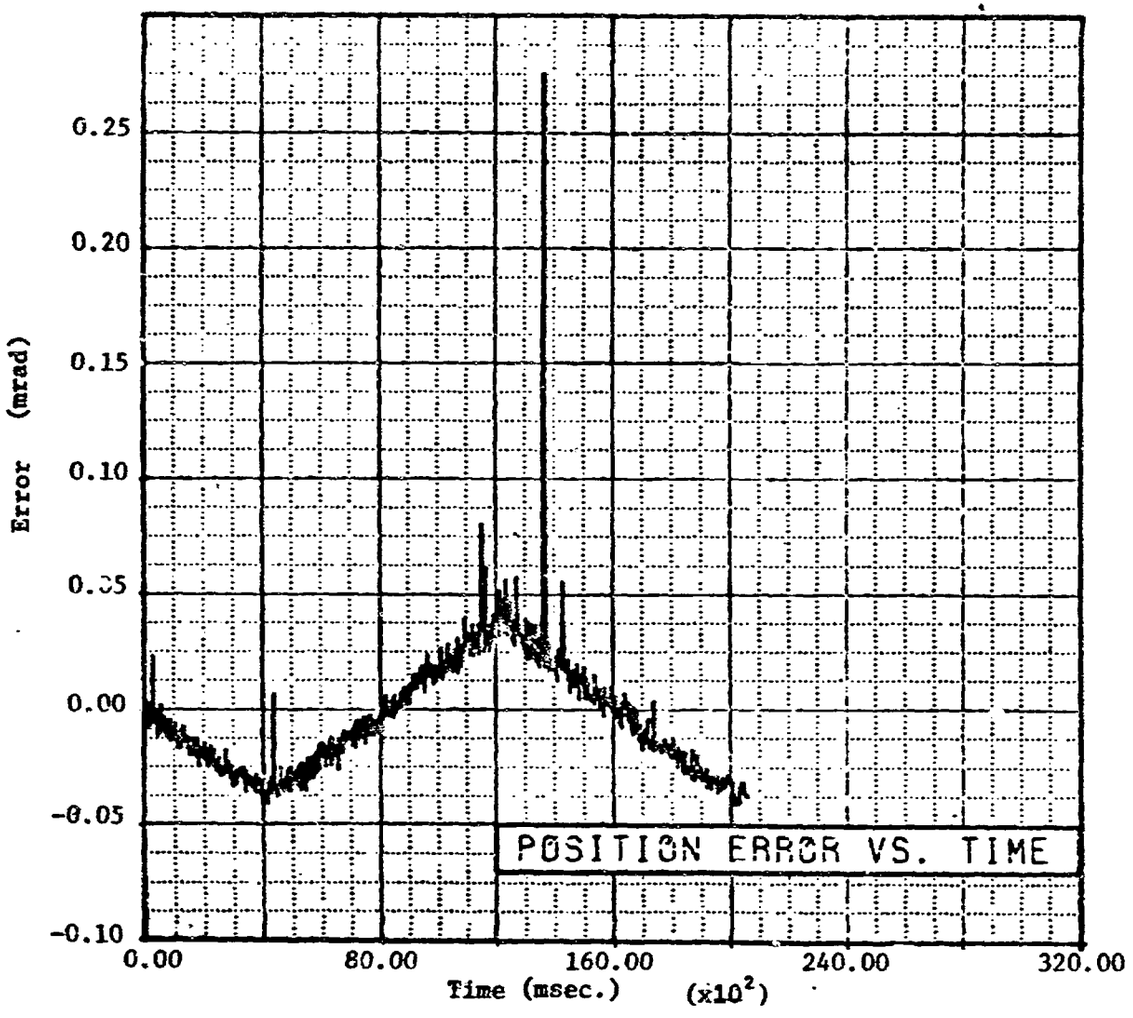

Figure 12 Error for Mosaic Tracker; Irr. = 0.165, Contr. = -99.8%, Vel. = 5.24, F.R. = 46; Run #2060. (CALIBRATION FACTOR ADJUSTED)

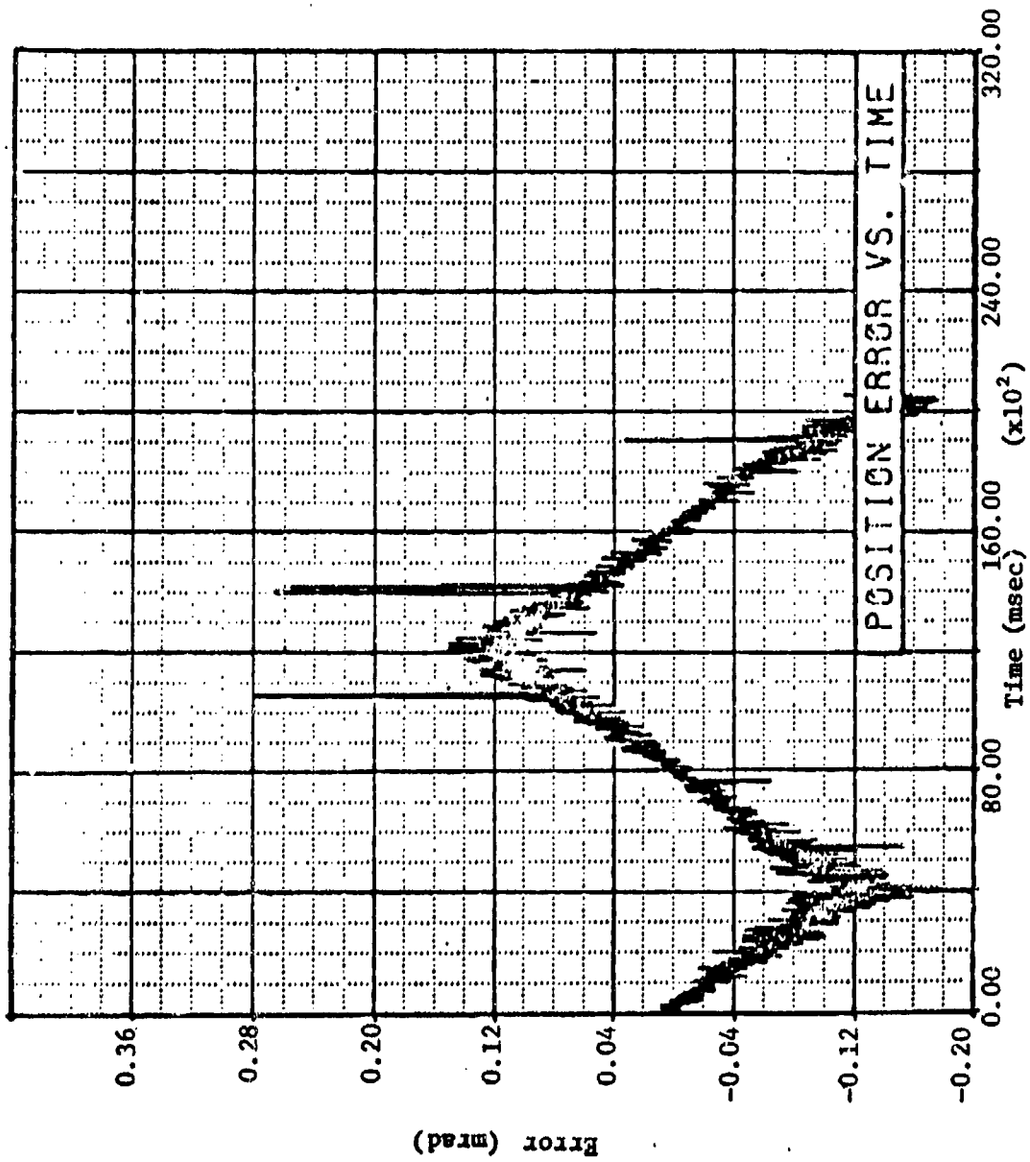

Figure 13. Error for Mocaic Tracker; Irr. = 0.396, Contr. = -100.0%, Vel. = 5.24, F.R. = 46; Run #2034. (CALIBRATION FACTOR ADJUSTED)

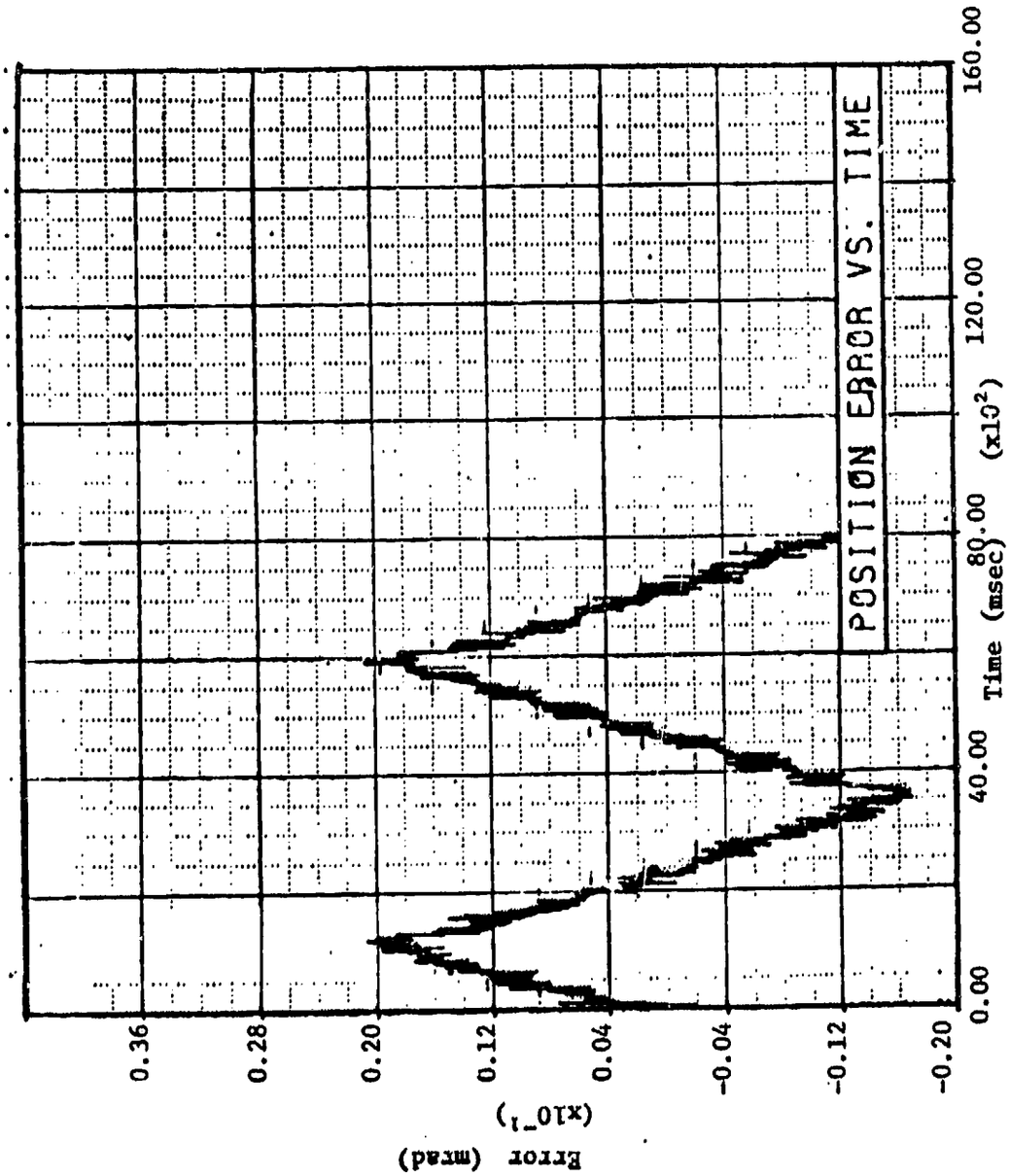

Figure 14. Error for Correlation Tracker; Irr. = 0.0413, Contr. = -69.3%, Vel. = 5.43, F.R. = 1191; Run #3031.

CHAPTER IV

RESULTS OF PARAMETER STUDY

The sources of the tracker test and analysis are a statistical data reduction program written for the available Univac 1106 Multiprocessor facility and ZOTS data from the laboratory evaluation of the five solid state imaging arrays. Some of the latter is available from previous reports and repeated on the local facility for comparison purposes. The minimum and maximum values of E_s are used to determine if loss of track occurs in each run. Loss of track is defined to have occurred when an extreme value of E_s is significantly greater than one-half the appropriate x or y dimension of the target image on the sensor. Since the trackers have no provisions for reacquisition of the target, such occurrences are also defined as loss of track.

The data shown in Tables 3 through 7 provide an analysis of tracker accuracy of the five trackers as a function of irradiance of the tracker lens. These data are used to determine the irradiance range over which each tracker can successfully track. The upper irradiance level is chosen safely below the level necessary to saturate the sensor or cause blooming. The lowest reported irradiance level is defined as the lower limit, which is immediately above the non-tracking level. x and y motion refer to independent target motion along that respective axis. The quantity Δ is the difference E_s and σ is the standard deviation, both of which are averaged over all runs of a particular test series, expressed in milliradians.

Table 3. Tracking Accuracy Versus Irradiance, Tracker No. 1.

Error in Milliradians

Irradiance	x Motion		y Motion		Diagonal Motion			
μ Watt/cm^2	Δ	σ	Δ	σ	Δ(x)	σ(x)	Δ(y)	σ(y)
2.57[a]	-0.028	0.334	-0.006	0.237	0.077	0.347	-0.091	0.260
1.48[a]	-0.046	0.308	0.308	0.268	0.073	0.351	-0.034	0.262
0.725[a]	0.050	0.347	0.046	0.263	0.164[c]	0.343	-0.013[c]	0.240
0.312[a]	0.077[c]	0.344	-0.018	0.265	0.233	0.355	-0.007	0.263
0.260[a]	0.094	0.425	-0.087	0.283	_[d]	_[d]	_[d]	_[d]
0.603[b]	0.047	0.260	-0.049[c]	0.229	0.027	0.245	0.043	0.253
0.157[b]	0.040	0.255	0.023[c]	0.230	0.105	0.260	-0.034	0.252
0.075[b]	_[d]		-0.073[e]	0.223	0.194[d,f]	0.279	-0.082[d,f]	0.236
0.048[b]	_[d]		-0.074	0.247	0.296[d,g]	0.306	0.056[d,g]	0.276
0.033[b]	-	-	0.024[h]	0.256	-	-	-	-

Notes:
- a Tracker frame rate 92.6 frames/sec, contrasts 56.1 to 81.7% with mean 70.0%, target velocities: x = y = 13.2 mrad/sec, diagonal = 18.7 mrad/sec.
- b Tracker frame rate 23.1 frames/sec, contrasts 64.8 to 84.7% with mean 76.1%, target velocities: x = y = 3.2 mrad/sec, diagonal = 4.5 mrad/sec.
- c Lost track 10% of runs
- d Lost track all runs
- e Lost track 22% of runs
- f Automatic gain control defeated, lost track 33% of runs
- g Automatic gain control defeated, lost track 16.7% of runs
- h Automatic gain control defeated

Table 4. Tracking Accuracy Versus Irradiance, Tracker No. 2.

Error in Milliradians

Irradiance	x Motion		y Motion		Diagonal Motion			
μ Watt/cm^2	Δ	σ	Δ	σ	Δ(x)	σ(x)	Δ(x)	σ(x)
1.94	-0.099	0.514	-0.288	0.309	-0.103	0.510	-0.286	0.312
1.06	0.198	0.742	-0.580	0.548	0.177	0.692	-0.529	0.563
0.396	-0.099	0.842	-0.595	0.657	-0.030	0.907	-0.680	0.803
0.275	-0.199	0.939	-0.595	0.644	-0.124	1.078	-0.628	0.797
0.165	0.260	5.604	-0.851	2.223	0.384	3.830	-0.956	3.192

Notes: Tracker frame rate, 46 frames/sec

Contrast 70.2 to 100%, Mean 88.9%

Target Velocities: x motion = y motion = 5.2 mrad/sec

Diagonal motion = 7.4 mrad/sec

Table 5. Tracking Accuracy Versus Irradiance, Tracker No. 3.

Irradiance	Error in Milliradians							
	x Motion		y Motion		Diagonal Motion			
μ Watt/cm^2	Δ	σ	Δ	σ	Δ(x)	σ(x)	Δ(x)	σ(x)
0.278	-0.094	0.323	-0.009	0.129	-0.105	0.287	-0.076	0.117
0.0835	-0.018	0.311	-0.044	0.131	0.030	0.285	-0.075	0.124
0.0413	0.070	0.310	-0.034	0.128	-0.027	0.290	-0.057	0.131
0.0253	0.068	0.302	-0.056	0.129	-0.054	0.274	-0.080	0.140
0.0149	0.130	0.344	-0.094	0.155	-0.055	0.286	-0.100	0.177

Notes: Tracker frame rate, 119 frames/sec
Contrast 69.3 to 86.3%, mean 78.9%
Target Velocities: x motion = y motion = 6.4 mrad/sec
Diagonal motion = 9.1 mrad/sec

Table 6. Tracking Accuracy Versus Irradiance, Tracker No. 4.

Error in Milliradians

Irradiance	x Motion		y Motion		Diagonal Motion			
μ Watt/cm^2	Δ	σ	Δ	σ	Δ(x)	σ(y)	Δ(x)	σ(y)
0.211	-0.032	0.176	0.097	0.145	0.030	0.225	0.098	0.157
0.103	-0.078	0.193	0.082	0.141	-0.072	0.226	0.087	0.155
0.0483	-0.155	0.197	-0.019	0.136	-0.130	0.243	-0.014	0.166
0.0208	-0.021	0.191	-0.030	0.162	-0.013	0.235	-0.023	0.203
0.0081	-0.207[a]	0.214	0.095	0.175	-0.205[b]	0.228	0.039[b]	0.289
0.0070	-0.228	0.208	0.057[c]	0.171	-0.157[d]	0.221	0.082[d]	0.368
0.0070[e]	-	-	0.051	0.191	-0.146	0.228	0.012	0.181
0.0045[e]	-0.222	0.208	0.044	0.205	-0.237	0.223	0.003	0.219

Notes: Tracker frame rate, 124 frames/sec

Contrast 71.8 to 80.2%, mean 76.4%

Target Velocities: x motion = 6 motion = 8.6 mrad/sec
Diagonal Motion = 12.1 mrad/sec

a Lost track 20% of runs
b Lost track 40% of runs
c Lost track 66.7% of runs
d Lost track 75% of runs
e Adaptive gate disabled

Table 7. Tracking Accuracy Versus Irradiance, Tracker No. 5.

Error in Milliradians

Irradiance	x Motion		y Motion		Diagonal Motion			
μ Watt/cm^2	Δ	σ	Δ	σ	Δ(x)	σ(x)	Δ(x)	σ(x)
0.30	-0.120	0.468	-0.015	0.162	-0.175	0.477	0.020	0.342
0.11	0.043	0.609	-0.028	0.290	0.012	0.508	-0.002	0.340
0.026	-0.158[a]	0.631	0.099[b]	0.194	-0.364	0.550	-0.021[c]	0.332

Notes: Tracker frame rate, 30 frames/sec

Target Velocities: x motion 3.48 mrad/sec

y motion 2.00 mrad/sec

Diagonal Motion 4.01 mrad/sec

Contrast 78.9 to 99.1% with mean 90.6%

a Lost track 40% of runs
b Lost track 20 of runs
c Lost track 60% of runs

Tracking accuracies as a function of contrast are shown in Tables 8 through 12. The contrasts used are defined in the following manner.

$$C = 100\left[\frac{L_T - L_B}{L_B}\right] \tag{13}$$

where C is the contrast in percent, L is the measured luminance in foot-lamberts, and subscripts T and B refer to target and background respectively.

This test determines the lowest possible photometric contrast at which each tracker could successfully track.

Tables 13 through 20 present tracking accuracies as a function of target rate with both irradiance and target contrast variable. The purpose of this test is to determine the maximum tracking rate capability of each of the trackers at the extreme limits of the irradiance and contrast tests. The initial target velocity in array cells/second is approximately 60% of the tracker frame rate. At each irradiance or contrast level, the target rate is increased until either the tracker ceases to track or the ZOTS limit is reached. Rate tests are performed in x, y, and diagonal axes when unrestricted by ZOTS nonuniformity or test time limitations.

The five trackers prove to be very accurate, reliable and to have wide dynamic ranges in both irradiance and target contrast. These capabilities are presented in Table 21. The irradiance capabilities are expressed as the dynamic ranges of successful operation; since absolute limits may be modified by changes in tracker optics

Table 8. Tracking Accuracy Versus Contrast, Tracker No. 1.

Error in Milliradians

Contrast	x Motion		y Motion		Diagonal Motion			
%	Δ	σ	Δ	σ	Δ(x)	σ(x)	Δ(y)	σ(y)
56.1[a]	-0.028	0.334	-0.006	0.237	0.077	0.347	-0.091	0.260
39.0[a]	-0.045	0.339	-0.122	0.285	0.022	0.342	0.003	0.265
12.2[a]	0.032[c]	0.321	-0.132	0.280	0.157	0.331	0.025	0.270
1.5[a]	0.056	0.348	0.023	0.272	0.097	0.338	-0.011	0.255
-0.5[a]	0.116[d]	0.338	-0.016[c]	0.275	0.094[e]	0.351	-0.003[e]	0.267
64.8[b]	0.047	0.260	0.049	0.230	0.027	0.245	0.043	0.253
6.5[b]	0.034	0.258	-0.102[f]	0.227	0.006	0.247	-0.042	0.231
2.1[b]	0.081	0.271	-0.008	0.235	0.144[g]	0.261	0.004	0.256

Notes:
a Tracker frame rate 92.6 frames/sec, irradiances 0.968 - 2.70 μw/cm^2, mean 1.75 μw/cm^2, Target Velocities: x = y = 13.2 mrad/sec, diagonal = 18.7 mrad/sec

b Tracker frame rate 23.1 frames/sec, 0.337 - 0.603 μwatt/cm^2, mean 0.437 μwatt/cm^2, Target Velocities: x = y = 3.2 mrad/sec, diagonal = 4.5 mrad/sec

c Lost track 10% of runs

d Lost track 90% of runs

e Lost track 50% of runs

f Lost track 14% of runs

g Lost track 11% of runs

Table 9. Tracking Accuracy Versus Contrast, Tracker No. 2.

Error in Milliradians

Contrast	x Motion		y Motion		Diagonal Motion			
%	Δ	σ	Δ	σ	Δ(x)	σ(x)	Δ(y)	σ(y)
70.2	-0.099	0.514	-0.288	0.309	-0.103	0.510	-0.286	0.312
20.3	-0.158	1.013	-0.356	0.760	-0.198	1.023	-0.508	0.966
12.2	-0.261	1.300	-0.413	1.280	-0.286	1.401	0.591	1.357

Notes: Tracker frame rate, 46 frames/sec

Irradiance 1.33 - 1.94, mean 1.62 $\mu watt/cm^2$

Target Velocities: x motion = y motion = 5.2 mrad/sec

Diagonal Motion = 7.4 mrad/sec

Table 10. Tracking Accuracy Versus Contrast, Tracker No. 3

Error in Milliradians

Contrast	x Motion		y Motion		Diagonal Motion			
%	Δ	σ	Δ	σ	Δ(x)	σ(x)	Δ(y)	σ(y)
79.1	-0.094	0.323	-0.009	0.129	-0.105	0.287	-0.076	0.117
39.2	-0.100	0.299	-0.054	0.127	0.050	0.286	-0.126	0.123
12.9	0.169	0.309	-0.066	0.129	0.084	0.296	-0.087	0.119
10.9	0.090	0.303	-0.025	0.131	0.022	0.291	-0.074	0.130
2.1	0.076	0.317	-0.087	0.161	-0.045	0.291	-0.114	0.163
0.9	0.204	0.365	0.105[a]	0.159	0.179[b]	0.349	0.247[b]	0.217
<0.5[c]	0.161[b]	0.326	0.039	0.192	0.114	0.346	0.062	0.227

Notes: Tracker frame rate, 119 frames/sec

Irradiance = 0.28 μwatt/cm^2

Target Velocities: x motion = y motion = 6.4 mrad/sec

Diagonal motion = 9.1 mrad/sec

a Lost track 40% of runs

b Lost track 20% of runs

c Automatic range closure function inhibited, irradiance = 0.457 μwatt/cm^2

Table 11. Tracking Accuracy Versus Contrast, Tracker No. 4.

Error in Milliradians

Contrast %	x Motion		y Motion		Diagonal Motion			
	Δ	σ	Δ	σ	Δ(x)	σ(x)	Δ(y)	σ(y)
71.8	-0.032	0.176	0.097	0.145	0.030	0.225	0.098	0.157
23.7	-0.133	0.202	0.091	0.122	-0.150	0.241	0.064	0.159
10.9	-0.053	0.193	0.050	0.148	-0.080	0.214	0.024	0.157
3.6	-0.129[a]	0.212	0.066	0.136	-0.151	0.214	0.011	0.170
2.1	-0.394	0.180	-0.013[b]	0.212	-0.149[c,d]	0.224[c,d]	-0.133[c,d]	0.193[c,d]
~0[d]	-0.315	0.217	-0.068	0.239	0.150[e]	0.211	-0.174[e]	0.367

Notes: Tracker frame rate, 124 frames/sec

Irradiance = 0.21 μwatt/cm^2

Target Velocities: x motion = y motion = 8.6 mrad/sec

Diagonal Motion = 12.1 mrad/sec

a Lost track 10% of runs
b Lost track 20% of runs
c Lost track all runs in normal mode
d Adaptive gate disabled
e Lost track 66.7% of runs

Table 12. Tracking Accuracy Versus Contrast, Tracker No. 5.

Error in Milliradians

Contrast	x Motion		y Motion		Diagonal Motion			
%	Δ	σ	Δ	σ	Δ(x)	σ(x)	Δ(y)	σ(y)
99.1	-0.120	0.468	-0.015	0.162	-0.175	0.477	0.020	0.342
11.7	0.242	0.495	0.101	0.134	-	-	-	-
11.7	0.211[a]	0.535	0.018[b]	0.129	-	-	-	-
1.7	0.509[c]	0.533	0.024[d]	0.176	-	-	-	-

Notes: Tracker frame rate, 30 frames/sec

Target Velocities: x motion 3.48 mrad/sec

y motion 2.00 mrad/sec

Diagonal motion 4.01 mrad/sec

Irradiances 2.7 - 3.4 $\mu w/cm^2$ with mean 3.1 $\mu w/cm^2$

a Target Velocity 0.58 mrad/sec
b Target Velocity 0.34 mrad/sec
c Lost track 33% of runs
d Lost track 60% of runs

Table 13. Tracking Accuracy Versus Target Rate, Tracker No. 1.

Error in Milliradians

Irradiance	Contrast	10.7 mrad/sec		12.4 mrad/sec		14.4 mrad/sec	
μWatt/cm^2	%	Δ	σ	Δ	σ	Δ	σ
0.562	78.3	0.057	0.279	0.094	0.290	0.059	0.302
0.081	88.3	-0.076	0.287	0.023	0.295	-0.020	0.311
0.028	83.3	0.221[a]	0.326	-[b]		-[b]	
0.154	15.1	-0.027[c]	0.312	-0.040[d]	0.329	-0.074[e,f]	0.342
0.153	5.9	-0.068[c]	0.280	-0.108[d]	0.301	-0.086[e]	0.312

Notes: Tracker frame rate 23.1 frames/sec

Target motion in y axis

Lost track all runs at 15.4 mrad/sec

a Lost track 80% of runs
b Lost track all runs
c Target velocity 10.2 mrad/sec
d Target velocity 11.7 mrad/sec
e Target velocity 13.7 mrad/sec
f Lost track 33% of runs

Table 14. Tracking Accuracy Versus Target Rate, Tracker No. 2.

Error in Milliradians

Irradiance	Contrast	16.4 mrad/sec		32.8 mrad/sec		54.1 mrad/sec	
μWatt/cm^2	%	Δ	σ	Δ	σ	Δ	σ
1.01	79.6	-0.645	0.591	-0.575	0.673	-0.547[a]	0.599[a]
0.233	81.8	-0.661	1.764	-0.734	3.945	-0.813	3.814
0.220	78.9	-0.550	1.511	-0.441	1.379	-0.441	1.538
1.75	12.2	-0.794	1.521	-0.731	1.593	-0.916	2.117
1.61	11.5	-0.820	0.990	-0.686	1.077	-0.690	1.191
2.00[b]	55.2	0.055	0.758	0.032	1.013	0.144	0.573
0.600[b]	64.8	0.216	1.902	0.213	3.247	0.012	2.076
2.46[b]	23.5	0.214	1.236	0.248	1.004	-0.366	4.124

Notes: Target motion in y axis

Tracker frame rate, 46 frames/sec

a Target velocity 45.8 mrad/sec
b Tracker frame rate of 63 frames/sec

Table 15. Tracking Accuracy Versus x-Axis Target Rate, Tracker 3.

Error in Milliradians

Irradiance	Contrast	16.1 mrad/sec		24.1 mrad/sec		32.1 mrad/sec	
μWatt/cm^2	%	Δ	σ	Δ	σ	Δ	σ
0.277	79.1	-	-	0.088	0.399	0.032	0.487
0.0254	85.6	0.130	0.363	0.167	0.391	0.061	0.457
0.0150	86.2	0.067	0.401	0.019	0.423	-	-
0.276	9.8	0.044	0.360	0.165	0.406	-	-
0.277	2.1	0.039	0.401	0.031	0.478	-	-
0.0298[a]	1.0	0.228[b]	0.470				

Notes: Tracker frame rate, 119 frame/sec

a Tracker frame rate of 20 frames/sec, target velocity 6.4 mrad/sec
b Lost track 40% of runs

Table 16. Tracking Accuracy Versus y-Axis Target Rate, Tracker No. 3

Error in Milliradians

Irradiance	Contrast	16.1 mrad/sec		24.1 mrad/sec		36.1 mrad/sec	
μWatt/cm^2	%	Δ	σ	Δ	σ	Δ	σ
0.277	79.1	-	-	0.064	0.197	0.070	0.307
0.0254	85.6	0.047	0.153	0.039	0.196	0.239[a]	0.339
0.0150	86.2	0.193	0.216	0.209[b]	0.256	0.124[c,d]	0.241[c,d]
0.276	9.8	0.063	0.154	0.063	0.201	-0.084	0.342
0.277	2.1	0.231	0.273	0.163[a]	0.284	-[c]	-[c]
0.0298[e]	1.0	0.079[f]	0.146	0.075[g]	0.489		

Notes: Tracker frame rate, 119 frames/sec

a Lost track 20% of runs
b Lost track 40% of runs
c Lost track all runs
d Automatic range closure function inhibited, tracked all runs in this mode
e Tracker frame rate of 20 frames/sec
f Target velocity 1.1 mrad/sec
g Target velocity 6.4 mrad/sec, lost track 80% of runs

Table 17. Tracking Accuracy Versus Diagonal Target Rate, Tracker No. 3

Error in Milliradians

Irradiance	Contrast	22.7 mrad/sec		34.1 mrad/sec		51.1 mrad/sec	
μWatt/cm^2	%	Δ	σ	Δ	σ	Δ	σ
				x - Component			
0.277	79.1	-	-	-0.228	0.443	-0.041[c]	0.579
0.0254	85.6	0.093	0.329	0.128	0.439	0.135	0.503
0.0150	86.2	0.132	0.360	-[a]	-[a]	-0.072[b]	0.399[b]
0.276	9.8	0.090	0.347	0.114	0.439	-0.157[d]	0.460
0.277	2.1	-0.201[c]	0.422	-[a]	-[a]	-0.055[b]	0.431[b]
0.0298[e]	1.0	0.031	0.237				
				y-Component			
0.277	79.1	-	-	0.330	0.236	0.373[c]	0.612
0.0254	85.6	0.054	0.156	0.159	0.222	0.049	0.531
0.0150	86.2	0.339	0.224	-[a]	-[a]	0.134[b]	0.211[b]
0.276	9.8	0.102	0.165	0.160	0.250	0.143[d]	0.436
0.277	2.1	0.400[c]	0.334	-[a]	-[a]	0.032[b]	0.209[b]
0.0298[e]	1.0	0.009	0.236				

Notes: Tracker frame rate, 119 frames/sec

a Lost track all runs

b Automatic range closure function inhibited, tracked all runs in this mode

c Lost track 20% of runs

d Lost track 60% of runs

e Tracker frame rate of 20 frames/sec, target velocity of 1.5 mrad/sec, lost track all runs at 9.1 mrad/sec

Table 18. Tracking Accuracy Versus x-Axis Target Rate, Tracker No. 4

Error in Milliradians

Irradiance	Contrast	16.1 mrad /sec		28.9 mrad/sec		38.6 mrad/sec	
μWatt/cm^2	%	Δ	σ	Δ	σ	Δ	σ
0.211	77.4	0.222	0.362	-	-	0.216	0.382
0.0278	82.1	0.018	0.339	0.009	0.408	0.004	0.368
0.0075	78.5	0.024	0.356	0.027	0.389	0.066	0.305
0.0055[a]	80.2	0.081	0.337	0.103	0.347	0.052[b]	0.256
0.211	3.5	-0.274	0.350	-0.293	0.410	-0.306	0.359
0.214	2.2	-0.363	0.358	-0.298	0.399	-0.318	0.346
0.218[a]	0.04	-0.297	0.289	-0.333[b]	0.313	-	-

Notes: Tracker frame rate, 124 frames/sec

a Adaptive gate disabled
b Lost track 60% of runs

Table 19. Tracking Accuracy Versus y-axis Target Rate, Tracker No. 4

Error in Milliradians

Irradiance μWatt/cm^2	Contrast %	16.1 mrad/sec Δ	16.1 mrad/sec σ	28.9 mrad/sec Δ	28.9 mrad/sec σ
0.211	77.4	0.046	0.158	0.032	0.211
0.0278	82.1	0.071	0.167	0.187	0.191
0.0075	78.5	0.155	0.171	0.134	0.207
0.0055[a]	80.2	0.120	0.236	0.103	0.324
0.211	3.5	0.101	0.177	0.072	0.203
0.214	2.2	-0.089	0.208	-0.063	0.201
0.218[a]	0.04	0.043	0.164	0.066	0.214

Notes: Tracker frame rate, 124 frames/sec

a Adaptive gate disabled

Table 20. Tracking Accuracy Versus Target Rate, Tracker No. 5

Error in Milliradians

Irradiance μWatt/cm^2	Contrast %	Velocity mrad/sec	Δ mrad	σ mrad
0.096	92.4	14.9	0.233	0.485
0.096	92.4	15.7	0.288	0.464
0.096	92.4	16.1	0.235[a]	0.647
0.069	70.5	3.48	0.012	0.537
0.069	70.5	6.97	0.188[b]	0.488
1.7	4.6	4.65[c]	0.258	0.519

Notes: Tracker frame rate, 30 frames/sec

Target motion in x-axis

a Lost track 40% of runs, would not track at 16.6 mrad/sec
b Lost track 20% of runs, would not track at greater target velocities
c Would not track at 5.23 mrad/sec

Table 21. Array Tracker Capabilities

Tracker No.	Frame Rate (f/sec)	Irradiance Range (I_{max}/I_{min})	Min Contrast %	Max Target Rate mrad/sec
1	92.6	10	1.5	-
2	46	12	12.2	>54
3	119	19	2.1	>36
4	124	26	3.6	>39
5	30	11	>1.7	16.1

and/or frame rate. The maximum target rate for trackers 2, 3, and 4 are not determined due to rate limitations of the ZOTS.

One major advantage of Tracker Number 1 is that it requires no adjustments throughout the complete series of tests at a given frame rate. Trackers Number 3 and 4 require adjustments for the conversion from a high-irradiance range to a low-irradiance range. Trackers Number 2 and 5 require adjustments for each parametric change of irradiance or contrast.

The tracking accuracy of a particular tracker (except Tracker Number 2) is essentially independent of irradiance until the marginal level is approached. The tracking accuracy is usually degraded by 10 - 20% at the marginal level. Tracker Number 2 is the only tracker exhibiting greater errors than 0.36 milliradians or greater standard deviation than 0.63 milliradians under all irradiance conditions. The accuracies of Tracker Number 2 are much lower and decrease with irradiance level.

The tracking accuracy of the trackers (excepting Tracker Number 2) are less than 0.51 milliradians with standard deviations of less than 0.54 milliradians for all contrasts. The accuracy is again essentially independent of target contrast for contrasts above the level at which the tracker ceases to operate. Tracker Number 2 is much lower and decreases with target contrast.

Target rate effects were different for each of the trackers. The only trackers showing independence to target rates are Trackers Number 2 and 5, Trackers Number 1 and 3 showing linear increases in error with target rate. Tracker Number 4 shows a linear increase

in error in the y direction, but the x-axis error approximately doubles between the rates of 8.6 and 16.1 mrad/sec. The x-direction error remains essentially constant for higher velocities. The maximum target rate capabilities of Trackers Number 1 and 5 are 0.93 times the theoretical value of one cell/frame, except for the tests at the marginal irradiance and contrast limits, where it drops to 0.40 and 0.27 times the design rate limit, respectively.

Data from Tracker Number 1 indicate the tracking accuracy at a frame rate of 92.6 is essentially five times that at 23.1. Trackers Number 2 and 3 demonstrate no significant differences at different frame rates. Lower target velocities account for the increase in accuracy at the lower frame rate of Tracker Number 1.

At higher target velocities the tracker tracks the target but lags behind. When the lag accumulates to the degree where the target leads by more than one cell, the target is lost.

Array response has some degree of nonuniformity. This nonuniformity contributes to tracker failure at marginal conditions of irradiance and contrast. The array used in Tracker Number 1 has a column of "hot" cells and the array of both Trackers Number 3 and 4 have several irregularly shaped areas of non-uniform cells. Under extremely low irradiance or contrast conditions, the target is lost if its image passes over these areas. An operational tracker is limited by such nonuniformities.

The five trackers using the solid state arrays are extremely reliable. No failure of any of the tracker's electronics or

detectors under several hundred hours of testing exhibits promising performance.

Two of the trackers previously discussed use a 100 x 100 CCD array (Martin Marietta). With the recent developments in MOS technology, it seems apparent that the charge coupled concept will gradually play a more dominant role in the imagery technology.

The parameters which seem to be sensor oriented rather than algorithm oriented are contrasts and transfer time, or transfer efficiency. The latter affects the frame or scan rate and thus the maximum target velocity. The dependence of a tracker on these parameters depends on what type of tracker is employed and what type of target recognition scheme is used.

Several systems are available utilizing acquisition and tracking algorithms, providing reliable tracking of missile plumes. Here the missile plume is assumed to have a positive contrast ratio with respect to the background. However, many cases do not offer such conveniences. It is desirable to track the target pattern itself, such as missile body tracking, aircraft tracking, or projectile tracking. If a system is available capable of such a task, then the possibility of real-time data reduction can be considered. The parameters influencing sensor behavior or response evidently control the upper limit on tracker efficiency.

A very good idea of how these parameters influence device behavior, is obtained through investigation of the modulation transfer function. This modulation transfer function describes the

response of the CCD to each parameter as a function of frequency. It is analogous to the frequency response of a network.

Also, aliasing occurs due to the discrete nature of the sensor elements. In other words, the imaging surface is not continuous but samples the image plane. Thus, the spatial frequency response beyond the sampling limit, or Nyquist limit, is a design consideration. This characteristic, however, is not as severe as has been supposed. If it proves to be a problem, it can be removed by prefiltering or defocussing the image to render the edges and lines continuous. This also tends to blur the image and reduce edge contrast by spreading the energy of the scene elements to adjacent areas.

If the sensor is to be used to detect subresolution sized objects, such as point images of stellar objects, it is a definite disadvantage to have unresponsive intensities in the image plane. It is preferable then to have the sensors contiguous, or for the scene to be prefiltered to that degree. However, if sensitivity is the goal, prefiltering is not advised.[6]

The modulation transfer function (MTF) is the ratio of device output to input in a particular observation domain. In the frequency domain, the MTF relates the amplitude and phase of a sinusoidal output to the corresponding sinusoidal input signal. The argument gives the phase shift and the modulus gives the attenuation. Generally the normalization used is unity amplitude and zero argument at zero frequency. In the case of a linear system, the MTF is simply the Fourier transform of the impulse response function. In

the case of a sampled data system, such as a CCD, a single input frequency gives rise to several output frequencies. These additional signals are multiples and sidebands of all of the multiples of the sampling frequency. Because the additional output signals represent no additional information the MTF is calculated using the component of the output having the same frequency as the input. Hence the MTF becomes simply the frequency response of the system. Here, the Nyquist frequency becomes the spatial sampling limit.

The MTF is an excellent way of expressing the operational imaging characteristics of the CCD. The overall MTF of the chip is composed of three factors:

1. The loss of spatial frequency due to the geometry of the integrating cell (MTF_{integ})
2. The loss of frequency response due to transfer inefficiency ($MTF_{transfer}$)
3. The loss of frequency response due to the diffusion of charge between photon absorption and photoelectron collection (MTF_{diff}).

1. MTF_{integ}:

The integration MTF is given by the Fourier transform of the basic integration cell. For a rectangular cell of length Δx repeated with periodicity p, i.e., p is cell to cell spacing; the MTF is

$$MTF_{integ} = \frac{\sin\left(\frac{f}{f_N}\,\frac{w\Delta x}{p}\right)}{\frac{f}{f_N}\,\frac{w\Delta x}{p}} \qquad (14)$$

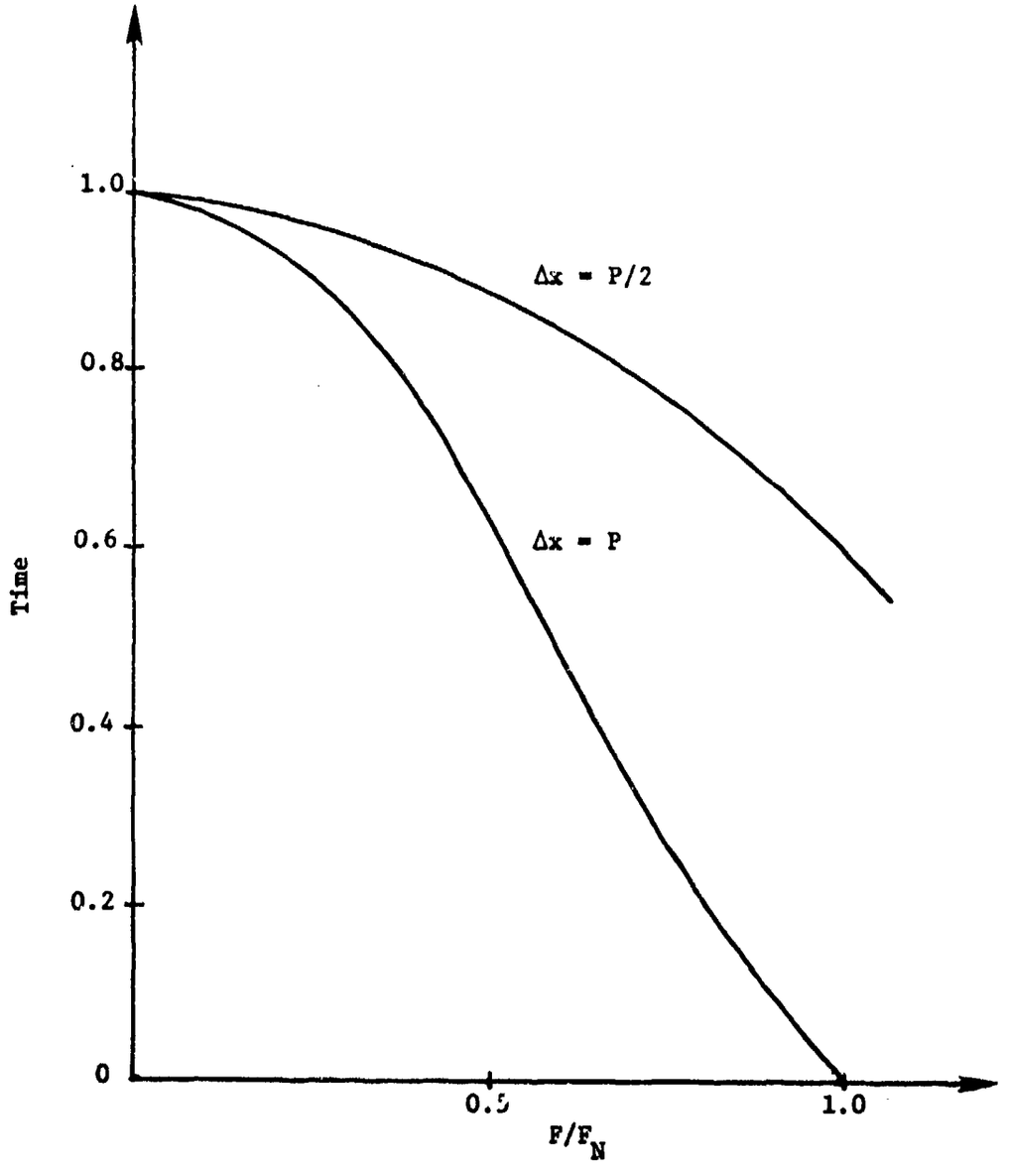

Figure 15. MTF_{integ} Versus Normalized Spatial Frequency.

where f_N is the Nyquist frequency. For $\Delta x = p$, the first zero occurs at $f = f_N = 1/p$. For $\Delta x = p/2$, the first zero occurs at $f_N = 2/p$. Figure 15 gives the integration MTF versus normalized spatial frequency. For the backside illuminated frame transfer (BIFT) device, $\Delta x = \Delta y = p$, and for frontside illuminated interline transfer (FIIT) devices, $\Delta x = \Delta y = p/2$.

2. $MTF_{transfer}$

During the transfer of a sampled sinusoidal signal along a CCD shift register, a fraction of the charge ε is lost from each of the samples at each transfer, and this charge is added to trailing samples. The effect of this dispersion on MTF is given by

$$MTF_{transfer} = \exp\left\{-\eta\varepsilon\left[1 - \cos\left(\pi \frac{f}{f_N}\right)\right]\right\} \qquad (15)$$

where η is the number of transfers.

Figure 16 shows the transfer MTF versus the normalized spatial frequency with the $\eta\varepsilon$ product as the parameter.

The number of transfers in the x direction is the same for both frame-transfer and interline-transfer arrays. Therefore, the horizontal MTF degradation due to transfer is the same for both arrays. The number of transfers in the y direction is greater for the frame-transfer chip by the amount PN_y, where P is the number of phases and N_y is the number of y-direction cells. Therefore, the vertical MTF for the frame-transfer chip is lower than that for the interline-transfer chip.

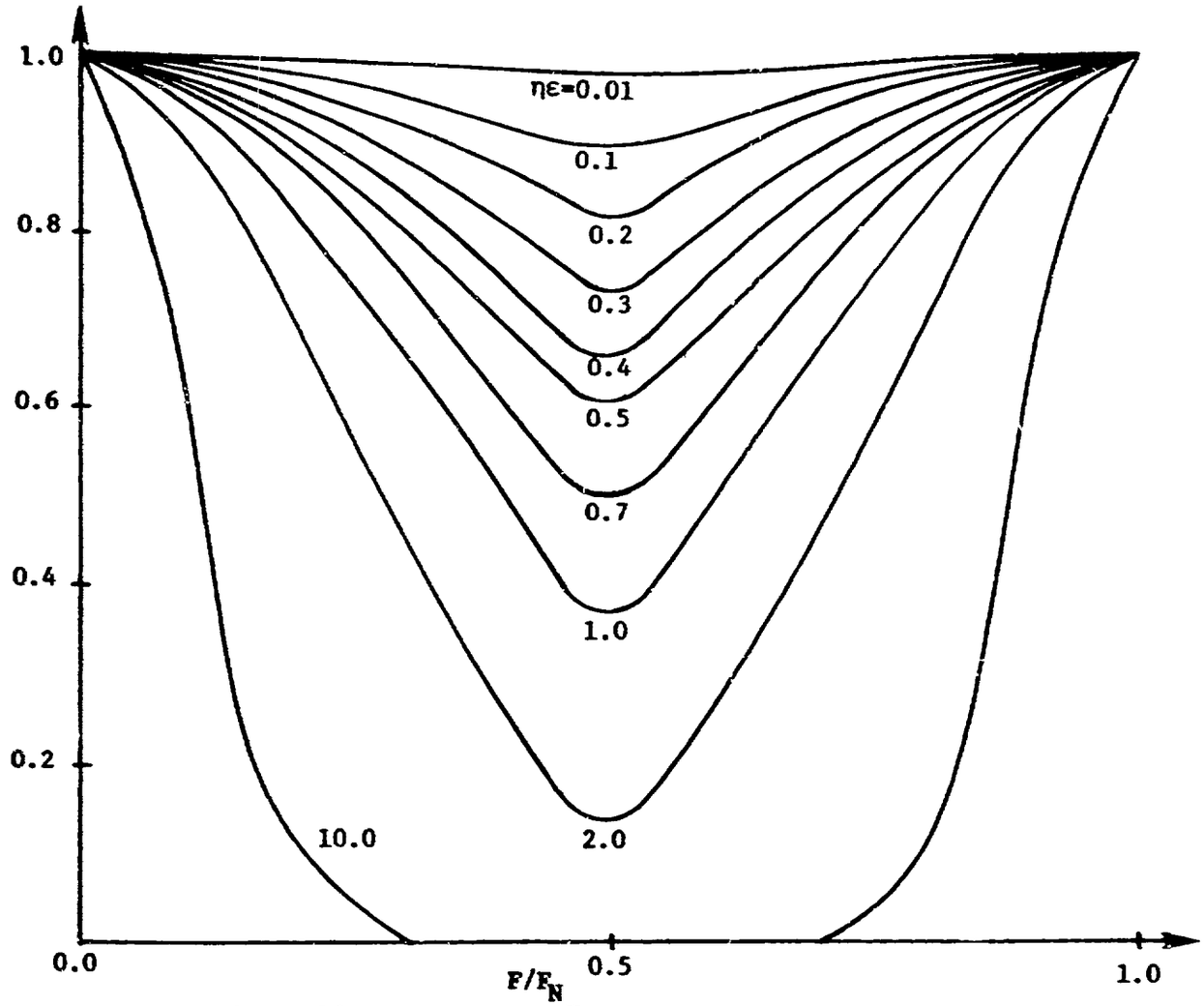

'gure 16. $MTF_{transfer}$ Versus Normalized Spatial Frequency.

3. MTF_{diff}

If photons are absorbed within the depletion regions, then the collection is assumed 100% efficient. However, if photons are absorbed away from the depletion regions, then the charge configuration will spread as it diffuses toward the depletion regions with a resulting decrease in MTF.

If photons are absorbed a distance d from the depletion region and if the diffusion length in the silicon is L_1, then the MTF due to the diffusion of charge is given by

$$MTF_{diff} = \frac{\cosh(d/L_1)}{\cosh(d/L)} \quad , \tag{16}$$

where $L^{-2} = L_1^{-2} + (2\pi f)$.

Figure 17 shows the diffusion MTF versus normalized spatial frequency with d as the parameter.

The responsivity of each photo element is a description of the efficiency of each cell in converting incident photons to the photo electrons eventually collected in the potential well beneath the sensor gate.

The photoelement responsivity is determined by the efficiency with which photons are absorbed and the resulting photoelectrons are collected. Basically four mechanisms act to reduce the photoelement responsivity ($R_{element}$) .

1. Reflection at layer interfaces before the photons reach the silicon.

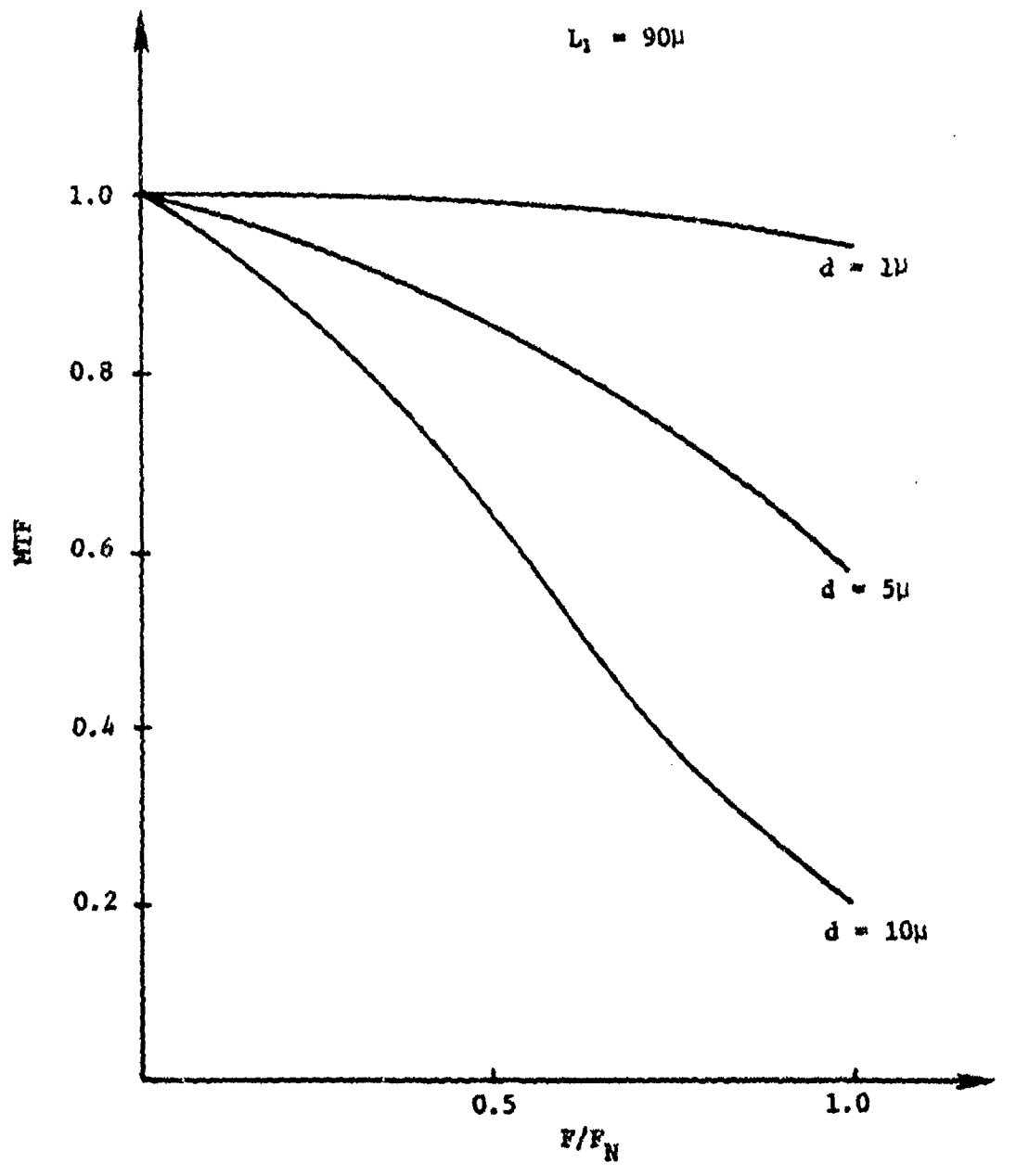

Figure 17. MTF_{diff} Versus Normalized Spatial Frequency.

2. Aborption in these layers before the photons reach the silicon.
3. Recombination at the Si-SiO_2 interface after hole-electron generation.
4. Absorption too far away from potential wells for the photoelectrons to be collected.

Mechanisms 2 and 3 cause a reduction in $R_{element}$ in the blue, mechanism 4 causes a reduction in $R_{element}$ in the infrared, and mechanism 1 causes interference fringes throughout the spectrum. Mechanism 1 is mainly responsible for $R_{element}$ being different for BIFT and FIIT structures.[6]

As previously mentioned, dark current is not completely uniform throughout a device. The dark current signature of a device is obtained by integrating in the dark. If the element-to-element nonuniformity is ΔN_d, then the minimum signal that can be detected will be limited to $N_s \simeq \Delta N_d$. If the element-to-element variation of ΔN_d is 10 percent, then at room temperature this will limit the minimum detectable signal to about 1000 electrons. The dark current is a strong function of temperature, decreasing by a factor of 2 every 10° C decrease in temperature.

Three-phase charge coupled devices with transfer efficiencies of 99.99% are available providing operating frequencies of up to 10 MHz. Since nonuniformities are characteristics of the manufacturing process, the parameter of the device itself in need of experimental investigation is this transfer efficiency as it is related to

image degradation, target acquisition, tracking and the overall MTF. In the discussion of the effects of transfer inefficiency on images, a single element with stored charge Q is observed. This charge is placed in a well (i = 0), then after N transfers, the distribution of charge in cells i = 0,1,2,... is given by

$$D(i,N) = \frac{Q_i}{Q} = \frac{N!}{(N-i)!i!} (1 - \alpha)^i \alpha^{N-i} \tag{17}$$

where α is the fractional loss incurred by the charge packet in moving from one cell to the next. The phenomenon is illustrated in Figure 18 for the first two transfers. The fractional loss from the charge packet after N cell transfers is given by 1 - D(N,N);

$$\text{loss} = 1 - (1 - \alpha)^N \tilde{=} N\alpha \qquad \text{for} \qquad N\alpha << 1 \tag{18}$$

The equation D(N,N) = D(N - 1,N) gives the value of N for which the first trailing packet and the leading packet have equal amounts of charge. This value is calculated in the following manner.

$$D(N,N) = \frac{N!}{(N-N)!N!} (1 - \alpha)^N \alpha^{N-N} \tag{19}$$

$$D(N,N) = \frac{N!}{N!} (1 - \alpha)^N \alpha^0 \tag{20}$$

$$D(N,N) = (1 - \alpha)^N \quad . \tag{21}$$

Likewise,

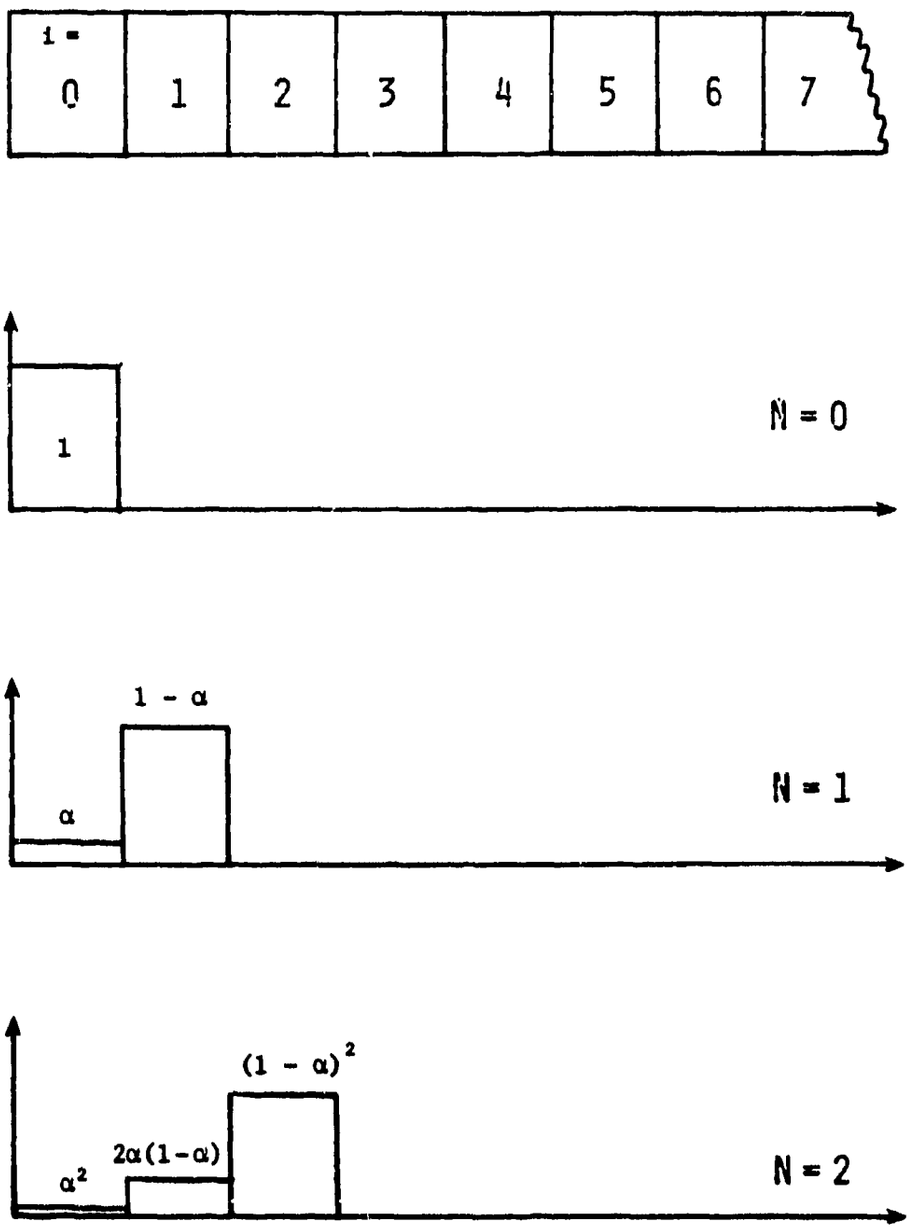

Figure 18. Representation of Charge Loss After Two Transfers.

$$D(N-1,N) = \frac{N!}{(N-N+1)!(N-1)!} (1-\alpha)^{N-1} \alpha^{N-N+1} \tag{22}$$

$$D(N-1,N) = \frac{N!}{(N-1)!} (1-\alpha)^{N-1} \alpha \tag{23}$$

$$D(N-1,N) = N(1-\alpha)^{N-1} \alpha \quad ; \tag{24}$$

thus,

$$D(N,N) = D(N-1,N) \Rightarrow (1-\alpha)^{N} = N(1-\alpha)^{N-1} \alpha \quad . \tag{25}$$

Therefore,

$$N\alpha = \frac{(1-\alpha)^{N}}{(1-\alpha)^{N-1}} \tag{26}$$

$$N\alpha = 1-\alpha \tag{27}$$

$$N = \frac{1-\alpha}{\alpha} \tag{28}$$

For

$$\alpha \ll 1 \quad , \quad N \cong 1/\alpha \quad . \tag{29}$$

Thus, for every $1/\alpha$ transfers, the peak of the charge distribution shifts back one cell, i. e., after $2/\alpha$ transfers, the second trailing packet contains the largest charge quantity. This constitutes a delay in addition to the delay time N/f_c required to clock a packet out of the CCD.[4]

This development is used to create a simulation of the CCD as used as an imager for tracking applications. The simulation is a

bit more complicated, however, since each cell has some charge stored in its depletion well. The concept is the same. In order to illustrate this concept, an image is placed on the 100 x 100 simulated array. The test pattern resembles that shown in Figure 19. Each cell has a sensitivity to 9 grey levels (this may be changed to achieve desired results), each level described in Table 22.

Table 22. Grey Level Response of CCD

Level	Voltage Range	Symbol
1	0.0 - 0.2	
2	0.2 - 0.3	.
3	0.3 - 0.4	+
4	0.4 - 0.5	*
5	0.5 - 0.6	&
6	0.6 - 0.7	X
7	0.7 - 0.8	#
8	0.8 - 0.9	$
9	0.9 - 999.9	■

The image is clocked from the array with any desired transfer efficiency or contrast ratio. With a transfer efficiency of 93% and the interline-transfer method used, the observed image becomes that of Figure 20. Note the degradation of the image as well as the delay encountered. This delay is not related to clock frequency

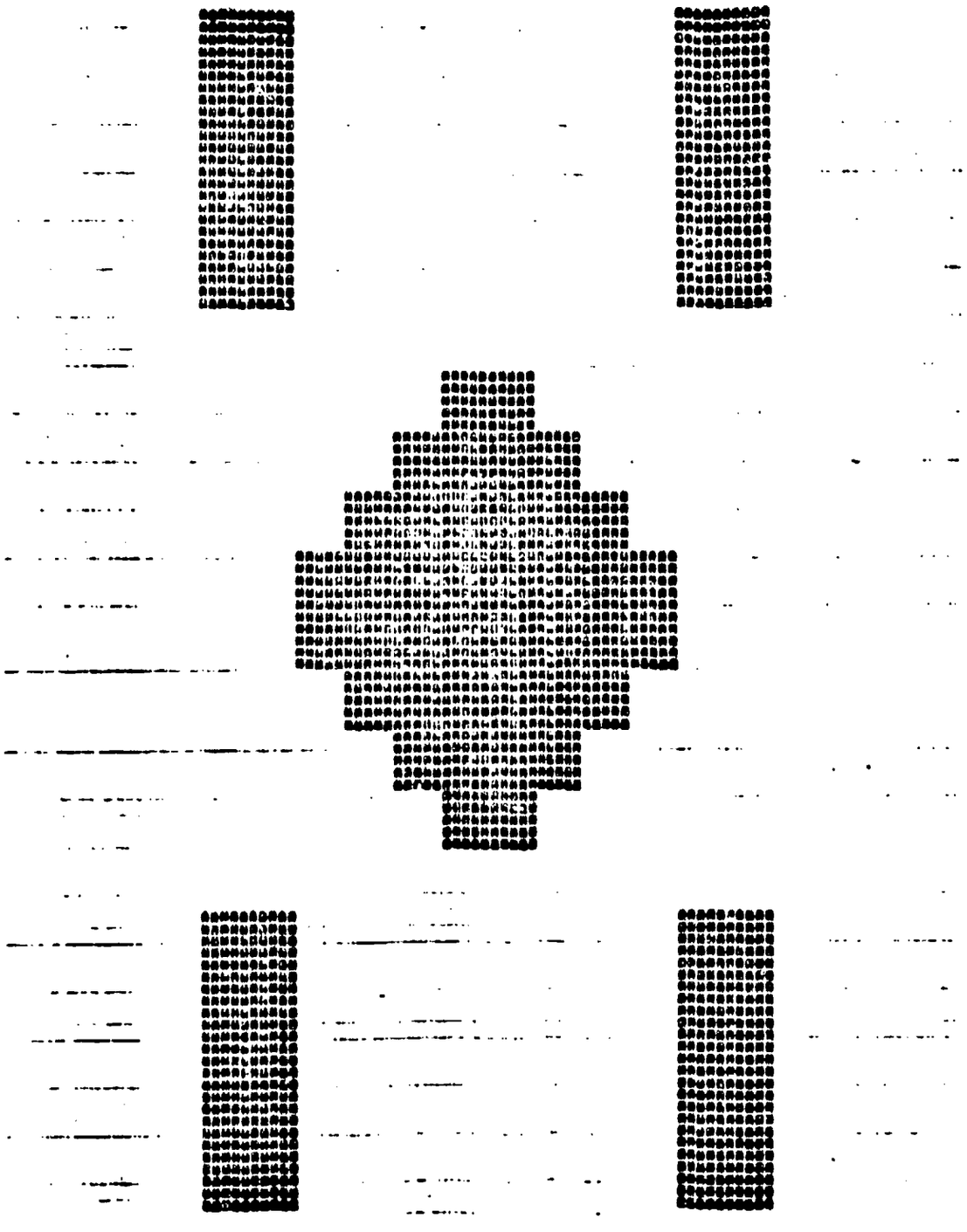

Figure 19. 100 x 100 CCD Array Test Pattern.

Figure 20. CCD Array after clocking at 93% transfer efficiency.

other than through the transfer efficiency. When pattern tracking, to maintain no delay due to charge distribution changes, the transfer efficiency must be well above 99% as illustrated by Figure 21. Of course, the position of the target on the sensor face does have some bearing on the target pattern degradation. The amount of degradation is directly proportional to the number of transfers necessary to remove the image scene from the sensor. The simulation removes the image by clocking the cells up and to the left. Therefore, the target is more easily found in the upper left-hand corner than the lower right-hand corner.

The determination of the minimum transfer efficiency for target recognition begins with the generation of a complicated background on which to view the target. The pseudo-random background of Figure 22 provides possibly worst-case results for pattern recognition. The output of the program using the target shown in Figure 23 is tabulated for evaluation in Table 23. The contrast ratio is set at 0 to once again provide worst-case results and to give an honest feel for pattern tracking rather than positive contrast tracking. The target pattern is positioned at x = 50, y = 50, resulting in approximately 100 transfers for each cell. The pattern cell tolerance is set at 0.09 volts, giving approximately one grey level of tolerance. The transfer efficiency must, therefore, be greater than 99.90% in order to maintain track under these conditions. This efficiency is of course dependent on several factors other than placement of the target on the image surface. The complexity of the target itself is an important factor. The grey

level tolerance of the pattern cell can be raised to provide tracking or acquisition at lower transfer efficiencies. However, the possibility of locating a "false" target increases with an increase in tolerance.

An estimation of the lowest transfer efficiency allowing acquisition of the target may be calculated for the above situation. Assuming no addition from preceding charge packets, tolerance of 0.09 volts and pattern location of $x = 50$, $y = 50$; the largest number of transfers is 108 and the value of that cell is 1 volt. Therefore,

$$(\eta)^N (V) = (V) - (tol) \quad , \tag{30}$$

where η is the transfer efficiency, N is the number of transfers, V is the value stored in the cell, and tol is the cell pattern tolerance. This gives

$$(\eta)^{108} (1) = 1 - (0.09)$$

$$\eta^{108} = 0.91$$

$$108 \ln \eta = \ln 0.91$$

$$\ln \eta = \frac{\ln 0.91}{108}$$

$$\ln \eta = -0.00087$$

or,

$$\eta = 0.99913$$

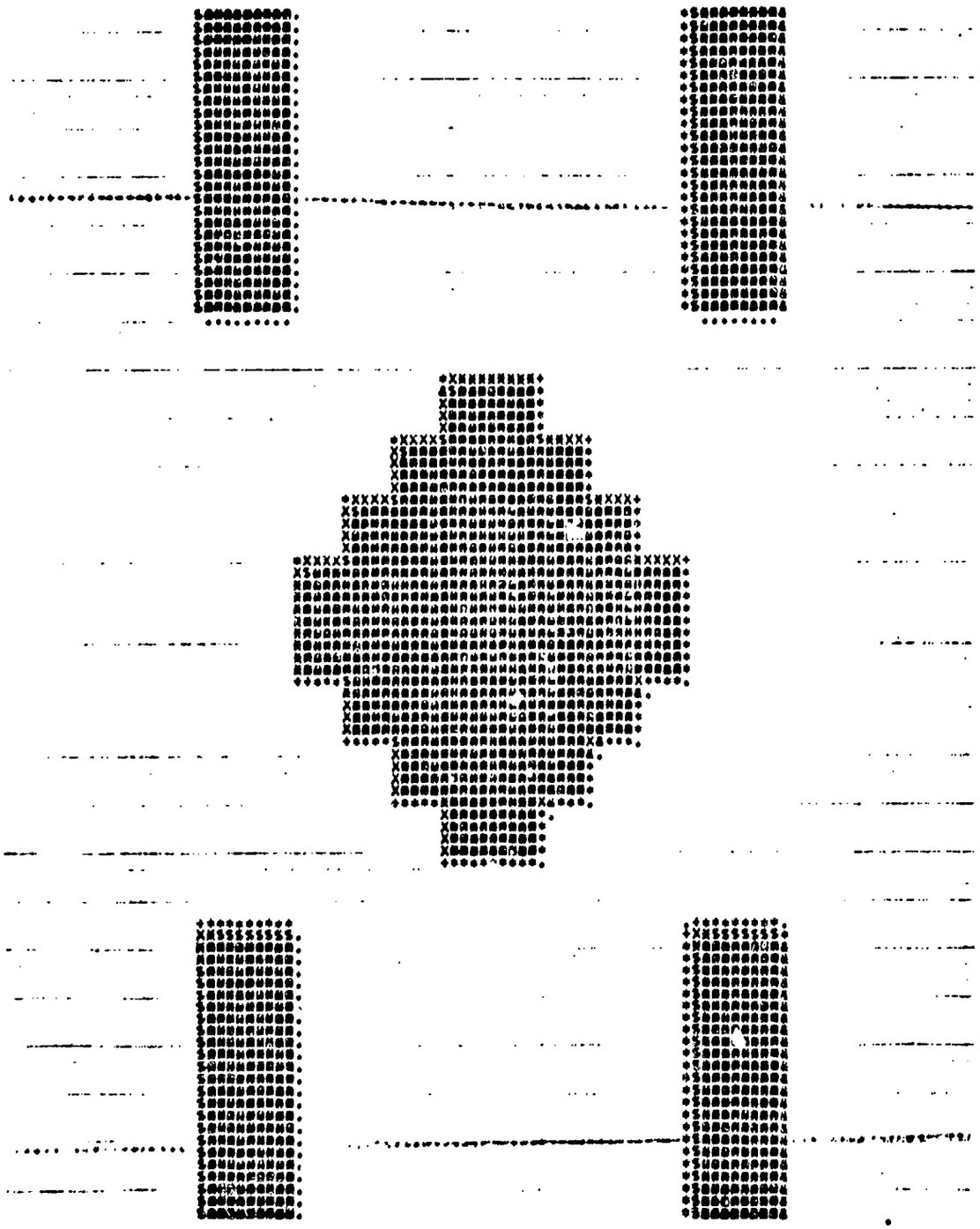

Figure 21. CCD Array after clocking at 99% transfer efficiency.

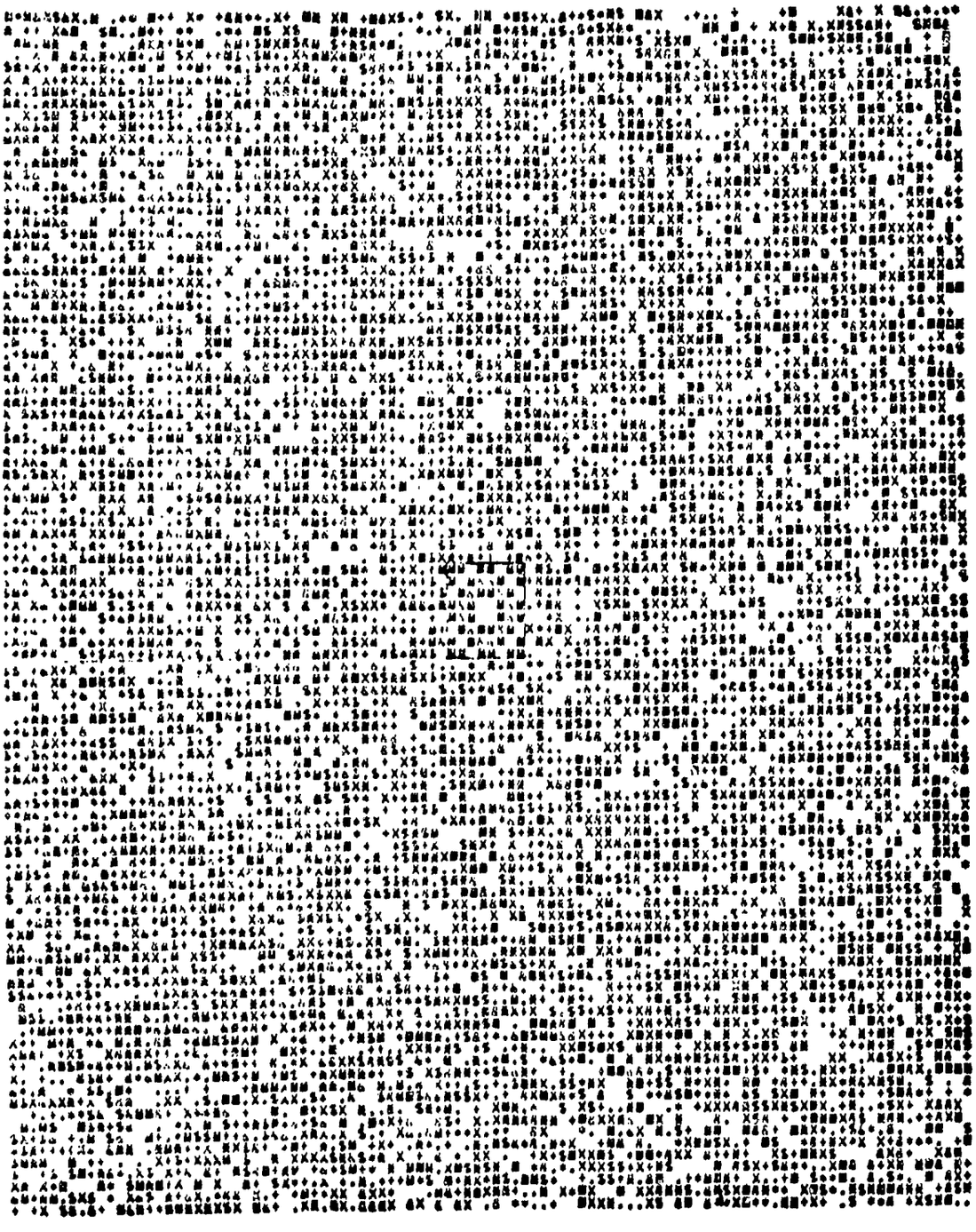

Figure 22. CCD Array with pseudo-random background and target image.

TARGET PATTERN SIGNATURE

1	1	0	1	1	0	1	1
1	0	1	½	½	1	0	1
0	1	½	1	1	½	1	0
1	½	1	0	0	1	½	1
1	½	1	0	0	1	½	1
0	1	½	1	1	½	1	0
1	0	1	½	½	1	0	1
1	1	0	1	1	0	1	1

Figure 23. 8 x 8 CCD Array Used as Target.

Table 23. Output of CCDSIM.SEARCH

Iteration	Output
1	GOOD SEARCH, TRANSFER EFFICIENCY IS 100.00%
	THE TARGET WAS LOCATED AT x = 50, y = 50
2	GOOD SEARCH, TRANSFER EFFICIENCY IS 99.90%
	THE TARGET WAS LOCATED AT x = 50, y = 50
3	GOOD SEARCH, TRANSFER EFFICIENCY IS 99.98%
	THE TARGET WAS LOCATED AT x = 50, y = 50
4	GOOD SEARCH, TRANSFER EFFICIENCY IS 99.97%
	THE TARGET WAS LOCATED AT x = 50, y = 50
5	GOOD SEARCH, TRANSFER EFFICIENCY IS 99.96%
	THE TARGET WAS LOCATED AT x = 50, y = 50
6	GOOD SEARCH, TRANSFER EFFICIENCY IS 99.95%
	THE TARGET WAS LOCATED AT x = 50, y = 50
7	GOOD SEARCH, TRANSFER EFFICIENCY IS 99.94%
	THE TARGET WAS LOCATED AT x = 50, y = 50
8	GOOD SEARCH, TRANSFER EFFICIENCY IS 99.93%
	THE TARGET WAS LOCATED AT x = 50, y = 50
9	GOOD SEARCH, TRANSFER EFFICIENCY IS 99.92%
	THE TARGET WAS LOCATED AT x = 50, y = 50
10	GOOD SEARCH, TRANSFER EFFICIENCY IS 99.91%
	THE TARGET WAS LOCATED AT x = 50, y = 50
11	BAD CCD SYSTEM--TARGET LOST!!!!!!
	TRANSFER EFFICIENCY TOO LOW AT 99.90%
	LAST AVAILABLE POSITION WAS x = 50, y = 50

This corresponds to a transfer efficiency of 99.913%, which corresponds very closely to the simulation output.

It should be pointed out that the simulation is for interline transfer. If line--or interline--transfer is used, the number entered as TREFF is actually the cube of the transfer efficiency for a three-phase device since three transfers are made for each sensing element. For frame- or field-transfer, two parts must be used. For the transfer to the storage section the number entered is also the cube of the transfer efficiency but the only vertical transfer is made, so half as many transfers are made for a square device. The second part is identical to the line transfer, having both vertical and horizontal transfer. An efficiency of at least 99.91% is presently attainable with state-of-the-art MOS fabrication.

For actual simulation of known device characteristics, the contrast of target to background may be varied as is necessary. Any target may be used for the recognition scheme. The only provision is that the target approximation must cover a rectangular array of cells. Digitized target patterns are easily obtainable and may be used directly by the scheme. With slight revision, the program can also provide target acquisition as well as tracking.

One great advantage of the CCD mechanism is that it is self-scanning. This mechanism provides the ability to observe the cells one at a time as one might observe bits in a shift register. The grey levels are easily chosen and implemented. The uses for the CCD imager as a tracker necessitate compactness and agility. In

order to process the information from the CCD where several grey levels are not necessary the information may be encoded directly as it is clocked from the array sensor. If the information is bi-level (0 or 1), as shown in Figure 24, the black and white information may be encoded as run-lengths of cells. If several grey levels are necessary, the difference between grey levels is encodable with large dynamic sensitivity. A great deal of redundancy exists in black and white imaging. If a priori knowledge is available on the background, a good "educated" guess can be made as to the probability of various run-lengths. With this knowledge, the information can be encoded with a large savings in the number of bits necessary for reconstruction for the image scene. A one-zero representation of Figure 24 is presented in Figure 25. If this "scene" background is assumed to have a Poisson probability distribution with an average run-length of 5, it can be encoded as it is clocked from the array using the Huffman code generated from the appropriate distribution. The encoded sequences are given in Table 24 for lines 40 through 60 of Figure 25. Since the target is not accurately represented by the Poisson distribution, it is easily recognizable. Even though the image of Figures 24 and 25 is not accurately represented by the Poisson distribution, the number of bits necessary for description is reduced and the target pattern is easily found in the sequence. Perhaps a better distribution for description of the scene is the modified binomial distribution previously described. A program is presented for this encoding, along with the code to be used in its table look-up procedure in Appendix B.

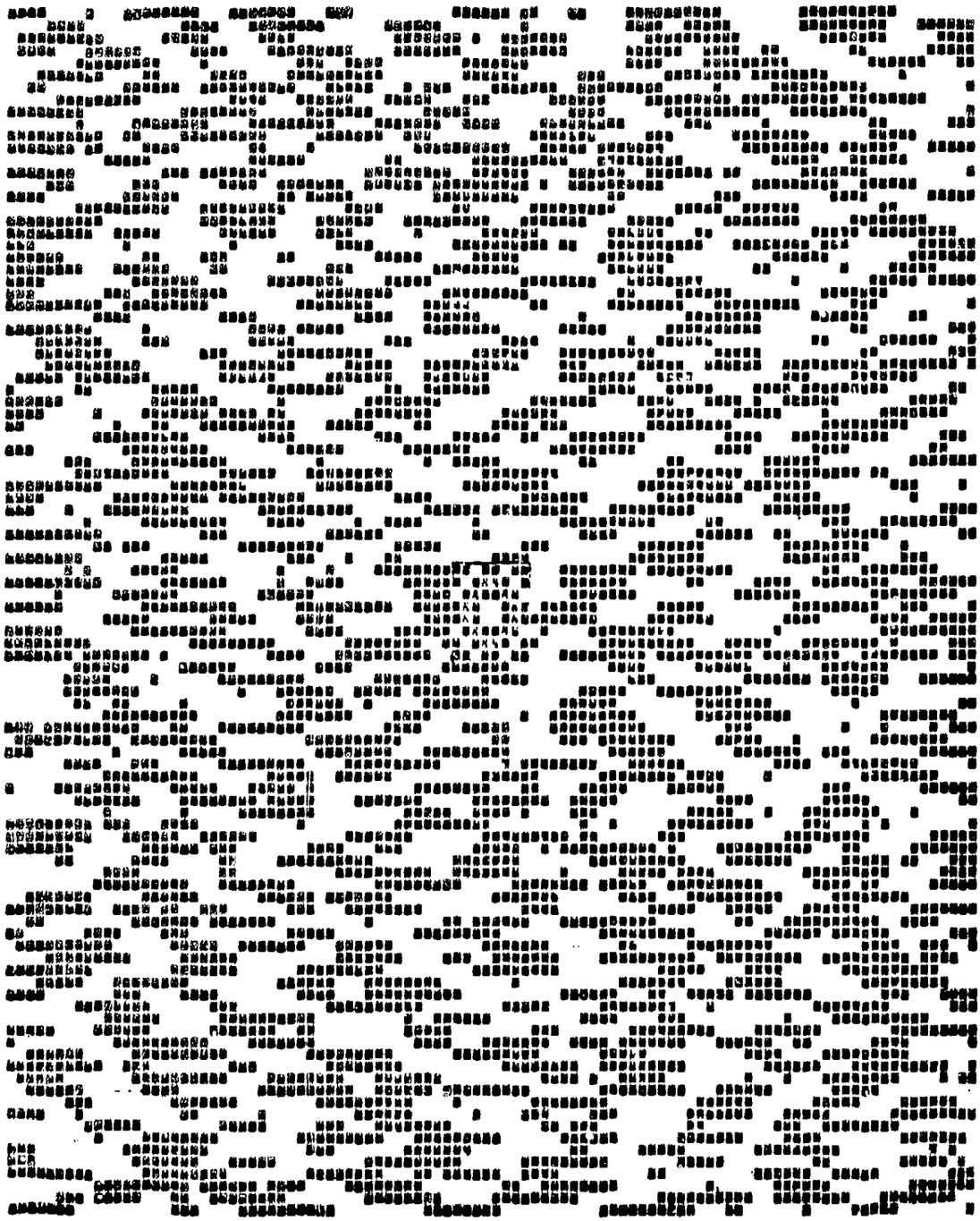

Figure 24. CCD Array with bi-level representation for Huffman Coding.

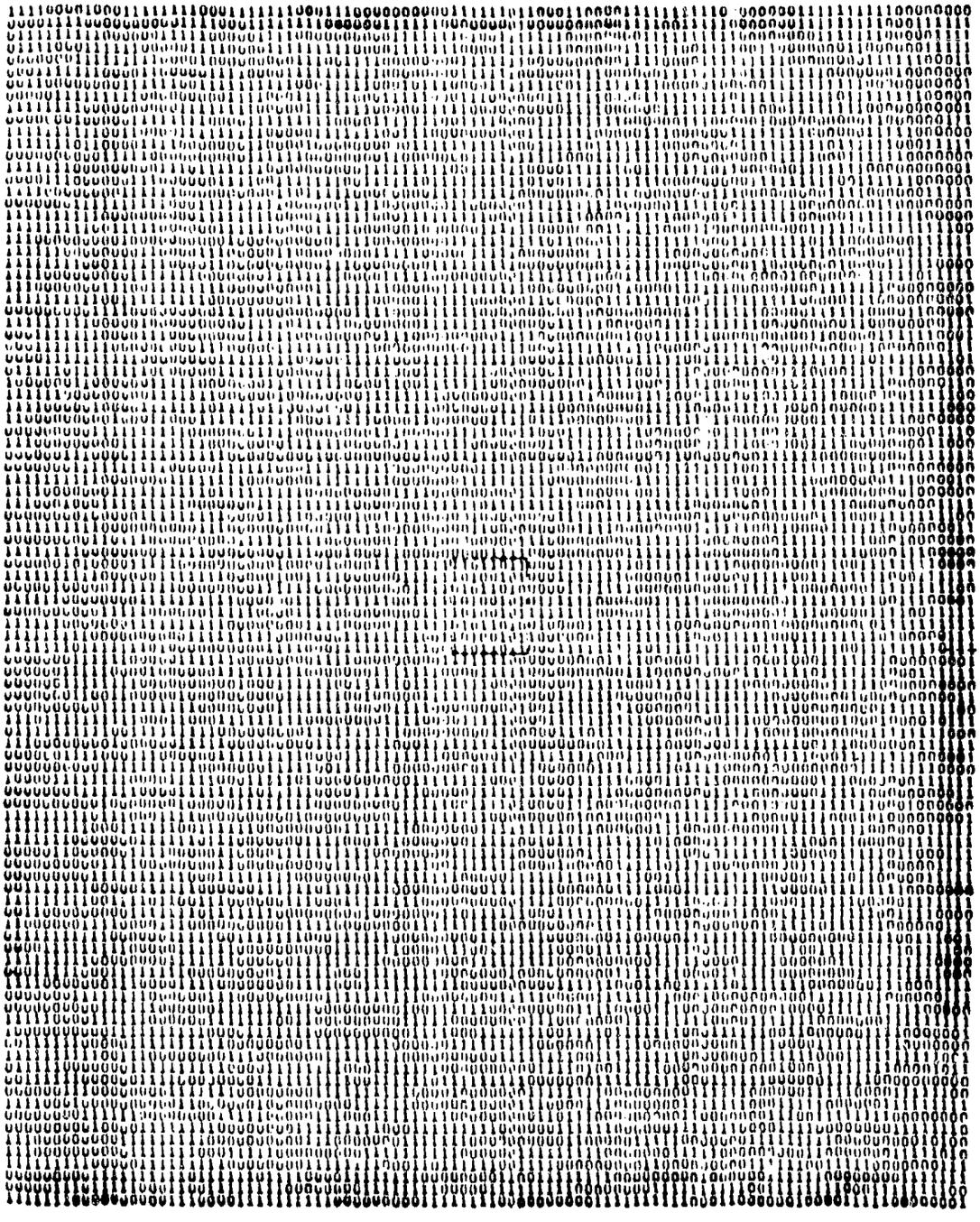

Figure 25. One-Zero representation of Figure 24 for coding.

Table 24. Encoded Sequences for Lines 40 Through 60 of Figure 25.

1*011	0*1010	1*011	0*0010	0*1011000
0*010	1*011	0*100	1*1011000	1*1010
1*00110	0*100	1*000	0*0010	0*1010
0*1011000	1*1011000	0*00111	1*00111	1*00111
1*1010	0*11	1*00111	0*1010	0*00111
0*1010	1*1010	0*011	1*011	1*100
1*011	0*011	1*000	0*00110	0*011
0*1010	1*011	0*010	1*100	1*00110
1*010	0*11	1*00111	0*100	0*000
0*010	1*1011000	0*1010	1*100	1*010
1*1010	0*00111	1*00111	0*011	0*11
0*0010	1*011	0*1011000	1*0010	1*1011000
1*11	0*11	1*0010	0*11	0*00111
0*1010	1*1011000	0*1010	0*000	1*011
1*1011000	0*100	1*1010	1*1011000	0*000
0*000	1*00110	0*010	0*1011000	1*000
1*0010	0*11	1*11	1*1011000	0*1011000
0*0010	1*00111	0*100	0*011	1*1011000
1*1011000	0*00110	1*0010	1*11	0*00111
0*0010	1*0010	0*1010	0*00110	1*1011000
1*1010	0*0010	1*010	1*1011000	0*1011000
0*010	1*100	0*100	0*011	1*1011000
1*00110	0*00111	1*1010	1*1011000	0*0010
0*010	1*00110	0*0010	0*011	1*010
1*000	0*00110	1*1011000	1*00110	0*000
0*1011000	1*0010	0*010	0*1011000	1*00111
1*1010	0*00110	1*100	1*00111	0*11
0*0010	1*000	0*100	0*1011000	1*011
1*1010	0*1010	1*11	1*00111	0*00111
0*010	1*00111	0*100	0*0010	1*100
1*1010	0*1010	1*0010	1*100	0*0010

Table 24. (Continued)

1*000	0*1011000	1*11	0*1011000	0*00111
0*11	1*1011000	1*000	1*00111	1*100
1*1011000	0*1011000	0*010	0*000	0*1011000
0*11	1*000	1*00110	1*00110	1*0010
1*010	0*000	0*100	0*0010	0*010
0*100	1*11	1*011	1*11	1*000
1*000	0*1010	0*11	0*0010	0*11
0*00110	1*1010	1*000	1*100	1*000
1*011	0*00111	0*1011000	0*1011000	0*100
0*1011000	1*0010	1*1011000	1*1011000	1*011
1*1011000	0*011	0*1011000	0*11	0*1010
0*1011000	1*1011000	1*00111	1*0010	1*010
1*00111	0*00110	0*1011000	1*010	0*00110
0*1011000	1*11	1*1011000	0*1011000	1*011
1*1011000	0*000	0*00111	1*010	0*11
0*11	1*11	1*1011000	0*1011000	1*000
1*010	0*011	0*011	1*1011000	0*0010
0*00110	1*011	1*1010	0*00110	1*1011000
1*010	0*1010	0*00110	1*011	0*0010
0*010	1*011	1*1011000	0*0010	1*010
1*1010	0*1011000	0*00110	1*00110	0*100
0*00111	1*1011000	1*00110	0*00111	1*1011000
1*000	0*00111	1*1010	1*00111	0*000
0*100	1*1011000	0*00110	0*1011000	1*11
1*00110	0*1011000	1*1010	1*00111	0*011
0*000	1*100	0*010	0*1011000	1*1011000
1*00110	0*11	1*100	1*00111	0*000
0*00111	1*010	0*00111	0*0010	1*1010
1*11	0*010	1*00111	1*1010	0*010
0*1011000	1*011	0*1011000	0*1011000	1*010
1*1011000	0*11	1*1011000	1*00110	0*011
0*00111	1*011	0*00111	0*1011000	1*11
1*1011000	0*00111	1*1011000	1*100	0*00110

Table 24 (Continued)

1*0010	1*1011000	0*100	1*100
0*1010	0*11	1*011	0*0010
1*010	1*100	0*011	
0*1011000	0*000	1*11	
1*010	1*000	0*011	
0*0010	0*100	1*00110	
1*000	1*100	0*100	
0*000	0*100	1*0010	
1*100	1*1011000	0*1010	
0*00110	0*00110	1*1011000	
1*1011000	1*00111	0*0010	
0*0010	0*00110	1*1011000	
1*000	1*00110	0*011	
0*00111	0*100	1*10110000	
1*11	1*100	0*1011000	
1*1011000	0*011	1*0010	
1*100	1*011	0*1011000	
0*1010	0*1010	1*00110	
1*11	1*1011000	0*00111	
0*0010	0*00111	1*1010	
1*1010	1*1010	0*1010	
0*1010	0*000	1*00110	
1*11	1*00110	0*1010	
0*00110	0*1010	1*00111	
0*010	1*100	0*11	
1*00111	0*00111	1*0010	
0*00111	1*0010	0*1011000	
1*00111	0*1011000	1*100	
0*11	1*00110	0*011	
1*1011000	0*0010	1*11	
0*00110	1*00111	0*0010	
1*000	0*0010	1*1011000	
0*00111	1*1010	0*010	

CHAPTER V

CONCLUSIONS AND RECOMMENDATIONS

The CCD mechanism lends itself to imaging systems that are certainly commensurate with the device capabilities. Most of the parameters of the SSID as used as sensors in trackers are not the limiting characteristics. The parameters of the tracker provide the limitations in most cases. System degradation due to sensor characteristics are mostly charge transfer oriented. This study shows the CCD to be capable of handling up to 10 MHz operation which is sufficient for most tracking application.

The small size and low power requirement indicate the strong impact on image tracking where limited space and power availability are factors. As evidenced by this study, with adequate transfer efficiencies, the accuracy of the position of the target to which each emergent charge packet can be assigned, sensitivity, and dynamic range, give these sensors wide application in the field of target acquisition and tracking.

The devices are easily modeled, giving simulation results which can be used to predict the accuracy of a tracker utilizing the CCD or CID. The device parameters (transfer efficiencies, contrasts, target patterns, background distribution), are estimated and then used by the simulation program to predict the behavior of a tracker using the device as a sensor. The routine is easily incorporated into target recognition schemes and tracking algorithms. One such

algorithm is the correlation method for target or image tracking. The study of this tracking technique as applied to the CCD simulation is suggested as a possible extension of the work.

The issue of buried channel versus surface channel mode is resolved. Buried channel provides several major advantages in performance and also simplifies device design and operation. The charge transfer efficiency for the buried channel mode is high for the full range of electron packet size, from saturation charge of approximately 10^6 electrons to the order of 10 electrons or less. Obviously, this provides wide dynamic range in straightforward design whereas, with the surface channel mode, it is necessary to cope with the level of the variably required "fat zero" channel current. One criticism of the buried channel device is that the saturation signal charge density cannot be made as high as with the surface channel device, and therefore is more limited in dynamic range. On the contrary, the buried channel device offers orders of magnitude higher dynamic range by virtue of the relatively low noise levels.

Image blooming can only be remedied by the incorporation of over-flow sinks which must be applied to each sensor element in order to accomplish adequate anti-blooming. Even when an image is excessively intense, smearing occurs in device types where charge is transferred through illuminated areas. Both frame-transfer and line-transfer device organizations have this problem; the interline-transfer device does not because the photoelement sites are distinct from the transport register. Where it is a problem, the device must

be designed and operated in such a way that the smear-producing charge transfer process is carried out as fast as it is generated. A compromise solution to the problem is to incorporate only one anti-blooming charge sink per sensor column. This feature can prevent blooming between columns, but not within columns.

The recognition scheme used in this work is a simple pattern search. With a few modifications, the recognition scheme could be greatly improved to encompass more sophisticated pattern searches utilizing more complex digitized target patterns. This work is meant to be a foundation for the simulation of the device itself as well as its incorporation into tracking schemes.

The actual calculation of the parameters read into CCDMAIN can be accomplished to further the simulation before the sensor is manufactured. Determination of device response or MTF can be made from design specifications before the prototype is developed.

It can be seen that for a 100 x 100 CCD sensor array which utilizes 10,000 photosensing elements, a 1 MHz clockrate will yield a frame rate of up to 100 frame/sec. This frame rate is certainly high enough to maintain track in any of the trackers surveyed in the study. The transfer efficiency necessary to maintain pattern recognition in the simulated scheme (99.90%) is easily attainable at such a clock rate. Therefore, even with clock rates as low as 1 MHz, adequate missile trackers utilizing a CCD sensor are realizable.

When utilizing this method as a missile tracking mechanism, the need for data reduction is evident. The scheme for encoding the run-lengths of white and black cells as they are clocked from the array

is introduced. The Huffman coding scheme is used with the table look-up method of codeword assignment. Sample encodings are made using codes derived from Poisson probability distributions with a mean of five and with a modified binomial distribution utilizing consecutive runs of while and black cells. It is evident that more knowledge of the background scenery encountered is desirable. The more closely the distribution can be approximated, the more reduction that is possible. Other distributions should be investigated and actual digitized scenes should be analyzed to determine the optimum code for a particular application.

The encoders for these operations are very easily implemented using simple digital electronics and could be incorporated into the peripheral electronics of the clocking waveform generators and output amplifiers of the device. This possibility creates a need for special chip design for special applications such as trackers, both with onboard tracking and onboard transmission of data to ground stations.

The idea is already being used for storing pages of literary information by encoding the outputs of linear reticon arrays. These encoded data are available then for instant recall. Up to 30 to 1 reductions of such information are attainable in present systems. The need for an extension of this work into the area described above utilizing charge-coupled devices and area arrays is apparent.

APPENDICES

APPENDIX A

BIBLIOGRAPHY

BIBLIOGRAPHY

Altman, Laurence, "CCDs Show Influence on Design Quietly," Electronics, January 20, 1977.

Altman, Laurence, "Charge-Coupled Devices Move in on Memories and Analog Signal Processing," Electronics, pp. 91-101, August 8, 1974.

Altman, Laurence, "The New Concept for Memory and Imaging: Charge-Coupling," Electronics, pp. 50-59, June 21, 1971.

Amelio, G. F., "Computer Modeling of Charge-Coupled Device Characteristics," The Bell System Technical Journal, pp. 705-730, Vol. 51, No. 3, March, 1972.

Amelio, G. F., "The Impact of Large CCD Image Sensing Area Arrays," International Conference of Technology and Applications of Charge-Coupled Devices, pp. 133-152, September, 1974.

Barbe, David F., "Imaging Devices Using the Charge-Coupled Concept," Proceedings of the IEEE, Vol. 63, No. 1, pp. 38-67, January, 1975.

Barbe, D. R., and Saks, N. S., "A Tradeoff Analysis of Transfer Speed Versus Charge-Handling Capacity for CCDs," International Conference of Technology and Applications of Charge-Coupled Devices, pp. 114-122, September, 1974.

Bradley, Lester, "Use of Two Electro-Optical Sensors Driven by Computer Generated Scan Patterns to Form a Real Time Two-Station Tracking System," NAECON '75 RECORD, pp. 309-313, 1975.

Broderson, R. W., Buss, D. D., and Tasch, A. F., Jr., "Experimental Characteristics of Charge Transfer Efficiency in Surface Channel Charge-Coupled Devices," Texas Instruments Incorporated, pp. 169-178.

Burt, D. J., "Basic Operation of the Charge-Coupled Device," GEC Hirst Research Centre, Wembley, England, pp. 1-12.

Burt, D. J., "Performance Limitations of Charge-Coupled Devices," GEC Hirst Research Centre, Wembley, England, pp. 84-91.

Campana, Stephen B., "Charge-Coupled Devices for Low Light Level Imaging," Naval Air Development Center, pp. 235-246.

Campana, S. B., and Barbe, D. F., "Tradeoffs Between Aliasing and MTF," International Conference of Technology and Applications of Charge-Coupled Devices, pp. 165-176, September, 1974.

Chan, C. H., and Chamberlain, S. G., "Charge Transfer Analysis in Two-Phase Step Oxide Charge-Coupled Device," International Conference of Technology and Applications of Charge-Coupled Devices, pp. 29-37, September, 1974.

Chan, C. H., and Chamberlain, S. G., "Numerical Methods for the Charge Transfer Analysis of Charge-Coupled Devices", Solid State Electronics, Vol. 17, pp. 491-499, 1974.

Dyck, Rudolf H., and Jack, Michael D., "Low Light Level Performance of A Charge-Coupled Area Imaging Device," International Conference of Technology and Applications of Charge-Coupled Devices, pp. 154-161, September, 1974.

Kosonocky, W. F., and Carnes, J. E., "Basic Concepts of Charge-Coupled Devices," RCA Review, RCA Laboratories, Princeton, N. J., pp. 566-593.

Kosonocky, W. F., Carnes, J. E., and Levine, P. A., "Measurements of Noise in Charge-Coupled Devices," RCA Review. RCA Laboratories. Princeton. N. J.. pp. 556-565.

Kosonocky. W. F.. and Carnes. J. E.. "Two-Phase Charge-Coupled Devices with Overlapping Polysilicon and Aluminum Gates." RCA Review, RCA Laboratories, Princeton, N. J., pp. 164-203.

Kovac, M. G., Shallcross, F. V., Pike, W. S., and Weimer, P. K., "Design, Fabrication, and Performance of a 128 x 160 Element Charge-Coupled Image Sensor," RCA Laboratories, Princeton, N. J., pp. 37-42.

Nelson, R. D., and Waters, W. P., "CCD Modulation Transfer Function," Rockwell International, pp. 207-216.

Schmieder, David E., "Seeker Lock-On Model and Performance Projections with CCD Sensors," NAECON '75 RECORD, pp. 343-349, 1975.

Steckl, Andrew J., Nelson, Richard D., French, Barry T., Gudmundsen, Richard A., and Schechter, Daniel, "Application of Charge-Coupled Devices to Infrared Detection and Imaging," Proceedings of IEEE, Vol. 63, No. 1, pp. 67-74, January, 1975.

Tompsett, M. F., Sealer, D. A., and Sequin, C. H., "Charge-Coupled Devices for Image Sensing," Bell Laboratories, pp. 1-5.

Tompsett, M. F., "Using Charge-Coupled Devices for Analog Delay." Bell Laboratories. pp. 147-150.

Tompsett. M. F.. Bertrum. W. J.. Sealer. D. A.. and Sequin, C. H., "Charge-Coupling Improves Its Image, Challenging Video Camera Tubes," Electronics, pp. 162-169, January 18, 1973.

APPENDIX B

FORTRAN PROGRAM LISTING

A Synopsis of the Computer Routines Used in the Parameter Study

All of the software development, simulation, data retrieval and data reduction are done on the Univac 1106 Multiprocessor facility available on the Mississippi State University campus. A listing of the software used follows this synopsis. All of the programs except one are written in Fortran IV and Fortran V. The one program used for data retrieval from the 9-track IBM compatible tape is written in Univac 1106 assembler language. Since the data tapes use 16 bit words, the word lengths are changed and manipulated to achieve the 36 bit word length necessary for use on the Univac facility.

The computer software are discussed in three separate sections as related to their use in the study. The data retrieval programs and subroutines are discussed first. These programs include file manipulation on tape, word length translation, error calculation and a Gould plot routine for displaying either the data or the error incurred.

The next section listed is the CCD simulation using a 100 x 100 element array and facilities for element manipulation as well as the variation of parameters.

The last listing is that for the encoding of the array data as it is clocked from the CCD. The encoder uses the table look-up procedure and includes a listing of two of the codes used for experimental evaluation of the reduction of bit sequence length.

TAPEREAD

(Data Retrieval and Evaluation)

TAPEREAD.DRIVE1

DRIVE1 is used to apply scale or calibration factor manipulation to the data after they have been converted to the correct word length and stored in a buffer (BUFF3). The errors are also derived from the adjusted tracker output and target position for each time interval. Both x- and y-position errors are calculated and either may be transferred to the plot routine, PLOTIT. The program also contains the ability to test for tape translation errors.

TAPEREAD.CONVRT

Subroutine BRKOUT takes the 36 bit words stored in the 960 word buffer (BUFF1), some of which contain more than one piece of data information, and separates them out into individual computer words using the Fortran V FLD(I,J,M) function. The FLD function allows bits I through J from word M to be transferred to a bit sequence of another word. These words are stored in BUFF3.

TAPEREAD.ASMRD

TREAD* reads the data tape one record at a time. One record is equivalent to 960 16 bit words of 426.67 36 bit words. Therefore, three records must be read in order to fill an integer number of 36 bit words. The 36 bit words are stored in BUFF1 and the 16 bit words are stored in BUFF2.

CONVRT* takes the data from TREAD* and transforms the 16 bit words to the usable 36 bit words necessary for the subroutine BRKOUT.

TAPEREAD.PLOTIT

Subroutine PLOTIT uses the data transferred from DRIVE1 to generate a Gould plot so that the position error or actual position of the target can be evaluated for each run under consideration.

CCDSIM

(CCD Simulation)

CCDSIM.CCDMAIN

CCDMAIN is the main device simulation program on which any image can either be generated or read. The parameters for the device are also read into the routine, affect the charge transfer and target-backgound contrast, as well as provide the grey level determination for target recognition. Any target can be placed on the image surface on any row-column location desired.

The program utilizes degradation of the image scene as determined by the transfer efficiency, TREFF. Both charge loss and residual charge addition affect the clocked array image.

CCDSIM.SEARCH

This routine searches throughout the previously clocked array for any target pattern stored in the target array, TARGET. The location of the target area is given and the transfer efficiency of the device at which the array was clocked. The grey levels within

which the pattern of the target must lie are specified to enable the user to either track contrast differences or specific patterns. If the transfer efficiency is sufficiently small so as to inhibit target recognition, the CCD is said to have lost target track. In this case, the last available position is given along with the transfer efficiency at which the target was lost.

CCDSIM.PATGEN

PATGEN generates a random sequence of run-lengths of white and black cells used in the evaluation of the possibility of encoding the array data as they are removed. Once again, the area pattern of the target is placed at any convenient location on the scene image and is encoded as well.

CCDSIM

(Encoding)

CCDSIM.ENCODE

The routine used for encoding the scene image utilizing a modified binomial probability distribution is ENCODE. The run-length is counted and identified as either 1's or 0's (black cells or white cells). The next sequence is also counted. Therefore, a run-length would be described as n 1's and m 0's or vice-versa. The probability is assigned as

$$P(S) = p^n q^m \quad , \tag{B1}$$

where p is the probability of a 1 occurring and q is the probability

of a 0 occurring, such that $p + q = 1$. In the runs made, $p = 0.6$ and $q = 0.4$. A run sequence might appear as

11111000 ,

and characterized as p^5q^3. P(S) is thus 0.00498 and is associated with the Huffman codeword 00010110.

CCDSIM.ENCODE2

If the run-lengths are to be characterized by either a run of 1's or a run of 0's, but not both consecutively, a separate encoder is available. ENCODE2 counts each sequence and identifies it as a run of either 1's or 0's, then chooses a Huffman codeword from the code library to transmit or store.

CCDSIM.POISCODE5

POISCODE5 contains the codeword library used in the look-up procedure for an encoder similar to ENCODE2. The Huffman codewords are generated from a Poisson probability distribution with average wordlength 5. This codeword library is taken from an earlier work in the area of redundancy reduction.

CCDSIM.MODBICODE

This library contains the Huffman codewords generated from the modified binomial distribution previously described. The library will be given in Appendix B. This codeword listing is also taken from the work done previously in redundancy reduction.

CCDSIM

(Pictorial Description)

CCDSIM.IMAGE

The next program and subroutine are utilized in giving a pictorial description of the CCD image surface before or after the clocking from the array. The picture generation shows the degradation of the image as well as the delay produced by low transfer efficiencies. IMAGE uses the data on the CCD to generate each element in one of a possible nine grey levels that may be specified in any manner so desired.

CCDSIM.DATA1

DATA1 provides the array description to be used by IMAGE. The data are read from a temporary storage file (having previously been cataloged by CCDSIM.CCDMAIN).

CCDSIM

(Target and CCD Characteristics)

CCDSIM.TARGET

TARGET is the element used to describe the target pattern utilized in the SEARCH routine as well as in the main program for storage in the array.

CCDSIM.CCDCHAR

CCDCHAR contains the initial parameters of the charge coupled device. These are used for characterizing the operation of the device and, in addition, target placement, contrast, and grey level tolerances. The data available in CCDCHAR are used by CCDSIM.CCDMAIN.

TAPEREAD VARIABLE LISTING

BUFF1	BUFFER STORAGE FOR THE 36 BIT WORDS CREATED IN THE SUBROUTINE CONVRT* FROM THE 16 BIT WORDS IN BUFF2
BUFF2	BUFFER STORAGE FOR THE 16 BIT WORDS READ FROM THE DATA TAPE
BUFF3	DATA INFORMATION WORDS--CONTAINING ALL OF THE INDIVIDUAL TRACKER DATA, SUCH AS POSITION, ZOTS DATA, AND TIME
BUFF4	ZOTS VOLTAGE OUTPUT INDICATION OF THE X POSITION OF THE TARGET
BUFF5	ZOTS VOLTAGE OUTPUT INDICATION OF THE Y POSITION OF THE TARGET
BUFF6	TRACKER INDICATION OF THE TARGET POSITION IN THE Y DIRECTION
BUFF7	TRACKER INDICATION OF THE TARGET POSITION IN THE X DIRECTION
ERFX	TRACKER-ZOTS ERROR IN THE X DIRECTION
ERFY	TRACKER-ZOTS ERROR IN THE Y DIRECTION
SCLTM	TRACKING TIME
APPROX	LINEAR LEAST-SQUARES FIT TO REMOVE ELECTRONIC NOISE
ERFXA	TRACKER-ZOTS ERROR WITH ELECTRONIC NOISE REMOVED
SCALE1,SCALE2 SCALE3,SCALE4 NADJ	SCALE AND CALIBRATION FACTORS FOR ADJUSTING BOTH TRACKER POSITION AND ZOTS INDICATION

```
TAPEREAD(1),DRIVE1
      1       INTEGER BUFF1(427),BUFF2(960),BUFF3(50)
      2       DIMENSION BUFF4(1000),BUFF5(1000),SCLTM(1000),BUFF6(1000),
     3      1BUFF7(1000),ERRX(1000),ERRY(1000),APPROX(1000),ERXA(1000)
      4       JM=0
      5       READ(5,222) SCALE1,SCALE2,NADJ,SCALE3,SCALE4
      6     222 FORMAT(2E13.7,I4,2F10.3)
      7       READ(5,555)IN,M
      8       WRITE(6,400)N,M
      9     400 FORMAT(2I10)
     10       WRITE(6,50)
     11      50 FORMAT('1',5X,'MANUAL',4X,'RECORD',5X,'FRAME',5X,'TIME'
     12     *,6X,'IRKY',6X,'IRKX',6X,'ZOIX',6X,'ZOIY')
     13       WRITE(6,51)
     14      51 FORMAT(' ',6X,'DATA',5X,'NUMBER',5X,'NUMBER')
     15     555 CONTINUE
     16       CALL TREAD(BUFF1,BUFF2,ISTAT)
     17       CALL CONVRT(BUFF1,BUFF2,ISTAT)
     18       IF(ISTAT-4)1,4,6
     19       1 CONTINUE
     20       IF(ISTAT-1)9,4,9
     21       4 CONTINUE
     22       DO 10 I=1,40
     23       JJ=24*I-23
     24       CALL BRKOUT(BUFF2(JJ),BUFF3)
     25       IF(BUFF3(1)-1.)555,535,555
     26     535 JM=JM+1
     27       BUFF4(JM)=BUFF3(42)*SCALE1
     28       BUFF5(JM)=BUFF3(43)*SCALE2
     29       BUFF6(JM)=(BUFF3(5)-NADJ)*SCALE3
     30       BUFF7(JM)=(BUFF3(6)-NADJ)*SCALE4
     31       ERXA(JM)=BUFF4(JM)-BUFF7(JM)
     32       ERRY(JM)=BUFF5(JM)-BUFF6(JM)
     33       SCLTM(JM)=BUFF3(4)*.1
     34       APPROX(JM)=(-6.9E-5*SCLTM(JM))
     35       ERXA(JM)=APPROX(JM)-BUFF7(JM)
     36      10 CONTINUE
     37     666 MN1=M-1
     38       DO 11 K=1,MN1
     39       CALL TREAD(BUFF1,BUFF2,ISTAT)
     40       CALL CONVRT(BUFF1,BUFF2,ISTAT)
     41       IF(ISTAT-4)21,24,6
     42      21 CONTINUE
     43       IF(ISTAT-1)9,24,9
     44      24 CONTINUE
     45       DO 11 I=1,40
     46       JJ=24*I-23
     47       CALL BRKOUT(BUFF2(JJ),BUFF3)
     48       JM=JM+1
     49       BUFF4(JM)=BUFF3(42)*SCALE1
     50       BUFF5(JM)=BUFF3(43)*SCALE2
     51       BUFF6(JM)=(BUFF3(5)-NADJ)*SCALE3
     52       BUFF7(JM)=(BUFF3(6)-NADJ)*SCALE4
     53       ERXA(JM)=BUFF4(JM)-BUFF7(JM)
     54       ERRY(JM)=BUFF5(JM)-BUFF6(JM)
     55       SCLTM(JM)=BUFF3(4)*.1
     56       APPROX(JM)=(-6.9E-5*SCLTM(JM))
     57       ERXA(JM)=APPROX(JM)-BUFF7(JM)
     58      11 CONTINUE
     59       WRITE(6,100)(BUFF3(KL),KL=1,6),(BUFF3(LK),LK=42,43)
     60     100 FORMAT(/(6I10,4E10.6))
     61       CALL PLOT11(SCLTM,ERXA,JM)
     62       GO TO 12
     63       9 CONTINUE
     64       6 WRITE(6,200)
     65     200 FORMAT(//'AN ERROR HAS OCCURRED IN TRANSLATION')
     66      12 CONTINUE
     67       STOP
     68       END
```

```
[redacted]STAPEREAD(1).CONVRT
      1             COMPILER(FLD=R)
      2             SUBROUTINE BRKOUT(BUF1,BUF0)
      3             INTEGER BUF1(1),BUF0(2)
      4             BUF0(1)=BUF1(1)
      5             BUF0(2)=FLD(15,0,BUF1(2))
      6             BUF0(3)=FLD(7,8,BUF1(2))
      7             BUF1(4)=BUF1(4)*2**16+BUF1(3)
      8             BUF0(5)=FLD(15,0,BUF1(5))
      9             BUF0(6)=FLD(7,8,BUF1(5))
     10             BUF0(7)=FLD(15,1,BUF1(6))
     11             BUF0(8)=FLD(15,1,BUF1(6))
     12             BUF0(9)=FLD(13,1,BUF1(6))
     13             BUF0(10)=FLD(12,4,BUF1(6))
     14             BUF0(11)=FLD(7,8,BUF1(6))
     15             I=8
     16             DO 3 J=7,12
     17             I=I+4
     18             BUF0(I)=FLD(15,4,BUF1(J))
     19             BUF0(I+1)=FLD(11,8,BUF1(J))
     20             BUF0(I+2)=FLD(7,4,BUF1(J))
     21           3 BUF0(I+3)=FLD(3,4,BUF1(J))
     22             BUF0(36)=FLD(15,8,BUF1(13))
     23             BUF0(37)=FLD(7,8,BUF1(13))
     24             BUF0(38)=BUF1(14)
     25             BUF0(39)=FLD(15,0,BUF1(15))
     26             BUF0(40)=FLD(7,8,BUF1(15))
     27             BUF0(41)=BUF1(16)
     28             J=16
     29             DO 2 I=42,49
     30             J=J+1
     31             BUF0(I)=BUF1(J)*2**21/2**21
     32           2 IF(BUF0(1).LT.0)BUF0(1)=BUF0(1)-1
     33             RETURN
     34             END
```

BEST AVAILABLE COPY

```
[redacted]TAPERLAD(1).ASMRD
                      AXR$ .
        INPAK         I$OT          'INTAPE',R$    S-S,S-S
        $(1).
        TREAD*
                      L             A0,(1,0)
                      L,U           A1,426
                      A             A0,0,X11
        ZERO1         SZ            0,*A0
                      JGD           A1,ZERO1
                      L,U           A0,427
                      S,H1          A0,INPAK+4
                      L             A0,0,X11
                      S,H2          A0,INPAK+4
                      I$OW          INPAK
                      L,S1          A0,INPAK+3
                      S             A0,*2,X11
                      J             4,X11
        CONVRT*       L             A0,(1,0)
                      L,U           A1,959
                      A             A0,1,X11
        ZERO2         SZ            0,*A0
                      JGD           A1,ZERO2
                      L             A0,(1,0)
                      A             A0,1,X11
                      L             A1,(1,0)
                      A             A1,0,X11
                      L,U           A2,100
        LOOP1         L,U           A3,0
                      L             A4,0,*A1
                      LDSL          A3,16
                      S             A3,0,*A0
                      L,U           A3,0
                      LDSL          A3,16
                      S             A3,0,*A0
                      L,U           A3,0
                      LDSL          A3,4
                      L             A4,0,*A1
                      LDSL          A3,12
                      S             A3,0,*A0
                      L,U           A3,0
                      LDSL          A3,16
                      S             A3,0,*A0
                      L,U           A3,0
                      LDSL          A3,8
                      L             A4,0,*A1
                      LDSL          A3,8
                      S             A3,0,*A0
                      L,U           A3,0
                      LDSL          A3,16
                      S             A3,0,*A0
                      JZ            A2,OUT
                      L,U           A3,0
                      LDSL          A3,12
                      L             A4,0,*A1
                      LDSL          A3,4
                      S             A3,0,*A0
                      L,U           A3,0
                      LDSL          A3,16
                      S             A3,0,*A0
                      L,U           A3,0
                      LDSL          A3,16
                      S             A3,0,*A0
                      JGD           A2,LOOP1
        OUT           J             4,X11
```

```
TAPEREAD(1),PLOTIT
      SUBROUTINE PLOTIT(SCLTM,ERFX,JM)
      DIMENSION SCLTM(10000),ERFX(8000)
      NPA=0
      NP2=0
      IGRID=-3
      JOK=0
      IMPT=1
      PAD=0.0
      POD=0.0
      XORIG=2.0
      YORIG=1.0
      AXL=0.0
      OXL=0.0
      AFAC=0.0
      OFAC=0.0
      ABSMIN=0.0
      ORDMIN=0.0
      AINT=0.0
      OINT=0.0
      SIZ=0.0875
      XLGN=0.0
      YLGN=0.0
      SLGN=0.0
      NUGA=0
      NUGO=0
      NUCA=0
      NUCO=0
      KSYM=0
      JSYM=0
      LAT=0
      LOT=0
      NLAT=0
      NLOT=0
      SLAB=0
      NLGN=0
      LOGA=0
      LOGO=0
      CALL PLOTCO
      CALL GRAPH(SCLTM,ERFX,JM,NP1,NP2,IGRID,JOK,NPAT,PAD,POD,XORIG,
     1YORIG,AXL,OXL,AFAC,OFAC,ABSMIN,ORDMIN,AINT,OINT,SIZ,XLGN,YLGN,
     2SLGN,NUGA,NUCA,NUGO,NUCO,KSYM,JSYM,LAT,NLAT,LOT,NLOT,SLAB,NLGN,
     3LOGA,LOGO)
      CALL LABEL(10.55,4.00,.10,90.0,0,0,1,5)
      CALL LABEL(1.05,4.00,.10,90.0,0,0,1,5)
      CALL LABEL(5.0,2.0,0.2,0.0,-2,-2,1,23)
      CALL PLOTNO
      RETURN
      END
```

CCDSIM VARIABLE LISTING USED IN TRANSFER

TREFF	TRANSFER EFFICIENCY ASSOCIATED WITH THE CCD ASSUMING ONLY ONE TRANSFER PER PHOTOSENSITIVE ELEMENT (SEE TEST RESULTS FOR VARIATIONS FOR DIFFERENT NUMBERS OF PHASES)
CCD	CCD ARRAY BEFORE CLOCKING THE IMAGE OUT
XCCD	CCD ARRAY INFORMATION AFTER CLOCKING THE IMAGE OUT
TSTPT	DIGITIZED TARGET SIGNATURE
TRLESS	AMOUNT OF REDUCTION IN TREFF FOR EACH ITTERATION
CONTR	TARGET-BACKGROUND CONTRAST
TOLER	GREY-LEVEL TOLERANCE USED IN TARGET RECOGNITION
MAX	NUMBER OF ELEMENTS SUBTENDED BY THE TARGET
NN	NUMBER OF ELEMENTS IN THE FIRST ROW OF THE TARGET
IFLAG	TEST FOR RECOGNITION OF THE TARGET
TSTPM1	LOWER LIMIT ON THE GREY-LEVEL TOLERANCE FOR TARGET RECOGNITION
NXPOS	X POSITION OF THE TARGET
NYPOS	Y POSITION OF THE TARGET
TSTPP1	UPPER LIMIT ON THE GREY-LEVEL TOLERANCE FOR TARGET RECOGNITION

```
CCDSIM(1).CCDMAIN
      C
      C*****************************************************************
      C
      C     TREFF REPRESENTS THE TRANSFER EFFICIENCY
      C
      C*****************************************************************
      C
            DIMENSION CCD(101,101),TSYPT(100),XCCD(100,100),X(100)
            READ(5,3) TREFF,TRESS,CONTR,TOLER
          3 FORMAT(4E10.3)
            READ(5,19)MAX,NN
         19 FORMAT(2I4)
            READ(5,19) INXPOS,INYPOS
            IMIN=INXPOS-NN/2+1
            IMAX=INXPOS+NN/2
            IMIN=INYPOS-NN/2+1
            IMAX=INYPOS+NN/2
            READ(5,18)(TSIPT(IM),IM=1,MAX)
         18 FORMAT(6F4.1)
            WRITE(6,201)
        201 FORMAT('1')
      C
      C*****************************************************************
      C
      C     THE FOLLOWING ROUTINE GENERATES THE BACKGROUND FOR
      C     THE ARRAY IN STORED CHARGE
      C
      C*****************************************************************
      C
        100 X(1)=0.7
            IM=M
            DO 11 J=1,100
            X(I)=X(I)*13431.
            CALL RANDU(X,100)
            DO 11 I=1,100
            X(I)=X(I)*CONTR
         11 CCD(I,J)=X(I)
            DO 10 I=IMIN,IMAX
            DO 10 J=JMIN,JMAX
            IM=IM+1
         10 CCD(I,J)=TSIPT(IM)
            DO 200 JMAX2=1,101
            CCD(JMAX2,101)=0.0
        200 CCD(101,JMAX2)=0.0
            I=1
         50 N=1
          6 J=1
      C
      C*****************************************************************
      C
      C     THE FOLLOWING ROUTINE CLOCKS OUT THE FIRST LINE
      C     OF STORED DATA--DEGRADED BY IMPERFECT TRANSFER
      C
      C*****************************************************************
      C
            XCCD(I,N)=CCD(I,J)*TREFF
          5 CCD(I,J)=CCD(I,J)-CCD(I,J)*TREFF+CCD(I,J+1)*TREFF
            J=J+1
            IF(J.LE.100) GO TO 5
            N=N+1
            IF(N.LE.100) GO TO 6
            I=I+1
            IP1=I+1
      C
      C*****************************************************************
      C
      C     THE NEXT SEQUENCE SHIFTS DOWN ALL OTHER ROWS
      C     IN THE ARRAY--DEGRADED BY TRANSFER INEFFICIENCY
      C
      C*****************************************************************
      C
```

```
72              DO 20 J=1,100
73           20 CCD(1,J)=CCD(1-1,J)+CCD(1,J)*THEFF
74              DO 21 IN=IP1,100
75              DO 21 J=1,100
76           21 CCD(IN,J)=CCD(IN-1,J)*(1.0-THEFF)+CCD(IN,J)*THEFF
77              IF(1.LE.100) GO TO 50
78        C
79        C*****************************************************************
80        C
81        C     THE DEGRADED IMAGE IS EVALUATED AS DATA.
82        C
83        C*****************************************************************
84        C
85              CALL SEARCH(XCCD,IFLAG,MAX,NN,TSTPT,THEFF,TOLER)
86              THEFF=THEFF-TRLESS
87              IF(IFLAG.NE.1)GO TO 100
88              STOP
89              END
```

```
CCDSIM(1).SEARCH
      C
      C*****************************************************************
      C
      C     THIS ROUTINE SEARCHES THE DEGRADED IMAGE FOR
      C     A GIVEN TARGET WITHIN SPECIFIED GREY LEVEL TOLERANCES
      C
      C*****************************************************************
      C
            SUBROUTINE SEARCH(XCCD,IFLAG,MAX,NN,TSTPT,THEFF,TOLER)
            DIMENSION XCCD(100,100),TSTPT(100),TSTPM1(100),TSTPP1(100)
            IFLAG=0
            N=1
            II=0
            JI=0
            JJ=1
            DO 33 IJT=1,MAX
            TSTPM1(IJT)=TSTPT(IJT)-TOLER
         33 TSTPP1(IJT)=TSTPT(IJT)+TOLER
      C
      C*****************************************************************
      C
      C     THE FOLLOWING SEGMENT SEARCHES FOR THE FIRST
      C     AVAILABLE CORRECT LINE--IF ONE IS FOUND, TRANSFER
      C     IS MADE TO THE NEXT ALLOWABLE TARGET ELEMENT
      C
      C*****************************************************************
      C
          5 II=II+1
            JI=0
          2 JI=JI+1
         15 CONTINUE
            IF(XCCD(II,JI).LE.TSTPP1(JJ).AND.XCCD(II,JI).GT.TSTPM1(JJ))
           1GO TO 20
            JI=JI-JJ+2
            JJ=1
            IF(JI.LE.100-NN-1) GO TO 15
            IF(II.LT.100) GO TO 5
         20 JJ=JJ+1
            IF(JJ.GT.JN) GO TO 4
            IF(II.EQ.100.AND.JI.GE.100-NN-1) GO TO 9
            GO TO 2
          3 JI=JI-MM+1
         13 MEN=1
            NNMAX=MEN
            IF(NNMAX.GT.MAX) GO TO 8
            II=II+1
            IF(II.GT.100) GO TO 9
      C
      C*****************************************************************
      C
      C     THIS SEGMENT CHECKS THE REMAINING PROPOSED TARGET
      C     ELEMENTS UNTIL EITHER THE ENTIRE TARGET IS FOUND
      C     OR AN ELEMENT DOES NOT CORRESPOND WITHIN GIVEN
      C     TOLERANCES.
      C
      C*****************************************************************
      C
            DO 4 JI=JI,100
            IF(XCCD(II,MI).LE.TSTPP1(JT).AND.XCCD(II,JI).GT.TSTPM1(JT))
           1GO TO 30
            JI=JI-MOD(JT,NN)+2
            II=II-N+1
            JJ=1
            N=1
            GO TO 15
         30 JT=JT+1
            IF(JT.GT.NNMAX) GO TO 13
          4 CONTINUE
          8 IXPOS=JI+MM/2-1
            NYPOS=II-NN/2
            WRITE(6,41) THEFF
```

```
      41 FORMAT(' ',' GOOD SEARCH, TRANSFER EFFICIENCY IS',2PF7.2,'%')
         WRITE(6,40) NXPOS,NYPOS
      40 FORMAT(' ',' THE TARGET WAS LOCATED AT X=',I4,4X,'Y=',I4)
         GO TO 111
       9 WRITE(6,50)
         DO 101 JR=1,100
     101 WRITE(10)(ACCU(IR,JR),JR=1,100)
         IFLAG=1
      50 FORMAT(' ',' BAD CCU SYSTEM -TARGET LOST!!!!!')
         WRITE(6,51) TREFF
      51 FORMAT(' ',' TRANSFER EFFICIENCY--TOO LOW AT',2PF7.2,'%')
         WRITE(6,52) NXPOS,NYPOS
      52 FORMAT(' ',' LAST AVAILABLE POSITION WAS X=',I4,4X,'Y=',I4)
     111 RETURN
         END
```

CCDSIM(I).TARGET

1	1.0	1.0	0.0	1.0	1.0	0.0	1.0	1.0
2	1.0	0.0	1.0	0.0	0.0	1.0	0.0	1.0
3	0.0	1.0	0.0	1.0	1.0	0.0	1.0	0.0
4	1.0	0.0	1.0	0.0	0.0	1.0	0.0	1.0
5	1.0	0.0	1.0	0.0	0.0	1.0	0.0	1.0
6	0.0	1.0	0.0	1.0	1.0	0.0	1.0	0.0
7	1.0	0.0	1.0	0.0	0.0	1.0	0.0	1.0
8	1.0	1.0	0.0	1.0	1.0	0.0	1.0	1.0

```
[redacted]CCDSIM(1).CCDCHAR
1          10.0E-01   1.0E-04  10.0E-01   9.0E-02
2          64   8
3          50   50
```

```
GOOD SEARCH. TRANSFER EFFICIENCY IS 100.00%
THE TARGET WAS LOCATED AT X=  50    Y=  50
GOOD SEARCH. TRANSFER EFFICIENCY IS  99.99%
THE TARGET WAS LOCATED AT X=  50    Y=  50
GOOD SEARCH. TRANSFER EFFICIENCY IS  99.98%
THE TARGET WAS LOCATED AT X=  50    Y=  50
GOOD SEARCH. TRANSFER EFFICIENCY IS  99.97%
THE TARGET WAS LOCATED AT X=  50    Y=  50
GOOD SEARCH. TRANSFER EFFICIENCY IS  99.96%
THE TARGET WAS LOCATED AT X=  50    Y=  50
GOOD SEARCH. TRANSFER EFFICIENCY IS  99.95%
THE TARGET WAS LOCATED AT X=  50    Y=  50
GOOD SEARCH. TRANSFER EFFICIENCY IS  99.94%
THE TARGET WAS LOCATED AT X=  50    Y=  50
GOOD SEARCH. TRANSFER EFFICIENCY IS  99.93%
THE TARGET WAS LOCATED AT X=  50    Y=  50
GOOD SEARCH. TRANSFER EFFICIENCY IS  99.92%
THE TARGET WAS LOCATED AT X=  50    Y=  50
GOOD SEARCH. TRANSFER EFFICIENCY IS  99.91%
THE TARGET WAS LOCATED AT X=  50    Y=  50
BAD CCU SYSTEM---TARGET LOST!!!!!
TRANSFER EFFICIENCY--TOO LOW AT  99.90%
LAST AVAILABLE POSITION WAS X=  50    Y=  50

OFIN
```

CCDSIM VARIABLE LISTING USED IN ENCODING

CCD	CCD INFORMATION ARRAY TO BE ENCODED
CODE	CODEWORDS ASSOCIATED WITH THE VARIOUS RUN-LENGTHS FOR THE MODIFIED BINOMIAL DISTRIBUTION OR FOR THE POISSON DISTRIBUTION
MAXRUN	THE MAXIMUM NUMBER OF CONSECUTIVE ONES OR ZEROS EXPECTED IN A RUN

CCDSIM(1).ENCODE

```
      SUBROUTINE ENCODE(CCD)
      DIMENSION CCD(100,100),CODE(10,10,4)
      DO 1 I=1,1000
    1 READ(10)((CCD(I,J),J=1,100)
      DO 21 IC=1,6
      DO 21 JC=1,9
   21 READ(5,22) (CODE(IC,JC,KC),KC=1,4)
   22 FORMAT(4A6)
      IF(CCD(1,1).LE.0.6) GO TO 2
      WRITE(6,3)
    3 FORMAT(' ','THE FIRST PORTION OF A CODE SEQUENCE
     1CONSISTS OF ONES')
      ITEST=1
      JTEST=1
    6 CONTINUE
      ICO=0
      IC1=0
    5 CONTINUE
      IF(CCD(ITEST,JTEST).LE.0.6) GO TO 4
      IC1=IC1+1
      JTEST=JTEST+1
      IF(JTEST.LE.100) GO TO 5
      JTEST=1
      ITEST=ITEST+1
      IF(ITEST.LE.100) GO TO 5
    4 ICO=ICO+1
      IF(CCD(ITEST,JTEST).GT.0.6) GO TO 8
      JTEST=JTEST+1
      IF(JTEST.LE.100) GO TO 4
      JTEST=1
      ITEST=ITEST+1
      IF(ITEST.LE.100) GO TO 4
    8 WRITE(6,9) (CODE(ICO,IC1,KC),KC=1,4)
    9 FORMAT(' ',4A6)
      IF(ITEST.LE.100) GO TO 30
    2 WRITE(6,10)
   10 FORMAT(' ','THE FIRST PORTION OF A CODE SEQUENCE
     2CONSISTS OF ZEROS')
      ITEST=1
      JTEST=1
   16 CONTINUE
      ICO=0
      IC1=0
   15 CONTINUE
      IF(CCD(ITEST,JTEST).GT.0.6) GO TO 14
      IC1=IC1+1
      JTEST=JTEST+1
      IF(JTEST.LE.100)GO TO 15
      JTEST=1
      ITEST=ITEST+1
      IF(ITEST.LE.100) GO TO 15
   14 CONTINUE
      ICO=ICO+1
      IF(CCD(ITEST,JTEST).LE.0.6) GO TO 8
      JTEST=JTEST+1
      IF(JTEST.LE.100) GO TO 14
      JTEST=1
      ITEST=ITEST+1
      IF(ITEST.LE.100) GO TO 14
      GO TO 8
   20 RETURN
      END
```

```
CCDSIM(I).ENCODE2
      1         DIMENSION CCD(100,100),CODE(100,3)
      2         READ(5,15) MAXRUN
      3         DO 16 IC=1,MAXRUN
      4      16 READ(5,14) (CODE(IC,IX),IX=1,3)
      5      15 FORMAT(I4)
      6      14 FORMAT(3A6)
      7         DO 1 I=1,100
      8       1 READ(10)(CCD(I,J),J=1,100)
      9         JJ=2
     10         II=1
     11       6 JJ=JJ-1
     12         ICU=0
     13         IC1=0
     14         IF(CCD(II,JJ).LE.0.6) GO TO 2
     15       4 IC1=IC1+1
     16         JJ=JJ+1
     17         IF(JJ.GT.100) GO TO 3
     18       9 CONTINUE
     19         IF(CCD(II,JJ).GT.0.6) GO TO 4
     20         WRITE(6,5) (CODE(IC1,IX),IX=1,3)
     21       5 FORMAT(' ',1H*,3A6)
     22         JJ=JJ+1
     23         GO TO 6
     24       2 ICU=ICU+1
     25         JJ=JJ+1
     26         IF(JJ.GT.100) GO TO 13
     27      11 CONTINUE
     28         IF(CCD(II,JJ).LE.0.6) GO TO 2
     29         WRITE(6,7) (CODE(ICU,IX),IX=1,3)
     30       7 FORMAT(' ',1H*,3A6)
     31         JJ=JJ+1
     32         GO TO 6
     33       3 II=II+1
     34         JJ=2
     35         WRITE(6,5)(CODE(IC1,IX),IX=1,3)
     36         IF(II.GT.100) GO TO 12
     37         GO TO 6
     38      13 II=II+1
     39         JJ=2
     40         WRITE(6,7)(CODE(ICU,IX),IX=1,3)
     41         IF(II.GT.100) GO TO 12
     42         GO TO 6
     43      12 STOP
     44         END
```

```
CCDS:M(1).PATGEN
      DIMENSION X(100),CCD(100,100),TSTPT(100)
      ID=0
      X(1)=13431.
      IM=1
      IF=1
      READ(5,11) INXPOS,INYPOS,NN,RUNLEN
   11 FORMAT(3I4,F6.1)
      READ(5,12)(TSTPT(ID),ID=1,64)
   12 FORMAT(8F4.1)
      JMIN=INXPOS-NN/2+1
      JMAX=INXPOS+NN/2
      IMIN=INYPOS-NN/2+1
      IMAX=INYPOS+NN/2
   19 CALL RANDU(X,100)
      DO 22 I=1,100
      IL=INT(X(I)*RUNLEN)+IF
      ID=MOD(I,2)
      DO 16 JM=IF,IL
      IF(IM.LT.100)GO TO 15
      IM=IM+1
      IF=1
      GO TO 24
   15 CONTINUE
      IF(ID.EQ.1)GO TO 17
      CCD(IM,JM)=0.0
      GO TO 16
   17 CCD(IM,JM)=1.0
   16 CONTINUE
   18 IF=IL+1
   24 CONTINUE
      IF(IM.LT.100)GO TO 21
   22 CONTINUE
      X(1)=13431.*X(1)
      GO TO 19
   21 CONTINUE
      DO 10 I=IMIN,IMAX
      DO 10 J=JMIN,JMAX
      ID=ID+1
   10 CCD(I,J)=TSTPT(ID)
      DO 102 IZ=1,100
  102 WRITE(10)(CCD(IZ,JZ),JZ=1,100)
      STOP
      END
```

```
CCUSIM(17).POISCODES
 1      1011000
 2      00111
 3      0010
 4      011
 5      11
 6      000
 7      010
 8      100
 9      1010
10      00110
11      10111
12      101101
13      10110010
14      101100110
15      1011001111
16      10110011110
17      101100111110
18      101100111111
```

	CCUSIM(I).MODBICODE
1	10
2	001
3	[illegible]
4	1100
5	01011
6	0100000
7	1101101
8	01111100
9	010100010
10	111
11	[illegible]
12	01001
13	0000100
14	011111
15	[illegible]
16	010001110
17	0001010010
18	0111110110
19	[illegible]
20	11011
21	011101
22	01010000
23	[illegible]
24	110100010
25	0111000110
26	0100011110
27	[illegible]
28	010101
29	01000010
30	000101000
31	[illegible]
32	0101000110
33	000101111110
34	110100111110
35	[illegible]
36	0100011111101
37	11010000
38	011100010
39	[illegible]
40	0000101011110
41	0111101110
42	0100011111111
43	[illegible]
44	1101000111100
45	01110001111011
46	0000101110
47	[illegible]
48	011100011110
49	000101111111
50	1101000111111
51	[illegible]
52	0101000111101111
53	000101111110011
54	011110111110111
55	[illegible]
56	000101011111
57	011110111111
58	011100111100
59	[illegible]
60	1101000111101111
61	011110111110110
62	01110001111010000
63	[illegible]
64	011100111111
65	010100111100
66	0100011111110000
67	[illegible]
68	011100111110101
69	010100111101001
70	000101111[illegible]001010
71	[illegible]

72	01110011110100101
73	00010111111000
74	01111011111010
75	010100111110101
76	010100111101000
77	00010111111001000
78	01110011111010011
79	000101111110010011
80	0111001111101001000
81	0111001111101001001

CCDSIM VARIABLE LISTING USED IN IMAGES

CTPTS	THE OUTPOINTS FOR THE DETERMINATION OF THE GREY LEVEL RANGE OF EACH POINT
NOPTS	NUMBER OF OVERPRINTS USED IN THE PRINTOUT
NGLEV	NUMBER OF GREY LEVELS UTILIZED
NX	STARTING X POSITION OF THE ARRAY
NY	STARTING Y POSITION OF THE ARRAY
TRAY	THE SYMBOLS USED FOR EACH OF THE OVERPRINTS
DLINE	DATA POINTS FOR EACH LINE OF THE ARRAY

BEST AVAILABLE COPY

```
CCDSIM(I).IMAGE
      DIMENSION DLINE(110),CTPTS(17),ITRAY(110),ORAY(6,110),IRAY(6,18)
     *,I(110),J(110),K(110),L(110),MSUM(20),INRANG(256)
      DO 10 M=1,110
       DO 10 N=1,6
   10 ORAY(N,M)=' '
C*****************************************************************************
C
C        THIS SECTION OF THE PROGRAM READS THE NUMBER OF COLUMNS
C        AND ROWS TO BE PROCESSED, THE NUMBER OF OVERPRINTS, NUMBER
C        OF DISCRETE LIGHT LEVELS AND THE COORDINATES OF THE NW
C        CORNER OF THE MAP ALL FROM THE FIRST DATA CARD(UNFORMATTED).
C        THE NEXT CARD PROVIDES THE UPPER BOUND CUTOFF POINTS(REAL)
C        IN UNFORMATTED LAYOUT.
C        FINALLY THE OVERPRINT SYMBOL TABLE IS READ INTO A TWO DIMENSIONED
C        ARRAY FROM THE NEXT 2-6 CARDS.
C
C*****************************************************************************
      CALL DATA0
      READ(5,100)NX,NY,NOPTS,NGLEV,NWX,NWY,FACTOR
      WRITE(6,200)NX,NY,NGLEV,NOPTS,NWX,NWY
      LAST=NGLEV-1
      READ(5,110)(CTPTS(M),M=1,LAST)
      READ(5,120)((IRAY(N,M),N=1,20),M=1,NOPTS)
      WRITE(6,210)(M,M=1,NGLEV)
      DUM=0.0
      WRITE(6,220)DUM,(CTPTS(M),M=1,LAST)
      DUM=999.9
      WRITE(6,220)(CTPTS(M),M=1,LAST),DUM
      DO 15 KGB=1,2
         PRINT 225
         DO 15 M=1,NOPTS
         WRITE(6,230)((IRAY(M,N),KK=1,5),N=1,NGLEV)
   15 CONTINUE
      NWX1=NWX
      DO 20 M=1,NX
      I(M)=NWX/1000
      II=I(M)*1000
      J(M)=(NWX-II)/100
      JJ=J(M)*100
      K(M)=(NWX-(II+JJ))/10
      KK=K(M)*10
      L(M)=(NWX-(II+JJ+KK))
      NWX=NWX+1
   20 CONTINUE
      WRITE(6,240)NWX1,NWY
      WRITE(6,250)I,J,K,L
      [illegible]
      KOUNT=1
      LKOUNT=NWY
   30 CALL DATA1(DLINE,NX)
C*****************************************************************************
C
C        IN THIS SECTION THE DATA RECEIVED FROM SUBROUTINE
C        DATA IS PROCESSED ONE ELEMENT AT A TIME TO DETERMINE WHICH
C        LEVEL CLASS THE ELEMENTS FALL IN.
C
C*****************************************************************************
      DO 50 M=1,NX
       DO 40 N=1,LAST
       IF(DLINE(M).LT.CTPTS(N))GO TO 35
       GO TO 40
   35  ITRAY(M)=N
      MSUM(N)=MSUM(N)+1
       GO TO 45
   40  CONTINUE
      ITRAY(M)=NGLEV
      MSUM(NGLEV)=MSUM(NGLEV)+1
      IF(FACTOR)50,50,45
   45 KL=DLINE(M)*FACTOR+1
      INRANG(KL)=INRANG(KL)+1
      MAXKL=MAX0(MAXKL,KL)
```

BEST AVAILABLE COPY

```
   50 CONTINUE
C*********************************************************************
C
C       IN THIS SECTION EACH PIXEL POINT IS ASSIGNED AN OVERPRINT SYMBOL
C       AND THE MAP IS PRINTED A SINGLE ROW AT A TIME. A FREQUENCY
C       DISTRIBUTION IS COMPUTED FOR EACH POSSIBLE PIXEL VALUE.
C
C*********************************************************************
      DO 70 M=1,NX
      KI=ITRAY(M)
       DO 60 N=1,NOPTS
   60  ORAY(N,M)=IRAY(N,KI)
   70 CONTINUE
      WRITE(6,260)LKOUNT,LKOUNT,((ORAY(I,J),J=1,110),I=1,NOPTS)
      IF(KOUNT.EQ.NY)GO TO 80
      LKOUNT=LKOUNT-1
      KOUNT=KOUNT+1
      GO TO 30
   80 WRITE(6,235)
      WRITE(6,250)I,J,K,L
      WRITE(6,280)
      DO 90 M=1,NGLEV
       WRITE(6,285)M,NSUM(M)
       WRITE(6,290)(ORAY(N,M),N=1,NOPTS)
   90 CONTINUE
      WRITE(6,300)
      DO 95 M=1,MAXKL
      N=M-1
   95 WRITE(6,310)N,ITRANG(M)
C-----FORMATS-------
  100 FORMAT()
  110 FORMAT()
  120 FORMAT(20A1)
  200 FORMAT('0',T20,'NUMBER OF COLUMNS PRINTED: ',I3,'.   NUMBER OF LIN
     *ES PRINTED: ',I4,'.   NUMBER OF GRAY LEVELS: ',I2,'.'//,T20,'NUMBE
     *R OF OVERPRINTS: ',I1,'.   COORDINATES OF NORTHWEST CORNER OF THIS
     * STRIP ARE: ',I4,'W,',I4,'N.')
  210 FORMAT('0',T20,'CLASS NUMBER/CLASS RANGE/CLASS SYMBOLOGY'///,T14,1
     *6(I2,4X)//)
  220 FORMAT(' ',I12,18(F5.1,1X)/)
  225 FORMAT(1X)
  230 FORMAT('+',T12,18(5A1,1X))
  235 FORMAT('0',//)
  240 FORMAT('0'///' \\\\\\\\\\\\\\\\\\\\\\\\\\\\\\\\\\\\\\\\\\\\\\\\\\\\\\\\\\\\
     *\\\\\\\\\\\\\\\\\\\\\\\\\\\\\\\\\\\\\\\\\\\\\\\\\\\\\\\\\\\\\\\\\\\\\
     *\\\\\\\\\\\\\\\\\\'//' NW CORNER COORDINATES=',2X,I4,',',I4///)
  250 FORMAT(' ',8X,110I1)
  260 FORMAT(' ',I4,1X,I4,I10,110A1/('+',8X,110A1))
  280 FORMAT('0',///,5X,'LEVEL',5X,'SYMBOL',5X,'FREQUENCY')
  285 FORMAT(' ',6X,I2,14X,I6)
  290 FORMAT('+',18X,A1)
  300 FORMAT('1DENSITY HISTOGRAM'//)
  310 FORMAT(' ',4X,I3,I9)
      STOP
      END
```

```
$CCUSIM(1).DATA1
      1         SUBROUTINE DATA(ALINE,N)
      2         DIMENSION XRAY(100),ALINE(110),HEADER(10)
      3         ENTRY DATA1(N)
      4            READ(5,1000)NPIX
      5            READ(5,1001)HEADER
      6            WRITE(6,1002)HEADER
      7            WRITE(6,1003)NPIX
      8            RETURN
      9         ENTRY DATA1(ALINE,N)
     10            READ(10)XRAY
     11            DO 40 I=1,N
     12         40 ALINE(I)=XRAY(NPIX+I)
     13            RETURN
     14      C-----FORMATS-----
     15      1000  FORMAT(I)
     16      1001  FORMAT(10A6)
     17      1002  FORMAT('1',10A6)
     18      1003  FORMAT('0',I4,' PIXELS SKIPPED FROM LEFT OF FILE.')
     19            END
```

REFERENCES

1. Burt, D. J., "Basic Operation of the Charge-Coupled Device," GEC Hirst Research Centre, Wembley, England, pp. 1-12.

2. Kosonocky, W. F., and Carnes, J. E., "Basic Concepts of Charge-Coupled Devices," RCA Review, RCA Laboratories, Princeton, N. J., pp. 566-593.

3. Burt, D. J., "Performance Limitations of Charge-Coupled Devices," GEC Hirst Research Centre, Wembley, England, pp. 84-91.

4. Amelio, G. F., "The Impact of Large CCD Image Sensing Area Arrays," International Conference of Technology and Applications of Charge-Coupled Devices, pp. 133-152, September, 1974.

5. Barbe, David F., "Imaging Devices Using the Charge-Coupled Concept," Proceedings of the IEEE, Vol. 63, No. 1, pp. 38-67, January, 1975.

6. Campana, S. B. and Barbe, D. F., "Tradeoffs Between Aliasing and MTF," International Conference of Technology and Applications of Charge-Coupled Devices, pp. 168-176, September, 1974.

Unclassified

SECURITY CLASSIFICATION OF THIS PAGE (When Data Entered)

REPORT DOCUMENTATION PAGE	READ INSTRUCTIONS BEFORE COMPLETING FORM
1. REPORT NUMBER: AFOSR-TR-78-0964	2. GOVT ACCESSION NO. / 3. RECIPIENT'S CATALOG NUMBER
4. TITLE (and Subtitle): SOLID STATE Imaging DEVICE PARAMETER STUDY for Use in Electro-Optic Tracking Systems	5. TYPE OF REPORT & PERIOD COVERED: Final Report. 1 May 76 - 31 Aug 77
	6. PERFORMING ORG. REPORT NUMBER: MSSU-EIRS-78-2
7. AUTHOR(s): Jerry W. Rogers, Wilson E. Taylor	8. CONTRACT OR GRANT NUMBER(s): Grant AFOSR-76-3022
9. PERFORMING ORGANIZATION NAME AND ADDRESS: Mississippi State University, Mississippi State, MS 39762	10. PROGRAM ELEMENT, PROJECT, TASK AREA & WORK UNIT NUMBERS: 61102F, 2305 D9
11. CONTROLLING OFFICE NAME AND ADDRESS: Air Force Office of Scientific Research/NE, Bolling Air Force Base, D.C. 20332	12. REPORT DATE: Oct 77
	13. NUMBER OF PAGES: 126 / 134 p.
14. MONITORING AGENCY NAME & ADDRESS (if different from Controlling Office)	15. SECURITY CLASS. (of this report): Unclassified
	15a. DECLASSIFICATION/DOWNGRADING SCHEDULE: N/A

16. DISTRIBUTION STATEMENT (of this Report)

Approved for public release; distribution unlimited

17. DISTRIBUTION STATEMENT (of the abstract entered in Block 20, if different from Report)

18. SUPPLEMENTARY NOTES

19. KEY WORDS (Continue on reverse side if necessary and identify by block number)

Optical Tracker
Solid State Image Tracker

20. ABSTRACT (Continue on reverse side if necessary and identify by block number)

The introduction of the solid-state imaging device provides a new concept in sensor types which may be utilized in target trackers. Solid-state imagers do not require the high voltage technology used in conventional vidicons. Also, the possibility of on-chip signal processing of the video information makes the device very attractive in the area of scene evaluation. However, the devices actually provide a sampled image and have certain characteristics which limit their utilization as trackers or target acquisition sensors.

DD FORM 1 JAN 73 1473 EDITION OF 1 NOV 65 IS OBSOLETE

UNCLASSIFIED

390 182

SECURITY CLASSIFICATION OF THIS PAGE (When Data Entered)

The purpose of this study is three-fold. The first part consists of evaluating five existing trackers which utilize solid-state imagers as sensors. These imagers are of three types: charge-coupled devices (CCDs), charge injection devices (CIDs), and photodiode arrays. These trackers are investigated as the contrast, irradiance, and target velocity are varied on the image plane.

Since the charge-coupled device shows great potential in this area, the next portion of the study is devoted to the evaluation of the CCD as a sensor in a tracking or target acquisition algorithm. Parameters are varied in a CCD simulation scheme to provide characteristics for the device. Contrast, target pattern signature, transfer efficiency, and grey level element tolerances can be varied for the simulation. The simulation provides a 100 x 100 element three-phase interline transfer device.

The last part of the study is devoted to the investigation of coding the video data as it is clocked from the array. The Huffman coding scheme is used to eliminate data redundancy by run-length encoding. The possibility of target acquisition from code sequences is also examined.